DOKUZ EYLÜL UNIVERSITY
GRADUATE SCHOOL OF NATURAL AND APPLIED SCIENCES

SEASONAL CHANGES OF THE ZOSTERIC ACID CONTENT IN ZOSTERA NOLTII DETRITUS

by
Gamze TOPÇAM

November, 2013
İZMİR

SEASONAL CHANGES OF THE ZOSTERIC ACID CONTENT IN ZOSTERA NOLTII DETRITUS

A Thesis Submitted to the
Graduate School of Natural and Applied Sciences of Dokuz Eylül University
In Partial Fulfillment of the Requirements for the Degree of Master of Science
in Chemistry

by

Gamze TOPÇAM

November, 2013
İZMİR

M.Sc THESIS EXAMINATION RESULT FORM

We have read the thesis entitled **SEASONAL CHANGES OF THE ZOSTERIC ACID CONTENT IN ZOSTERA NOLTII DETRITUS** completed by **GAMZE TOPÇAM** under supervision of **ASSOCIATE PROFESSOR LEVENT ÇAVAŞ** and we certify that in our opinion it is fully adequate, in scope and in quality, as a thesis for the degree of Master of Science.

.....

Assoc.Prof. Levent ÇAVAŞ

Supervisor

.....

Jury Member

.....

Jury Member

Prof.Dr. Ayşe OKUR

Director

Graduate School of Natural and Applied Sciences

ACKNOWLEDGMENTS

This thesis would not have been possible without the help, support and patience of my supervisor Assoc.Prof. Levent ÇAVAŞ. I also thank to master students in Dr.Cavas's group, Mr. Hakan ALYÜRÜK and Ms. Nazlı MERT, for their helps and friendships during my studies.

I would like to express my gratitude to The Scientific and Technological Research Council of Turkey (TÜBİTAK) for scholarship and supporting our research group with national research project grant (Grant no: 111T166).

Moravia Paint and Chemical Industry Trading Limited Company, Istanbul is gratefully acknowledged for providing raw materials and biocides for paint preparation. I am also thankful to Prof. Dr. George Pohnert and Mrs.Caroline Kurth from Friedrich-Schiller-University in Jena, Germany by providing the potassium zosterate standard.

Last, but by no means least, I would like to thank to my family for their limitless love and support.

Gamze TOPÇAM

SEASONAL CHANGES OF THE ZOSTERIC ACID CONTENT IN ZOSTERA NOLTII DETRITUS

ABSTRACT

Artificial surfaces are covered by micro and macro marine organisms, such as diatoms, barnacles and algae in marine ecosystem. This natural event is called as biofouling. Marine vehicles are negatively affected by fouling organisms. Therefore, ships' hull is coated with antifouling paints in order to prevent biofouling. Development of antifouling paints with less environmental impact is of great importance since the current paints contain some biocides such as TBT (tributyltin) that have genotoxic effects on non-target marine organisms. In contrast to artificial surfaces in marine ecosystem, some of marine plants do not allow fouling organisms to settle down their leave surfaces. They release secondary metabolites to prevent epibiosis on their leaf surfaces since they need sun light to do photosynthesis. It is known that *Zostera* sp. contains an antifouling agent, zosteric acid. These species are widely distributed along Turkish coastlines. In order to determine the zosteric acid levels in *Zostera noltii* from Turkish coastlines, dead leaves of *Zostera noltii* were collected monthly from Dikili, Urla and Erdek coastlines from November 2011 to October 2012. The zosteric acid levels in extracts of *Zostera noltii* were determined through RP-HPLC. In the present study, zosteric acid containing antifouling paints were also prepared and the antifouling performances of newly prepared paints were evaluated. It is found that, *Zostera noltii* samples collected from Urla contained higher zosteric acid than samples collected from Dikili and Erdek. According to the field test results, the zosteric acid contained paint was successful at preventing the settlement of macrofouling organisms compared to control plates. In conclusion, isolated zosteric acid or the extracts containing zosteric acid from *Zostera noltii* detritus or synthetic zosteric acid and the derivatives might be evaluated as a co-biocide source in the production of eco-friendly antifouling paints.

Key words: Antifouling, biofouling, RP-HPLC, Zostera noltii, zosteric acid.

ZOSTERA NOLTII ÖLÜ YAPRAKLARINDA ZOSTERİK ASİT DÜZEYLERİNİN SEZONAL DEĞİŞİMİ

ÖZ

Deniz ekosisteminde bulunan yapay yüzeyler kendiliğinden diyatomeler, kabuklu deniz hayvanları ve algler gibi mikro ve makro deniz organizmalarınca kaplanırlar. Bu doğal olay biyofouling olarak adlandırılır. Deniz araçları fouling organizmalardan olumsuz etkilenir. Bu nedenle biyofouling olayını önlemek için gemilerin karinaları antifouling boyalarla kaplanır. Mevcut boyalar hedef olmayan deniz organizmaları üzerinde DNA zehirleyici etkileri olan bazı biyositler içerdiğinden, TBT (tribütiltin) gibi, çevreye daha az etkili antifouling boyaların geliştirilmesi büyük önem taşımaktadır. Deniz içerisindeki yapay yüzeylerin aksine, bazı deniz bitkileri fouling organizmaların yaprak yüzeylerine yerleşmelerine izin vermez. Fotosentez için güneş ışığına ihtiyaç duyduklarından, yaprakları üzerindeki epibiosis olayını engellemek için sekonder metabolitler salgılarlar. *Zostera* cinsinin antifouling bir ajan içerdiği bilinir, zosterik asit (ZA). Bu cinse ait türler Türkiye kıyılarında geniş yayılım gösterir. Türkiye kıyılarındaki *Zostera noltii* türünde bulunan zosterik asit düzeylerini belirlemek için, *Zostera noltii* ölü yaprakları Kasım 2011'den Ekim 2012'ye kadar aylık olarak Dikili, Urla ve Erdek sahillerinden toplandı. *Zostera noltii* özütlerindeki ZA miktarları RP-HPLC ile belirlendi. Mevcut çalışmada ayrıca zosterik asit içeren antifouling boyalar hazırlanmış ve bu yeni hazırlanmış antifouling boyaların etkinlikleri değerlendirilmiştir. Urla'dan toplanan *Zostera noltii* örneklerinin, Dikili ve Erdek'ten toplanan örneklere göre daha fazla zosterik asit içerdiği bulundu. Alan testi sonuçlarına göre, zosterik asit içeren boya kontrol plakalarla karşılaştırıldığında makrofouling organizmaların tutunmalarını önlemede başarılı olmuştur. Sonuç olarak, *Zostera noltii* türünden izole edilen zosterik asit veya zosterik asit içeren ekstraktlar veya sentetik zosterik asit ve türevleri çevre dostu antifouling boya üretiminde yardımcı biyosit kaynağı olarak kullanılabilir.

Anahtar kelimeler: Antifouling, biyofouling, RP-HPLC, Zostera noltii, zosterik asit.

CONTENTS

Page

M.Sc THESIS EXAMINATION RESULT FORM ii
ACKNOWLEDGMENTS iii
ABSTRACT iv
ÖZ v
LIST OF FIGURES viii
LIST OF TABLES xiv

CHAPTER ONE-INTRODUCTION 1

1.1 Biofouling 1
1.2 Effects of the Biofouling on Marine Vehicles 2
1.3 Antifouling Paints 5
1.4 The Harmful Effects of Currently Used Biocides in Antifouling Paints 10
1.5 Zostera Noltii Hornemann 1832 13
1.6 Zosteric Acid: Biosynthesis and Antifouling Properties 17
1.7 The Aim of the Thesis 19

CHAPTER TWO-MATERIALS AND METHODS 20

2.1 Materials and Methods 20
2.2 Collection of the Z. Noltii Detritus 20
2.3 Preparation of the Extracts 22
2.4 Synthesis of the Sodium Zosterate 23
2.5 Synthesis of the Potassium Zosterate 24
2.6 Optimization of the HPLC and Seasonal Zosteric Acid Determination 24
2.7 Isolation of Zosteric Acid from Z. Noltii Extracts 26
2.8 The Preparation of the Antifouling Paints 26
2.9 The Field Tests 27
2.10 The Microscopic Analysis 30
2.11 The Statistical Tests 30

CHAPTER THREE-RESULTS AND DISCUSSION 31

3.1 The Characterization of the Synthesized Sodium Zosterate 31
3.2 The Characterization of the Synthesized Potassium Zosterate 32
3.3 The Optimization of the HPLC and Seasonal Zosteric Acid Determination . 34
3.4 Isolation of Zosteric Acid from Z. Noltii Extracts 54
3.5 The Field Test Results 57
3.6 The Results of the Microscopic Analysis 80
3.7 The Statistical Analysis Results 81

CHAPTER FOUR-CONCLUSION 82

REFERENCES 84

LIST OF FIGURES

Page

Figure 1.1 Schematic diagram of biofouling (Modified from illustration of Jack Cook, Wood Hole Oceanographic Institution)..... 1
Figure 1.2 A ship which was affected from biofouling (Photo: Gamze TOPCAM). .. 3
Figure 1.3 Bio accumulations on ships' hull (Photo: Gamze TOPCAM). 4
Figure 1.4 Detail of hard macrofoulers on ship's hull (Photo: Gamze TOPCAM). 4
Figure 1.5 The classification of the antifouling paints (original)..... 6
Figure 1.6 Biocide release mechanism of the self-polishing type antifouling paints (Illustrated by Gamze TOPÇAM). 7
Figure 1.7 Chemical formula of a repeating unit of a copolymer of tributyltin methacrylate and methyl methacrylate (Yebra et al, 2004). 8
Figure 1.8 Biocide release mechanism of the self-polishing copolymer type antifouling paints (Illustrated by Gamze TOPÇAM). 9
Figure 1.9 Biocide release mechanism of the insoluble type antifouling paints (Illustrated by Gamze TOPÇAM). 10
Figure 1.10 The molecule structures of the widely used booster biocides in commercial antifouling paints. 12
Figure 1.11 Taxonomy of *Zostera noltii* (from Taxonomy Browser: Algeabase). 13
Figure 1.12 *Z. noltii* Hornemann 1832 (Photo: Gamze TOPCAM)..... 14
Figure 1.13 The apex of the leave of *Z. marina* (rounded) and *Z. noltii* (emarginate). 15
Figure 1.14 The chemical structures of rosmarinic, caffeic and p-coumaric acid. 16
Figure 1.15 The chemical structure of ZA. 17
Figure 1.16 The metabolic pathway of p-sulfoxy cinnamic acid (Alberte & Smith, 2005). 18
Figure 1.17 Synthesis of sodium zosterate by sulfonation of p-coumaric acid with Py•SO3 complex in DMF. 19
Figure 2.1 Google Earth image of Urla, İzmir coastline where *Z. noltii* samples were collected (38° 19' 48.49" N, 26° 39' 07.99" E). 21

Figure 2.2 Google Earth image of Dikili, İzmir coastline where *Z. noltii* samples were collected (39° 07' 10.50" N, 26° 51' 12.61" E). 21
Figure 2.3 Google Earth image of Erdek, Balıkesir coastline where *Z. noltii* samples were collected (40° 24' 33.41" N, 27° 46' 59.42" E). 22
Figure 2.4 a) The dried *Z. noltii* sample, b) powdered *Z. noltii* sample and c) extraction apparatus. 23
Figure 2.5 Isolation system of HPLC a) semi-preparative column b) fraction collector. 26
Figure 2.6 Application of prepared antifouling paint. 27
Figure 2.7 Levent Marina, İzmir, Turkey, (38° 24' 21.79" N, 27° 04' 08.91" E). 28
Figure 2.8 Immersion test system with painted plates a) before immersion and b) after 144 days of immersion. 29
Figure 3.1 ^{1}H-NMR spectra of sodium zosterate. 31
Figure 3.2 FT-IR spectra of sodium zosterate. 32
Figure 3.3 ^{1}H-NMR spectra of potassium zosterate. 33
Figure 3.4 ^{13}C-NMR spectra of potassium zosterate. 34
Figure 3.5 The HPLC chromatograms with UV detection (280 nm) of 15 µg/mL ZA sodium salt. 35
Figure 3.6 The HPLC chromatograms with UV detection (280 nm) of 15 µg/mL ZA sodium salt. 36
Figure 3.7 The HPLC chromatograms with UV detection (280 nm) of 15 µg/mL ZA potassium salt. 37
Figure 3.8 Calibration curve for the potassium zosterate. 37
Figure 3.9 The HPLC chromatograms with UV detection (280 nm) of 10 µg/mL ZA potassium salt (blue) and *Z. noltii* extract (red). 38
Figure 3.10 The HPLC chromatogram with UV detection (280 nm) of November-2011-Urla sample. 39
Figure 3.11 The HPLC chromatogram with UV detection (280 nm) of December-2011-Urla sample. 39
Figure 3.12 The HPLC chromatogram with UV detection (280 nm) of January-2012-Urla sample. 40

Figure 3.13 The HPLC chromatogram with UV detection (280 nm) of February-2012-Urla sample. 40
Figure 3.14 The HPLC chromatogram with UV detection (280 nm) of March-2012-Urla sample. 41
Figure 3.15 The HPLC chromatogram with UV detection (280 nm) of April-2012-Urla sample. 41
Figure 3.16 The HPLC chromatogram with UV detection (280 nm) of May-2012-Urla sample. 42
Figure 3.17 The HPLC chromatogram with UV detection (280 nm) of June-2012-Urla sample. 42
Figure 3.18 The HPLC chromatogram with UV detection (280 nm) of July-2012-Urla sample. 43
Figure 3.19 The HPLC chromatogram with UV detection (280 nm) of August-2012-Urla sample. 43
Figure 3.20 The HPLC chromatogram with UV detection (280 nm) of September-2012-Urla sample. 44
Figure 3.21 The HPLC chromatogram with UV detection (280 nm) of October-2012-Urla sample. 44
Figure 3.22 The HPLC chromatogram with UV detection (280 nm) of November-2012-Dikili sample. 45
Figure 3.23 The HPLC chromatogram with UV detection (280 nm) of December-2012-Dikili sample. 45
Figure 3.24 The HPLC chromatogram with UV detection (280 nm) of January-2012-Dikili sample. 46
Figure 3.25 The HPLC chromatogram with UV detection (280 nm) of February-2012-Dikili sample. 46
Figure 3.26 The HPLC chromatogram with UV detection (280 nm) of March-2012-Dikili sample. 47
Figure 3.27 The HPLC chromatogram with UV detection (280 nm) of April-2012-Dikili sample. 47
Figure 3.28 The HPLC chromatogram with UV detection (280 nm) of May-2012-Dikili sample. 48

Figure 3.29 The HPLC chromatogram with UV detection (280 nm) of June-2012-Dikili sample. 48
Figure 3.30 The HPLC chromatogram with UV detection (280 nm) of July-2012-Dikili sample. 49
Figure 3.31 The HPLC chromatogram with UV detection (280 nm) of August -2012-Dikili sample. 49
Figure 3.32 The HPLC chromatogram with UV detection (280 nm) of September -2012-Dikili sample. 50
Figure 3.33 The HPLC chromatogram with UV detection (280 nm) of October -2012-Dikili sample. 50
Figure 3.34 The HPLC chromatogram with UV detection (280 nm) of January -2012-Erdek sample. 51
Figure 3.35 The HPLC chromatogram with UV detection (280 nm) of May-2012-Erdek sample. 51
Figure 3.36 The HPLC chromatogram with UV detection (280 nm) of July-2012-Erdek sample. 52
Figure 3.37 The HPLC chromatogram with UV detection (280 nm) of September-2012-Erdek sample 52
Figure 3.38 Seasonal variation of the ZA content in the *Z. noltii* detritus from three different regions. 53
Figure 3.39 HPLC chromatogram with UV detection (280 nm) of January-2012-Urla sample. 55
Figure 3.40 HPLC chromatograms of isolated ZA from July-2012-Urla sample, green: before the evaporation of mobile phase, red: after the evaporation of mobile phase by water bath for 4 h at 99°C. 56
Figure 3.41 HPLC chromatograms of isolated ZA from July-2012-Urla sample, green: before the evaporation of mobile phase, red: after the evaporation of mobile phase under N_2 stream at room temperature. 56
Figure 3.42 HPLC chromatograms of isolated ZA from July-2012-Urla sample, green: before the evaporation of mobile phase, red: after the evaporation of mobile phase with rotary evaporator at 70 °C. 57

Figure 3.43 The photographs belong to two sides of unpainted test plates (between January and March) (A: front, B: back, 1-3: parallel number). 59
Figure 3.44 The photographs belong to two sides of unpainted test plates (between April and July) (A: front, B: back, 1-3: parallel number). 60
Figure 3.45 The photographs belong to two sides of test plates painted with biocide free paint (between January to March) (A: front, B: back, 1-3: parallel number). 61
Figure 3.46 The photographs belong to two sides of test plates painted with biocide free paint (between April and July) (A: front, B: back, 1-3: parallel number). 62
Figure 3.47 The photographs belong to two sides of test plates painted with commercial paint (between January and March) (A: front, B: back, 1-3: parallel number). 63
Figure 3.48 The photographs belong to two sides of test plates painted with commercial paint (between April and July) (A: front, B: back, 1-3: parallel number). 64
Figure 3.49 The photographs belong to two sides of test plates painted with *Z. noltii* powder containing paint (between January to March) (A: front, B: back, 1-3: parallel number). 65
Figure 3.50 The photographs belong to two sides of test plates painted with *Z. noltii* powder containing paint (between April to July) (A: front, B: back, 1-3: parallel number). 66
Figure 3.51 The photographs belong to two sides of test plates painted with *Z. noltii* extract containing paint (between January and March) (A: front, B: back, 1-3: parallel number). 67
Figure 3.52 The photographs belong to two sides of test plates painted with *Z. noltii* extract containing paint (between April and July) (A: front, B: back, 1-3: parallel number). 68
Figure 3.53 The photographs belong to two sides of test plates painted with ZA containing paint (between January and March) (A: front, B: back, 1-3: parallel number). 69
Figure 3.54 The photographs belong to two sides of test plates painted with ZA containing paint (between April and July) (A: front, B: back, 1-3: parallel number). 70

Figure 3.55 The photographs belong to two sides of test plates painted with diuron containing paint (between January and March) (A: front, B: back, 1-3: parallel number). 71
Figure 3.56 The photographs belong to two sides of test plates painted with diuron containing paint (between April and July) (A: front, B: back, 1-3: parallel number). 72
Figure 3.57 The photographs belong to two sides of test plates painted with irgarol 1051 containing paint (between January and March) (A: front, B: back, 1-3: parallel number). 73
Figure 3.58 The photographs belong to two sides of test plates painted with irgarol 1051 containing paint (between April and July) (A: front, B: back, 1-3: parallel number). 74
Figure 3.59 The photographs belong to two sides of test plates painted with diuron + irgarol 1051 containing paint (between January and March) (A: front, B: back, 1-3: parallel number). 75
Figure 3.60 The photographs belong to two sides of test plates painted with diuron + irgarol 1051 containing paint (between April to July) (A: front, B: back, 1-3: parallel number). 76
Figure 3.61 The photographs belong to two sides of test plates painted with econea containing paint (between January and March) (A: front, B: back, 1-3: parallel number). 77
Figure 3.62 The photographs belong to two sides of test plates painted with econea containing paint (between April and July) (A: front, B: back, 1-3: parallel number). 78
Figure 3.63 Some diatoms observed on the test plates. 81

LIST OF TABLES

Page

Table 2.1 Antifouling paint compositions prepared for field test. 27
Table 3.1 Seasonal ZA contents in *Z. noltii* detritus from Turkish coastlines (DW: Dried weight, ±: standard deviation, LOD=0.035 mg ZA/mL). 53
Table 3.2 The assessment of fouling grades on the surface of antifouling paint test panels 79

CHAPTER ONE

INTRODUCTION

1.1 Biofouling

Biofouling or biological fouling defined as attachment of organic compounds, micro- organisms, plants and animals on a surface exposing to seawater (Abdul Azis, Al-Tisan, & Sasikumar, 2001; Armstrong, Boyd, & Burgess, 2000; Faÿ et al., 2010; Yebra, Kill, & Dam-Johansen, 2004). Such accumulations referred as epibiosis when the host surface is another organism and the association is not symbiotic (Wahl, 1989).

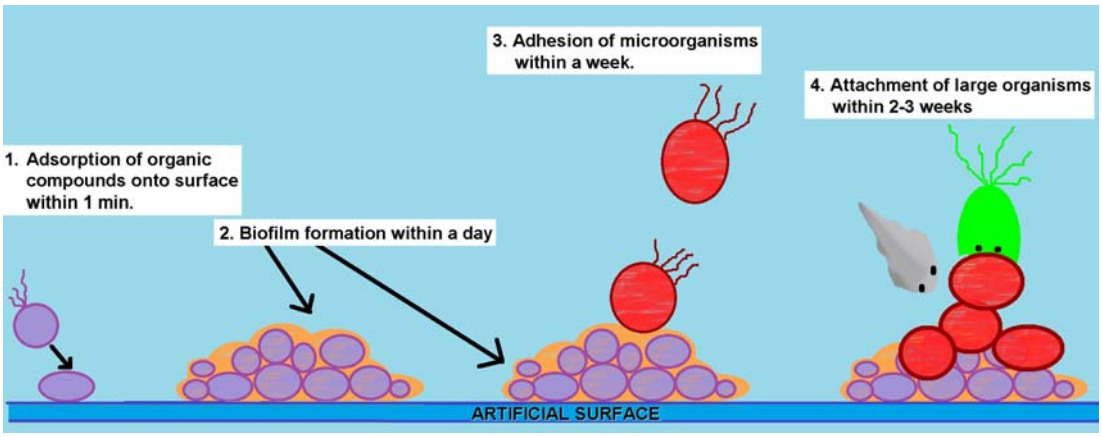


Figure 1.1 Schematic diagram of biofouling (Modified from illustration of Jack Cook, Wood Hole Oceanographic Institution)

As can be seen from Figure 1.1, this natural process starts with the adsorption of organic compounds, such as carbohydrates, polysaccharides and fatty acid on an artificial surface and it occurs in within a minute after contact of artificial surface with natural seawater (Abarzua & Jakubowski, 1995; Callow & Fletcher, 1994; Keough & Raimondi, 1995). Adsorption of these molecules is a result of the physical interactions between the organic compounds and the surface (Yebra et al, 2004). After the formation of organic film layer, presence of rich nutrients allows the attachment of microorganisms such as, bacteria and diatoms. This biofouling type is known as soft fouling. Soft fouling organisms are seaweed, hydroids, algae and

biofilm "slime". Colonization of the microorganisms on this artificial surface leads to the attachment of hard fouling organisms including barnacles, encrusting bryozoans, mollusks, polychaetes and other tube worms and zebra mussels (Brady, 1999; Yan et al., 2009).

The formation of biofouling depends on some parameters such as, under layer, the geographical location, the season and seawater temperature and competition etc. (Kirschner & Brennan, 2012). The most important parameter is temperature, since the temperature affects the growth rate of fouling organisms. The fouling event is generally heavier in seawater environment with high temperature. It is also known that biofouling is more problematic in coastal areas compared with the deep waters, since the marine organisms less abundant in oceans. The other effective parameter on the formation of biofouling is salinity of seawater. Most of the fouling organisms prefer the found in marine environment with high salinity but algae and bryozoa generally forms in low salinity waters (Yebra et al, 2004).

Biofilm formation is a problematic case in many industrial systems. In the heat exchangers and cooling water systems, there are two main encountered problems. Biofilms in this system reduce the heat transfer and cause thermal efficiency loss. Because of the reduction of flow, pressure drops across the heat exchanger. Moreover, corrosion of materials, unplanned shutdown for cleaning and increase of maintenance requirement are the other problems which are encountered (Tian, Chen, Yang, Chen, Shi, & Li, 2012; Murthy & Venkatesan, 2008). Biofilm formation in membranes is one of the most problematic fouling in industry and often causes stable permeability loss of and thus irreversible damage to the membranes (Liu, Zhang, He, Zhao, & Bai, 2010). Biofilms were also commonly observed in food industry. The attachment of the bacteria to the food product causes to hygienic problems and economic losses because of the spoilage of food (Peña, 2010).

1.2 Effects of the Biofouling on Marine Vehicles

Since marine vehicles contact with the seawater, ships' hull are covered with fouling organisms (Figure 1.2-1.4). In addition to the hull a lot of parts of the ship are

affected from the biofouling such as, propellers, external cooling pipes. Attachment of the fouling organisms onto ships' hulls increase the weight of the ship so, overall speed of ships decreases. Because of the high frictional resistance between the ship surface and sea water increases, the ships' maneuverability is reduced. Increase in the fuel consumption causes to extra carbon dioxide emission (Hall, Giddings, Soloman, & Balcomb, 1999; Hellio, De La Broise, Dufossé, Le Gal, & Bourgougnon, 2001). Extra carbon dioxide emission causes some effects such as, extreme weather changes, global temperature increase, the loss of ecosystems and potentially hazardous health effects for people.



Figure 1.2 A ship which was affected from biofouling (Photo: Gamze TOPCAM).



Figure 1.3 Bio accumulations on ships' hull (Photo: Gamze TOPCAM).

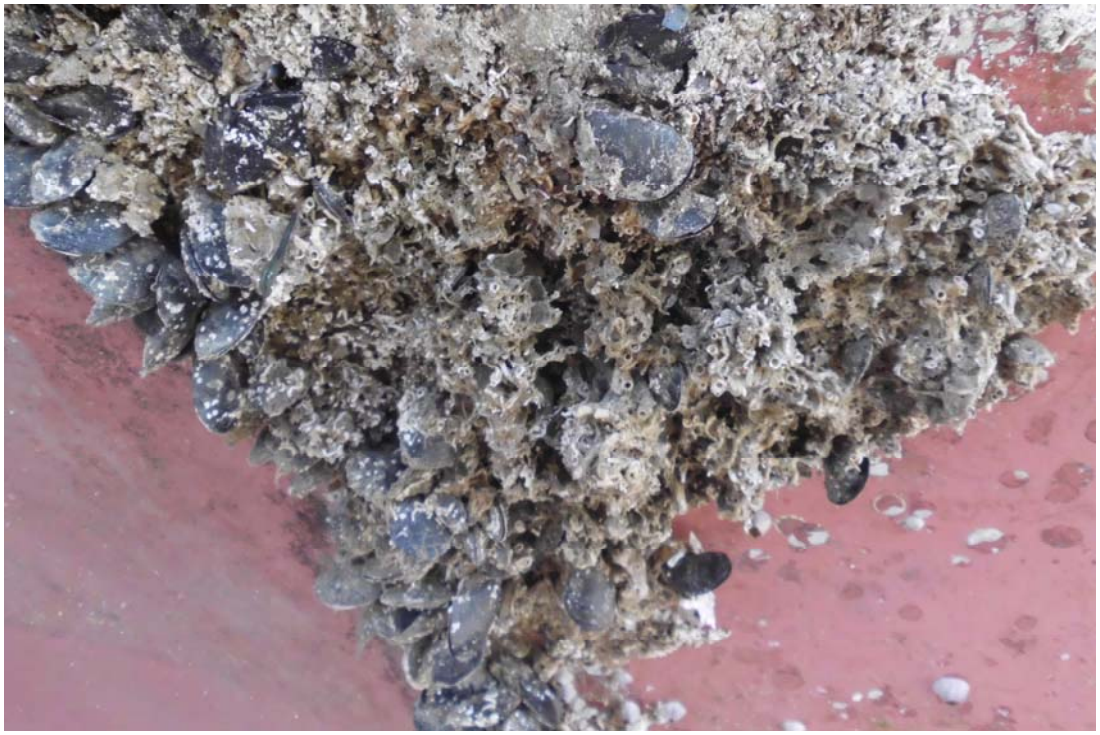


Figure 1.4 Detail of hard macrofoulers on ship's hull (Photo: Gamze TOPCAM).

In a study performed by Tobias Boren for International Paint it is reported that, an unprotected system may cover with 150 kg/m^2 in marine environment in less than six months. An example oil tanker with 40,000 m^2 underwater areas means that 6,000

tons of fouling. In this study it is also demonstrated that, while the ship's hull coated with antifouling paint, 39,420 metric tons fuel and so 28.5 million US dollars cost are saved in 15 years. Moreover, amount of CO_2 emission is reduced more than 125,000 metric tons in this period (Buskens, Wouters, Rentrop, & Vroon, 2013).

Abbott, Abel, Arnold, & Milne, (2000) summarized the additional expenses for fouled ships. According to Abbott, (2000) when a fouled ship voyage from San Francisco to Yokohama, ship's speed reduces from 14 knot to only 8.5 knot (1 knot=1.852 km/h) and the delay due to low speed (approximately 9 days) causes 65,700 US dollars additional coast. Increasing of the journey time means that need for more fuel and fresh water. It is reported that the net result is coast increases 77%, or 78,300 US dollars. Moreover, it is very expensive that placing a ship in a dry dock for cleaning and also during this process the ship is out of service.

Biofouling also causes some ecological problems (Yebra et al, 2004). Invasive or non-native species (exotics) introduce to many marine waters where they were not naturally present by shipping industry. These species are attached as fouling organisms or clung on ships' hull and transported across oceans and between coastal ports. Most of these species are invertebrates and plants, but fishes are also transported by marine vehicles (Brancato & MacLellan, 1999). %80 of these invasive species has not harmful effects on the indigenous species. However other species can be a threat to ecosystem diversity on where they were transported (Ribera, 1995). Invasive species compete with native species and can cause declines in native species. The transportation of fishes as fouler also affects the mariculture and commercial fishing, because the invading species are predators, and parasites. Moreover, some invasive species can carry disease such as bacteria can affect human health (Brancato & MacLellan, 1999).

1.3 Antifouling Paints

To prevent or inhibit the attachment and growth of fouling organisms on the ships' hull and also prevent the undesirable effects of biofouling, under water parts

of the ships are covered with special paints. These paints are known as antifouling paints. In the first years of shipping industry lime, arsenical and mercurial compounds and pesticides were used to protect the ships' hull from fouling organisms. In modern times, the antifouling paints are formulated with the toxic compounds or biocides.

After the first development of antifouling paints, different compositions, binders systems and biocides were tried. Today, a typical antifouling paint contains binder, solvent, biocide and other additives. In the literature, antifouling paints are mostly classified so far as their binder system as soluble, insoluble and foul release type antifouling paints. It is also possible to divide soluble type paints as self-polishing type and self-polishing copolymer type antifouling paints (Figure 1.5).

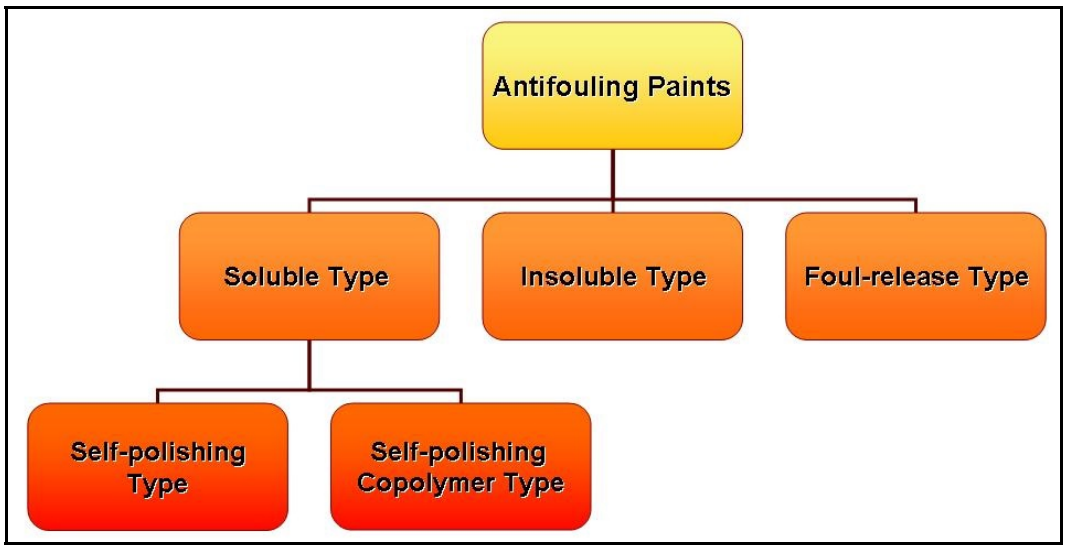


Figure 1.5 The classification of the antifouling paints (original).

Development of antifouling strategies was accelerated in mid 1800s (Yebra et al, 2004). James McInness used a metallic soap containing copper sulphate as antifoulant in 1860 and this composition is called as "hot-plastic paint" (WHOI, 1952; Yebra et al, 2004). At the same time Italian Moravian paint was developed which was mixture of rosin and copper compounds (WHOI, 1952; Yebra et al, 2004). Van de Kerk and co-workers made the first TBT-containing toxic compounds in the mid-1950s and TBT acrylate ester was first suggested for antifouling coatings

by Montermoso and co-workers in 1958 (WHOI, 1952; Yebra et al, 2004). Later, Milne and Hails obtained a patent on the use of TBT's in self-polishing copolymers in 1974 (Yebra et al, 2004).

Binder of self-polishing type antifouling paints is soluble resins and rosins. Copper(I) oxide is the main biocide (also pigment) used in these type antifouling paints. This biocide is highly toxic to marine organism. Dissolved Cu^{+} ions oxidize to more toxic Cu^{2+} ions. Because of the binder's solubility, the surface of the paint is rough and it contains fresh biocide all the time (Figure 1.6).

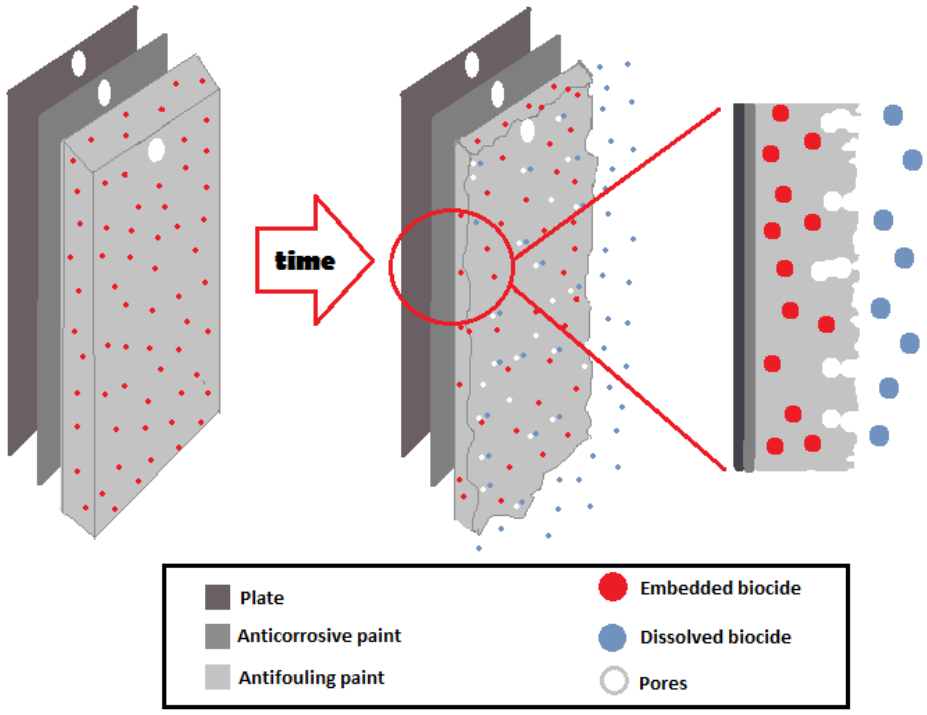


Figure 1.6 Biocide release mechanism of the self-polishing type antifouling paints (Illustrated by Gamze TOPÇAM).

Hence the surface is not smooth; self-polishing type paints cannot be used on some marine vehicles that need high speed, such as coast guard. This type antifouling paints are the most used antifouling paints all around world since the cost of this paint is cheaper than those of other type binders (Alyuruk, 2012; Karabay 2011; Yebra et al, 2004).

The most successful antifouling paints belong to Self-Polishing Copolymer Type antifouling group. These type antifouling paints are widely used because of their long service time and high performance. The highly toxic compounds such as tributyltin (TBT), co-biocides and copper (I) oxide play a role on the performance of this type paints.

Tributyltin (Figure 1.7) is found in self-polishing antifouling paints as an acrylic polymer (usually methyl methacrylate). TBT groups bond to polymeric backbone by an ester linkage and a soluble pigment, such as ZnO or Cu_2O (Alyuruk, 2012, Yebra et al, 2004).

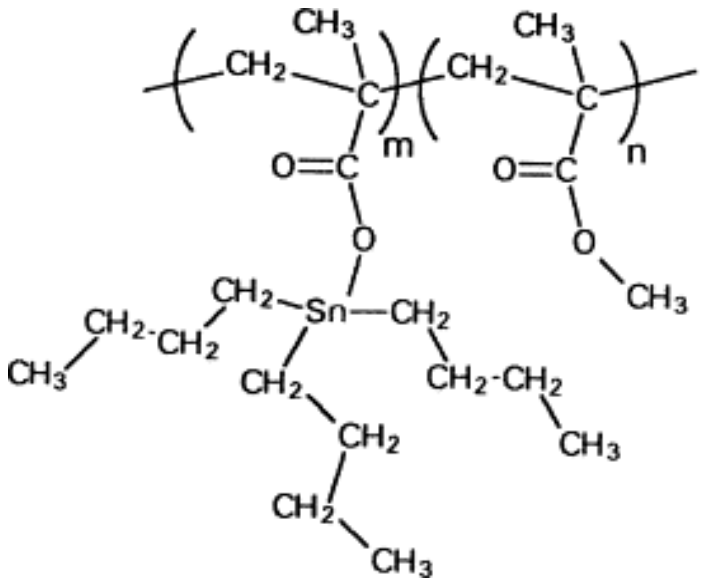


Figure 1.7 Chemical formula of a repeating unit of a copolymer of tributyltin methacrylate and methyl methacrylate (Yebra et al, 2004).

In this type antifouling paint TBT groups are released by hydrolysis of ester linkages between methyl methacrylate and TBT in seawater. Polymeric film releases layer by layer so the surface of paint always smooth and has fresh biocide (Alyuruk, 2012; Yebra et al, 2004). The biocide release mechanism of self-polishing copolymer type paints is given in Figure 1.8.

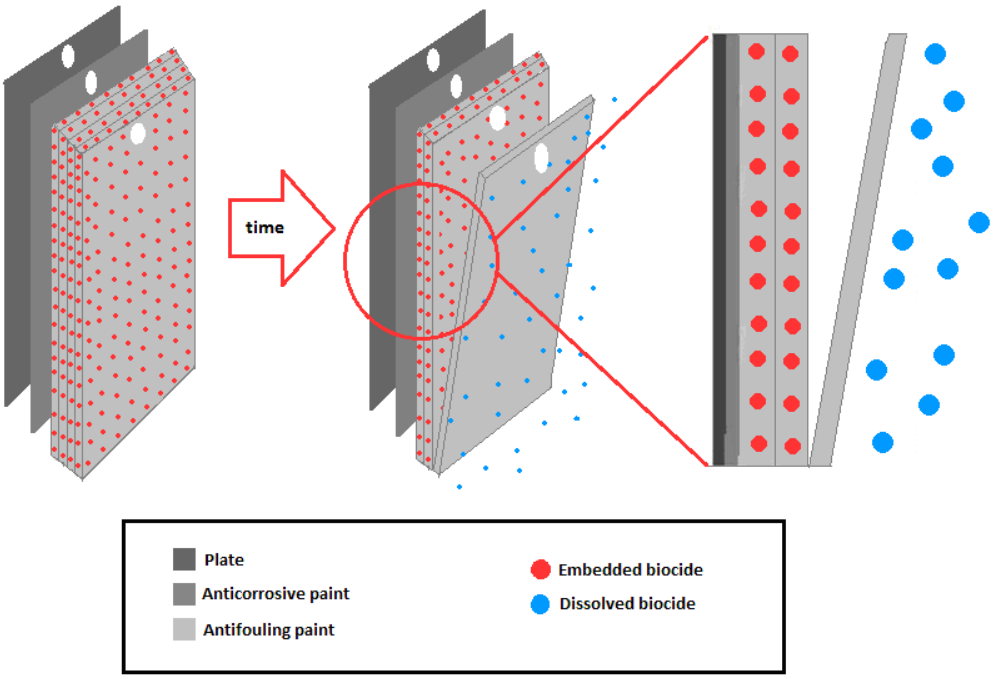


Figure 1.8 Biocide release mechanism of the self-polishing copolymer type antifouling paints (Illustrated by Gamze TOPÇAM).

Compared to soluble type antifouling paints, binder of insoluble type antifouling paint is not soluble in seawater and surface of insoluble type antifouling paint does not contain fresh biocide (Figure 1.9). Although the surface of paint is smooth, after releasing of biocides from paint surface, some pores are formed with in the binder and it is easy to attach these pores for fouling organisms.

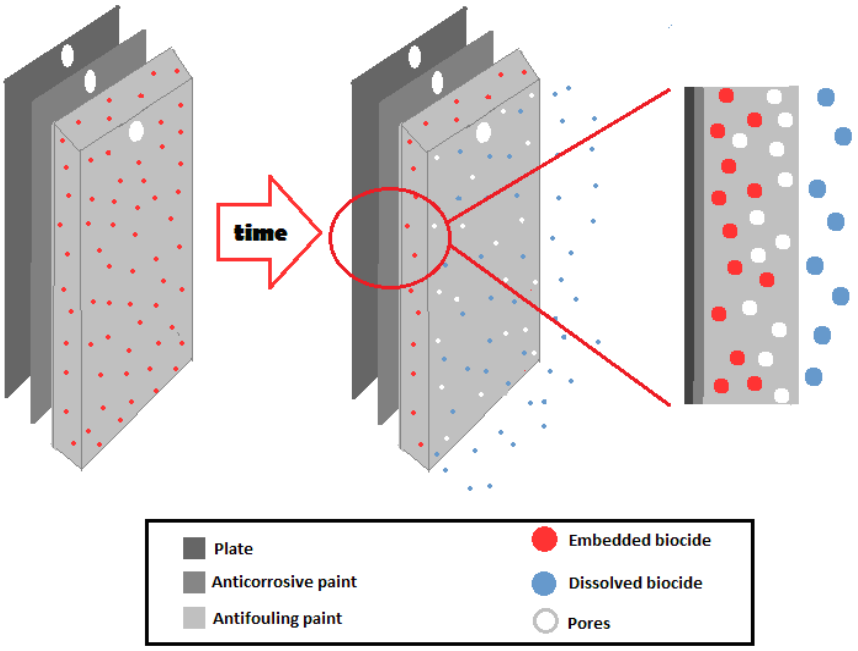


Figure 1.9 Biocide release mechanism of the insoluble type antifouling paints (Illustrated by Gamze TOPÇAM).

1.4 The Harmful Effects of Currently Used Biocides in Antifouling Paints

The binder of self-polishing copolymer type paints is acrylic copolymers (mainly methyl methacrylate derivatives) esterified with pendant groups such as organotin, organosilyl and organotitanium moieties. Tributyloxide (TBTO), tributyltin (TBT) fluoride, triphenyltin (TPT) fluoride, TBT chloride, TBT methacrylate copolymer, etc. are the organotin compounds used as antifoulant. They are very successful in preventing a wide range of fouling species (Omae, 2003).

Although TBT based paints prevent the fouling successfully, these type paints have harmful compounds in the formulations. These type paints have genotoxic and cytotoxic effects on non-target marine organisms such as, mussels, polychaetes, molluscs, fishes, etc. (David & Haydn, 1986; Hagger, Giddings, Soloman, & Balcomb 2002; Gibbs, Pascoe, & Bryan, 1991).

Because of their harmful effects, production of TBT based antifouling paints were banned in 2003 by International Maritime Organization (IMO). IMO also banned the application of TBT based antifouling paints in 2008 on vessels under 25 m. After banning of TBT, the antifouling paint manufacturers have started to use alternative biocides called “booster biocides” to increase the antifouling performances of antifouling paints.

The currently used booster biocides are;

- chlorothalonil (2,4,5,6-tetrachloroisophthalonitrile),
- dichlofluanid (N'-dimethyl-N-phenylsulphamide),
- diuron [3-(3,4-dichlorophenyl)-1,1-dimethylurea],
- irgarol 1051 (2-methylthio-4-t-butylamino-6-cyclopropylamino-s-triazine),
- zinc pyrithione (zinc complex of 2-mercaptopyridine-1-oxide),
- thiram [bis(dimethylthiocarbamoyl)disulphide],
- ziram [zinc bis(dimethyl thiocarbamate)],
- naneb (manganese ethylene bisdithiocarbamate),
- zineb (zinc ethylene bisdithiocarbamate),
- kathon 5287 (4,5-dichloro-2-n-octyl-4-isothiazolin-3-one) etc. (Voulvoulis et al, 1999).

Molecule structures of some of these booster biocides are given in the Figure 1.10. These booster biocides are generally herbicides or pesticides and they responsible the inhibition of primary growth of the fouling organisms (Faÿ et al., 2010). Diuron and irgarol 1051 are herbicides and the other biocides are fungicides which are used in agricultural applications (Voulvoulis et al, 1999).

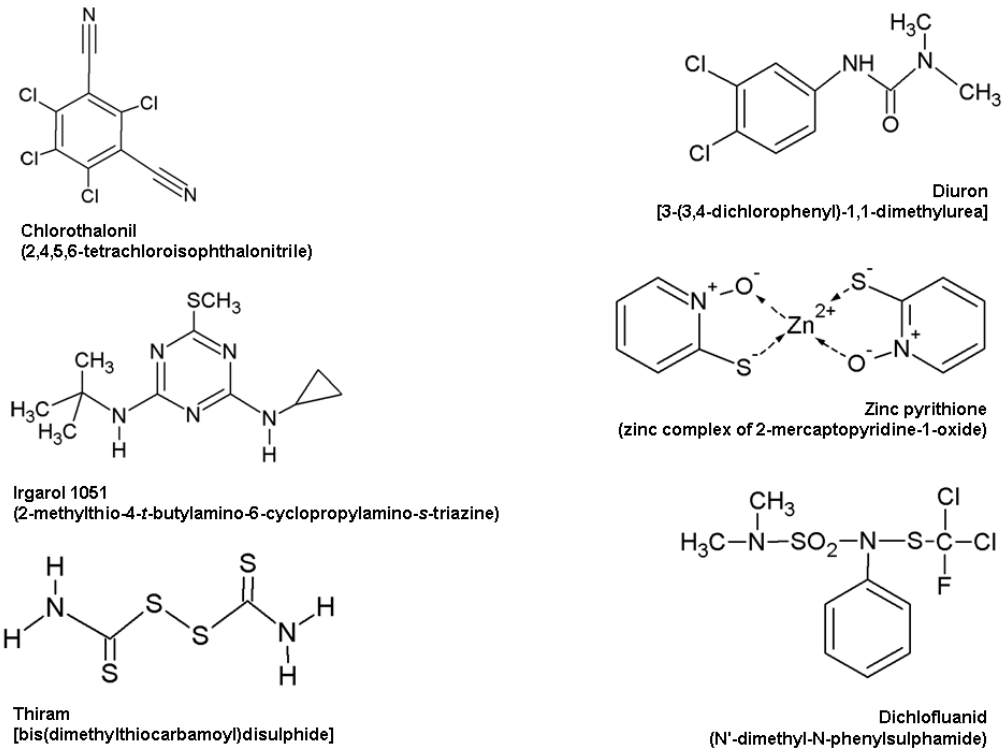


Figure 1.10 The molecule structures of the widely used booster biocides in commercial antifouling paints.

Diuron and irgarol are most popular booster biocides in the antifouling paint industry. However, the studies in last decades show that concentrations of these biocides or their degradation products in aqueous estuarines, marinas, ports, seawaters and sediments are very high (Chesworth, Donkin, & Brown, 2004; Haynes, Muller, & Carter, 2000; Readman et al., 1993a; Readman et al., 1993b; Thomas, Fileman, Readman, & Waldock, 2001; Voulvoulis, Scrimshaw, & Lester, 2000). Boxall et al., (2000) found the highest irgarol concentration in sediment samples from marinas as 1 μg/g. Half-lives of irgarol and diuron in seawater were reported as nearly 100 days and 14 days, respectively (Konstantinou & Albanis, 2004). Harmful effects of these antifouling herbicides on the seagrass *Zostera marina* Linnaeus (Chesworth et al 2004), on the phytoplankton species *Thalassiosira weissflogii* (Gronow), *Emiliania huxleyi* (Lohman), *Tetraselmis* F.Stein and *Fibrocapsa japonica* S.Toriumi & H.Takano (Anita et al., 2009) and on the early life history stages of corals *Acropora millepora* (Ehrenberg), *Montipora*

aequituberculata (Bernard) and *Pocillopora damicornis* (Linnaeus) (Negri et al., 2005) were reported.

Due to their harmful effects on the marine ecosystem, U.K. banned to use of irgarol as an antifouling paint ingredient in vessels lower than 25 m and use of diuron in any type of marine paint in November 2002 (Advisory Committee on Pesticides, 2000; Alyuruk & Cavas, 2013). Because of the negative effects of the booster biocides, it is of great importance to develop eco-friendly biocides and so eco-friendly antifouling paints.

1.5 Zostera noltii Hornemann 1832

Seagrasses are flowering plants which live in marine, saline ecosystem and Posidoniaceae, Zosteraceae, Hydrocharitaceae and Cymodoceaceae are member of Alismatales order. Zosteraceae family was found in temperate and subtropical coastal waters and this family includes two genera as *Phyllospadix* W.J.Hooker and *Zostera* Linnaeus (Figure 1.11).

Regnum: Plantae
Phylum: Tracheophyta
Subphylum: Euphyllophytina
Infraphylum: Spermatophytae
Superclassis: Angiospermae
Classis: Monocots
Ordo: Alismatales
Familia: Zosteraceae
Genus: Zostera
Species: *Zostera asiatica*, Miki
Zostera caespitosa, Miki
Zostera capensis, Setchell
Zostera capricorni, Ascherson
Zostera caulescens, Miki
Zostera chilensis, (J.Kuo) S.W.L.Jacobs & D.H.Les
Zostera japonica, Ascherson & Graebner
Zostera marina, Linnaeus
Zostera mucronata, den Hartog
Zostera muelleri, Irmisch ex Ascherson
Zostera nigricaulis, (J.Kuo) S.W.L.Jacobs & D.H.Les
Zostera noltei, Hornemann
Zostera novazelandica, Setchell
Zostera polychlamys, (J.Kuo) S.W.L.Jacobs & D.H.Les
Zostera tasmanica, Martens ex Ascherson

Figure 1.11 Taxonomy of *Zostera noltii* (from Taxonomy Browser: Algeabase).

There are fifteen different species in Genus *Zostera*. *Zostera noltii* Hornemann 1832 (here after *Z. noltii,* International Code of Nomenclature) is one of these species (Figure 1.12). *Nanozostera noltii* (Hornemann) Tomlinson & Posluszny is the homotypic synonym and *Zostera nana* Roth is the heterotypic synonym of *Z. noltii* (common name dwarf eelgrass).



Figure 1.12 *Z. noltii* Hornemann 1832 (Photo: Gamze TOPCAM).

Z. noltii has 2-4 leaves per branch and leaf sheath (1.25-6 cm) is wider than the leaf blade (0.75-1.5 mm). The leaf blades are 3-30 cm long and the leaf apices can become notched (emarginated) in mature leaves slightly (Figure 1.9). Approximate vein number of this species is 3 and they distributed parallel. Morphological variations in *Z. noltii* like other *Zostera* sp. may occurs dependent on some parameters such as plant age, location and tidal zone (Phillips & Menez, 1988).

Since the morphology of *Z. noltii* is close to *Z. marina*, these similarities cause problematic cases in systematic studies. Size of *Z. noltii* is smaller than *Z. marina*. Their colors and leave shapes are also different. The leaves of *Z. noltii* are dull grey-green whereas the *Z. marina* has shiny green leaves. Despite of *Z. noltii* has very narrow leaves with a notch in the tip (emarginated); *Z. marina* has leaves with rounded tips (Figure 1.13).



Figure 1.13 The apex of the leave of *Z. marina* (rounded) and *Z. noltii* (emarginate).

Z. noltii is widely distributed seagrasses within the coastal zones from the southern coasts of Norway to the Mediterranean Sea, the Black Sea, the Canary Islands, with the southern limit on the Mauritanian coast (Auby & Labourg, 1996; Milchakova, 1999; Philippart, 1995; Valle, Borja, Chust, Galparsoro, & Garmendia, 2011; Vermaat et al., 1993). *Z. noltii* forms with *Cymodocea nodosa* (Ucria) Ascherson, *Posidonia oceanica* (Linnaeus) Delile and *Zostera marina* Linnaeus in eastern Mediterranean country, in Greece, Syria and Egypt (Green & Short, 2003).

In the eastern Mediterranean, most seagrass beds are belong to one seagrass species only but *Z. noltii* often forms with *Cymodocea nodosa* (Ucria) Ascherson (Marbà, Cebrian, Enriquez, & Duarte, 1996).

Secondary metabolites are responsible for the protection of plants from pathogenic fungi and herbivorous arthropods. Seagrasses have also phenolic compounds in their leaves and they use these compounds to defense themselves against the marine microorganisms. These compounds play a role as antimicrobial agents in plants and protect the seagrasses from ultraviolet radiation (Grignon-Dubois, Rezzonico, & Alcoverro (2012). *Z. noltii* has different phenolic compounds such as caffeic acid, rosmarinic acid, p-coumaric acid and zosteric acid (Figure 1.12). Chemical structure of zosteric acid was given in Figure 1.14.

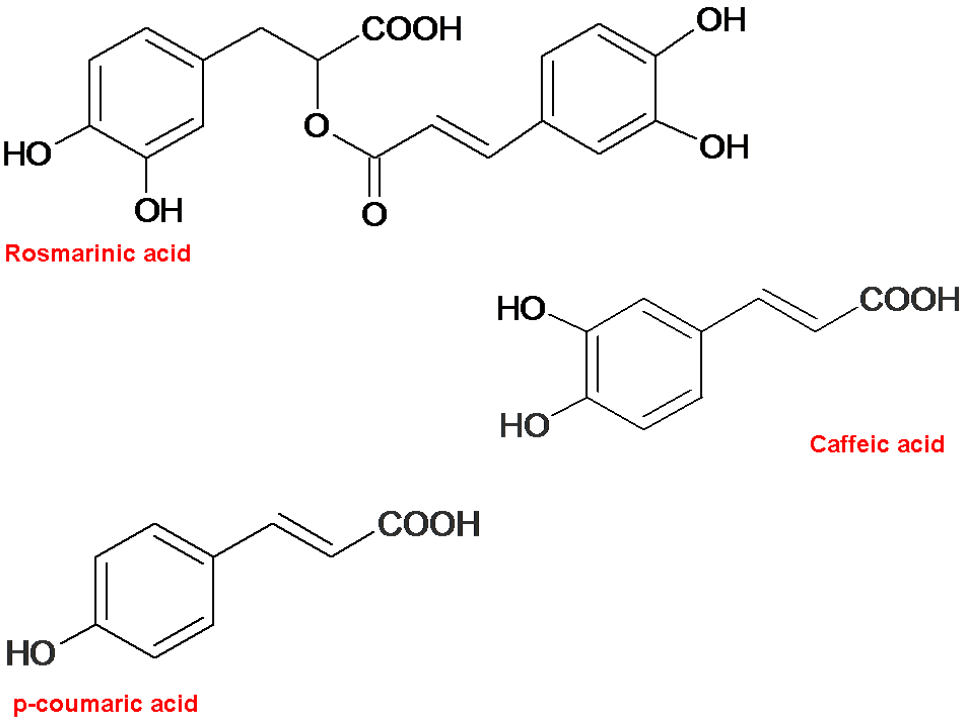


Figure 1.14 The chemical structures of rosmarinic, caffeic and p-coumaric acid.

Grignon-Dubois, et al., (2012) found three phenolic compounds in *Z. noltii* extract collected from four different region (French and Spanish Coast: Bay of Cadiz, Sa Nitja Bay, Alfacs Bay, Arcachon lagoon) and determined the level of these compounds through HPLC (Grignon-Dubois et al., 2012). Rosmarinic acid is an important phenolic compound because of its antibacterial, antioxidant, anti-inflammatory, anticarcinogenic, anti-allergenic activities and there are a lot of application area in pharmaceutical, cosmetic and food industries (Achamlale, Rezzonico, & Grignon-Dubois, 2009a). Isolation and HPLC quantification of rosmarinic acid in *Z. noltii* detritus from Arcachon lagoon was studied by Achamlale et al., (2009a).

Caffeic acid is well known and widely studied compound in the literature. Scientists reported its hepatoprotective effects against t-BHP-induced oxidative liver damage (Yang, Hong, Lee, Kim, & Lee, 2013), suppression of UV-B induced skin carcinogenesis (Kang et al, 2009), suppression of COX-2 expression (Kang et al, 2009), antioxidant activity (Gulcin, 2006), anti-hepatitis B virus activity (Wang et al, 2009), peripheral analgesic effect in mice and rats (Mehrotra, Shanbhag,

Chamallamudi, Singh, & Mudgal, 2011), inhibition of cancer cell metastasis (Hwang et al, 2006), anti-inflammatory and anti-coagulatory activity (Chao, Hsu, & Yin, 2009). Seasonal caffeic acid level in *Z. noltii* detritus from Turkish coastline was determined by our research group because of its vital importance. The study has been accepted for presentation in 40th CIESM Congress, Marseille, France under the title of "Determination of caffeic acid in *Zostera noltii* from Turkish Coastlines by HPLC" in 28 October - 1 November 2013.

Seagrass *Z. noltii* also have an important antifouling compound called as zosteric acid (hereafter ZA) (Achamlale et al., 2009b). Seasonal determination of ZA content in *Zostera* detritus from Arcachon Lagoon, France was studied and the detritus were proposed as a zosteric acid source by Achamlale et al., (2009b).

1.6 Zosteric Acid: Biosynthesis and Antifouling Properties

Seagrasses are rich source of phenolic substances, including phenolic acids, sulfated phenolic acids, flavones, condensed tannins, and also lignins. But some metabolites are found in single seagrass families or species, such as zosteric acid (Papenbrock, 2012).

p-(sulphooxy) cinnamic acid is the chemical name of zosteric acid (hereafter ZA). It contains a sulfate phenolic ester group and a carboxylic acid group in its structure (Figure 1.13).

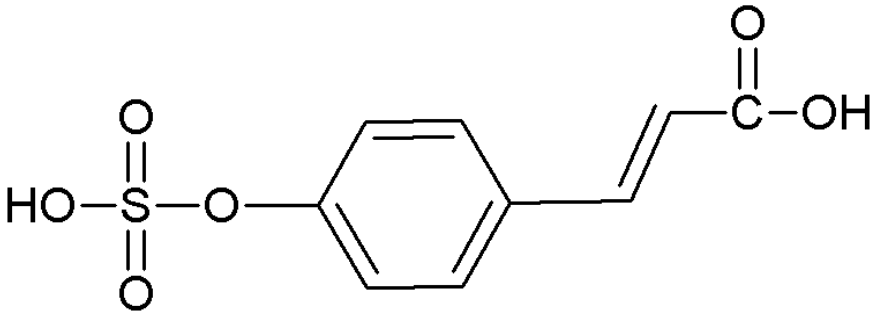


Figure 1.15 The chemical structure of ZA.

According to scientific literature, no paper is existed on the biosynthesis of ZA in *Zostera* sp. (Papenbrock, 2012). On the other hand there has been a patent (Alberte & Smith, 2005) where a possible biosynthesis mechanism is explained. According to Alberte & Smith, 2005 the biosynthesis of ZA by *Zostera* sp. starts with L-phenylalanine. L-phenylalanine is converted into t-cinnamic acid by the enzyme phenylalanine ammonia lyase (PAL). In the first step, PAL promotes removal of NH_3 from L-phenyalanine to yield t-cinnamic acid. The second step is the oxidation of t-cinnamic acid to p-hydroxy cinnamic acid, catalyzed by cinnamic acid-4-hydroxylase (C4H). The last step of this reaction is substation of OH with SO_3 by enzyme sulfoxytransferase (SULT) to yield p-sulfoxy cinnamic acid (Figure 1.14).

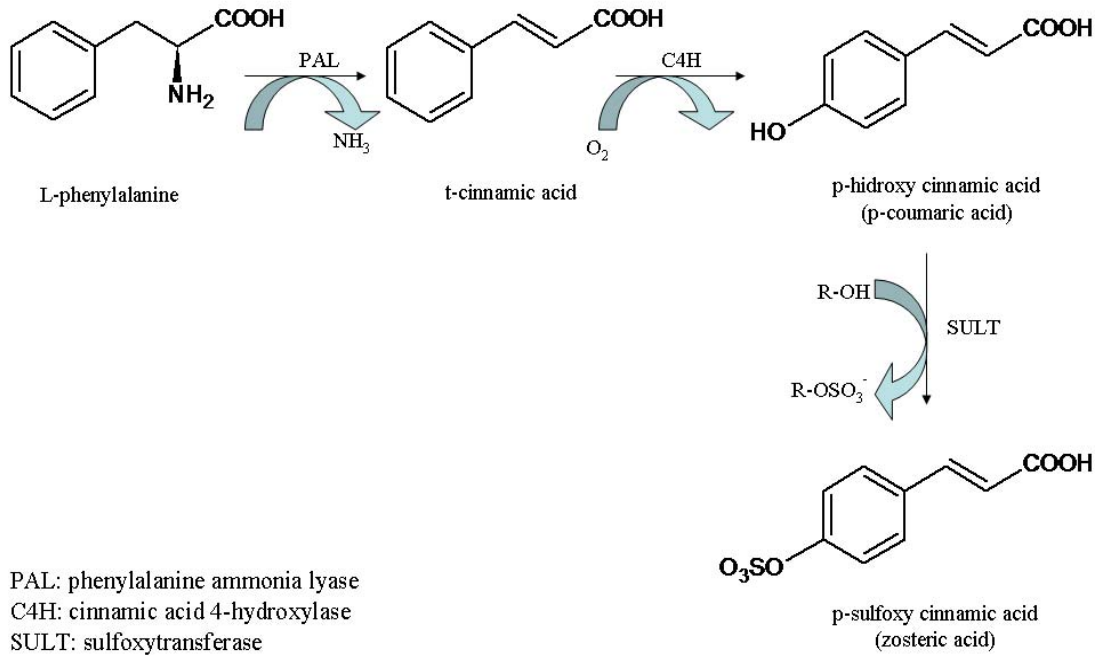


Figure 1.16 The metabolic pathway of p-sulfoxy cinnamic acid (Alberte & Smith, 2005).

The anti-adhesive compound ZA is soluble in water. Since free molecules directly interact with the organisms in marine environment, ZA easily prevent the attachment of fouling organisms (Sundberg, Vasishtha, Zimmerman, & Smith, 1997; Barrios, Xu, Cutright, & Newby, 2005). Barrios et al., 2005 evaluated antifouling performance of ZA by using fresh water bacteria. They used the silicone coating to

decrease the release rate of ZA. They reported that not only incorporated ZA but also ZA prevent the anti-bacterial attachment. Rees et al., 2008 studied on the antiviral properties of ZA against dengue virus and evaluated the toxicity to monkey kidney cell. They showed that ZA inhibited the dengue virus. 50% inhibitory concentration was 2mM (Rees et al, 2008). Villa et al., 2010 synthesized large amount of ZA by using p-coumaric acid and sulfur trioxide pyridine complex (Figure 1.17) and studied on the biofilm formation preventative ability of ZA. They found that ZA prevent the bacterial and fungal biofilm formation by 90% and 57%, respectively.

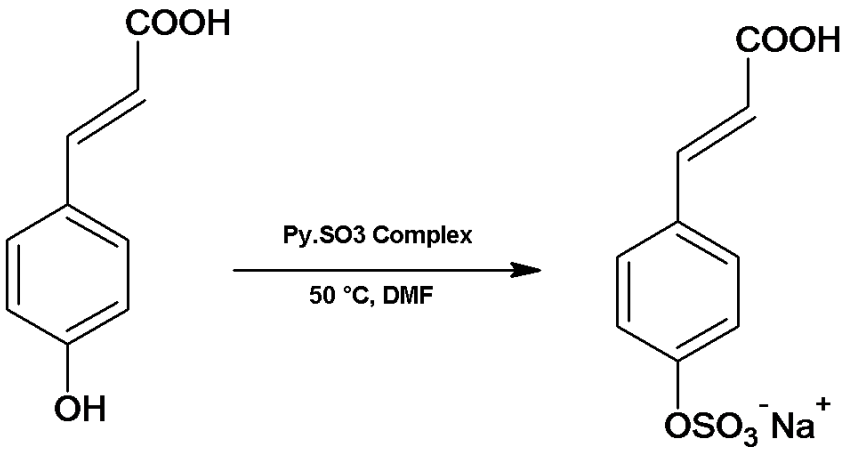


Figure 1.17 Synthesis of sodium zosterate by sulfonation of p-coumaric acid with Py•SO3 complex in DMF.

1.7 The Aim of the Thesis

This thesis aimed at determining the ZA level seasonally in *Z. noltii* detritus from Turkish coastlines and investigated the possibility of large scale ZA isolation from *Z. noltii* detritus for industrial applications. ZA was also synthesized in laboratory and the synthesized ZA was compared with the natural ZA in terms of yield, cost and antifouling activity. Antifouling performances of ZA containing rosin based antifouling paints were evaluated with a field test in marine environment. Antifouling performance of ZA was also compared with the current booster biocides such as diuron and irgarol in prepared antifouling paints. The main aim is to propose a natural agent, ZA, from *Z. noltii* detritus as a new eco-friendly biocide.

CHAPTER TWO

MATERIALS AND METHODS

2.1 Materials and Methods

All the solvents used in HPLC analyses were HPLC grade. Methanol with 0.1% trifloroacetic acid (TFA) and water with 0.1 % TFA as HPLC mobile phase, HPLC grade methanol for seagrass extraction and technical xylene as paint solvent were purchased from Sigma-Aldrich. The HPLC instrument used in the determination of compounds was Shimadzu Prominence LC-20A equipped with a DGU-20A5 solvent degasser, SPD-20A UV/VIS detector and CTO-10ASUP column oven. Inertsil C8 column (GL Sciences) (5 µm, 250 x 4.6 mm) and semi-preparative C8 column (10 µm, (250 x 10 mm)) were used. Analytical grade water was obtained using a Millipore MilliQ water purification system. The authentic sample of ZA potassium salt was kindly provided by Prof. Dr. George Pohnert and Mrs.Caroline Kurth from Friedrich-Schiller-University, Jena-Germany. Elementary Analysis was performed on a Vario EL III (Elementaranalysensysteme, Hanau), NMR on a Bruker Advance System (Bruker) for characterization of potassium zosterate. Oxford, NMR AS 400 system was used to obtain ^{1}H NMR spectrums of sodium zosterate.

2.2 Collection of the Z. noltii Detritus

The dead leaves of *Z. noltii* detritus were collected monthly from October 2011 to September 2012 from three different regions. The sampling areas were Urla-Turkey (Figure 2.1), Dikili-Turkey (Figure 2.2) and Erdek-Turkey (Figure 2.3). The dead leaves were washed with fresh water to remove salt, sand and epiphytes. Then, they were dried at room temperature.



Figure 2.1 Google Earth image of Urla, İzmir coastline where *Z. noltii* samples were collected (38° 19' 48.49" N, 26° 39' 07.99" E).



Figure 2.2 Google Earth image of Dikili, İzmir coastline where *Z. noltii* samples were collected (39° 07' 10.50" N, 26° 51' 12.61" E).



Figure 2.3 Google Earth image of Erdek, Balıkesir coastline where *Z. noltii* samples were collected (40° 24' 33.41" N, 27° 46' 59.42" E).

Turkish coastlines seasonally expose to sea tides because of meteorological and climatical forces or other reasons (Alpar et al., 2000). Many marine organisms were affected from sea tide. In winter 2012, a sea tide was observed over 1 km along the Dikili coastline with a distance of about 75 m from the coast. The affected and decomposed species and their economical values based on published reports were also studied. The results were published in *Hacettepe Journal of Biology and Chemistry*. Moreover, relative sea levels also affect the beaches. In Dikili coastlines landslide was also observed. As well as tide event, the collected seagrasess by authorities in these coasts cause the landslide.

2.3 Preparation of the Extracts

The dried detritus samples were powdered with coffee grinder for extraction. 20 g powdered samples were extracted with methanol by using soxhlet apparatus for 8 h (Figure 2.4). Before injection of the samples to HPLC, the extracts were filtered with filter paper and 0.45 µm syringe filter to remove impurities.

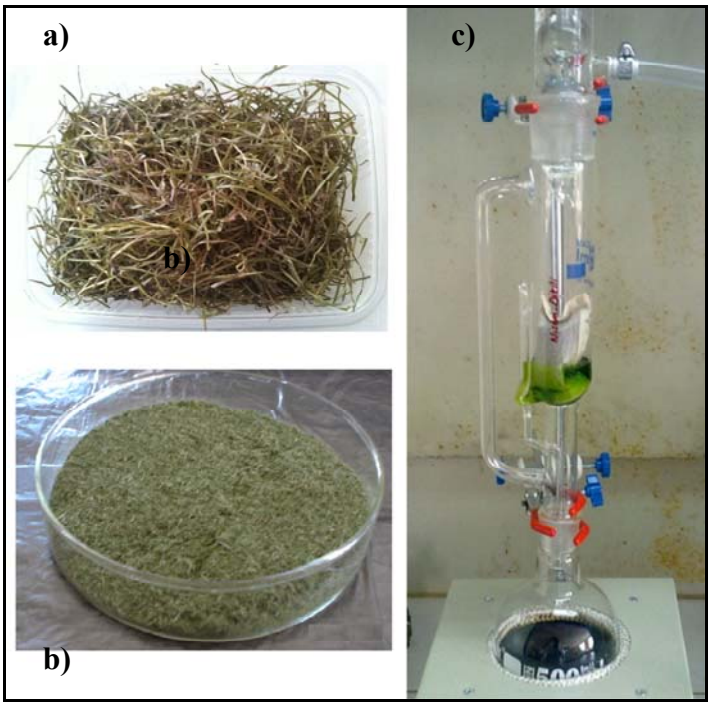


Figure 2.4 a) The dried *Z. noltii* sample, b) powdered *Z. noltii* sample and c) extraction apparatus.

2.4 Synthesis of the Sodium Zosterate

ZA sodium salt was synthesized based on the method described by Villa et al. (2010) in our laboratory. Briefly, 16.46 g of trans-4-hydroxycinnamic acid was dissolved in 30 mL of anhydrous N, N-dimethylformamide. Then, 25.68 g of sulfur trioxide pyridine complex (Py•SO_3) was added to reaction vessel and stirred at 50 °C for 2 h in water bath. In order to maintain a better agitation, reaction media was diluted with some water. After the reaction, reaction mixture was allowed to cool to room temperature and 30% NaOH was added dropwise to reaction media until the pH 7. The precipitated white solid was filtered and remaining solution was extracted three times with 20 mL of dichloromethane (CH_2Cl_2). Methanol was added to clear solution by dropwise causing the precipitation of a white solid that was removed with first filtration. The white precipitate was removed again by filtration and filtrate was evaporated to dryness. Finally, white sodium zosterate crystals were obtained after evaporation. ^{1}H-NMR and IR were used to characterize the synthesized ZA.

2.5 Synthesis of the Potassium Zosterate

Potassium zosterate was synthesized according to the Villa et al. (2010) by Prof. Dr. George Pohnert and Mrs.Caroline Kurth from Friedrich-Schiller-University in Jena, Germany.

2.6 Optimization of the HPLC and Seasonal Zosteric Acid Determination

Achamlale et al., (2009b) reported that they used p-coumaric acid as HPLC standard to determine the ZA level in *Z. noltii* extracts. In the present study, synthesized ZA salt was used as standard from 1 mg/L to 30 mg/L. The samples were analyzed with the gradient elution system with 1 mL/min flow rate and the column temperature was 40 °C. Injection volume was 20 µL. Peaks were obtained at 280 nm with UV detector.

The compounds were separated with the mobile phase of 0.1% (v/v) TFA in water (A) and 0.1% (v/v) TFA in methanol (B) (0 min, 1% B; 60 min, 99% B), and also water (A) and methanol (B) (0 min, 1% B; 60 min, 99% B) to observe the effects of trifloro acetic acid (TFA) in mobile phase. The analysis time was also optimized and it was reduced 20 min to reduce the solvent consumption.

Seasonal ZA determinations in the *Z. noltii* extracts were carried out with optimized method. The extracts were filtered with 0.45 µm syringe filter before injection and analysis. The determination of ZA levels in the samples of *Z. noltii* extracts was carried out by evaluating the peak area at 280 nm and using the calibration curve of ZA.

The ZA contents in seasonal samples were calculated as µg ZA/g DW and an example calculation was given in Equation 1 for the September-2012-Urla.

Example: 20 g dried powder of *Z. noltii* was extracted with 200 mL methanol, but the final volume of the extract was 190 mL because of evaporation of methanol. The

extract was diluted 5 fold before injection. The peak area measurements were carried out by evaluating the peak area at 280 nm. ZA content of the extract was calculated by using calibration curve of standard ZAK and correlation factor, 1.156, between ZA and ZAK.

Calculation: Peak areas belong to five injections were: 234772, 233894, 236019, 241968, and 239604.

$$y = 59556x \Rightarrow x = \frac{y}{59556} \quad (1)$$

where y was peak area of the ZAK and x was concentration of the ZAK.

$$\begin{aligned} y_1 = 234772 &\Rightarrow x_1 = 3.94\ \mu g/ml \\ y_2 = 233894 &\Rightarrow x_2 = 3.93\ \mu g/ml \\ y_3 = 236019 &\Rightarrow x_3 = 3.96\ \mu g/ml \\ y_4 = 241968 &\Rightarrow x_4 = 4.06\ \mu g/ml \\ y_5 = 239604 &\Rightarrow x_5 = 4.02\ \mu g/ml \end{aligned}$$

According to peak area of the first injection, 234772, ZA content in the *Z. noltii* sample was stoichiometrically-calculated as follow;

$$\mu g\ ZA \big/ g\ DW = \frac{3.94 \mu g\ ZAK}{1\ ml\ MeOH} \times \frac{190\ ml\ MeOH}{20\ g\ DW} \times \frac{1.156\ ZA}{1\ ZAK} \times 5 \quad (2)$$

where ZA, ZAK and g DW were zosteric acid, zosteric acid potassium salt and gram dry weight of *Z. noltii*.

Limit of detection (LOD) was also calculated by determination of solvent in same retention time with ZA (12.2 ± 0.0). Standard deviation of peak areas of the solvent was calculated for detection limit and used in below equation.

$$LOD = \frac{3\ x\ STD}{S} \quad (3)$$

where *STD* is standard deviation and *S* is the slope of calibration curve (Figure 3.8).

2.7 Isolation of Zosteric Acid from Z. Noltii Extracts

ZA was isolated from sample extracts in order to determine the yield of isolation. Fraction collector and semi-preparative column were used in HPLC system (Figure 2.5). The analytical C8 column (5 µm, (250 x 4.6 mm)) was changed with semi-preparative column (10 µm, (250 x 10 mm)) and the injection volume was increased from 20 µL to 2 mL. Retention time of ZA was optimized by increasing of flow rate from 1 mL/min to 4 mL/min. ZA was collected in the mobile phase and stored at 4°C.

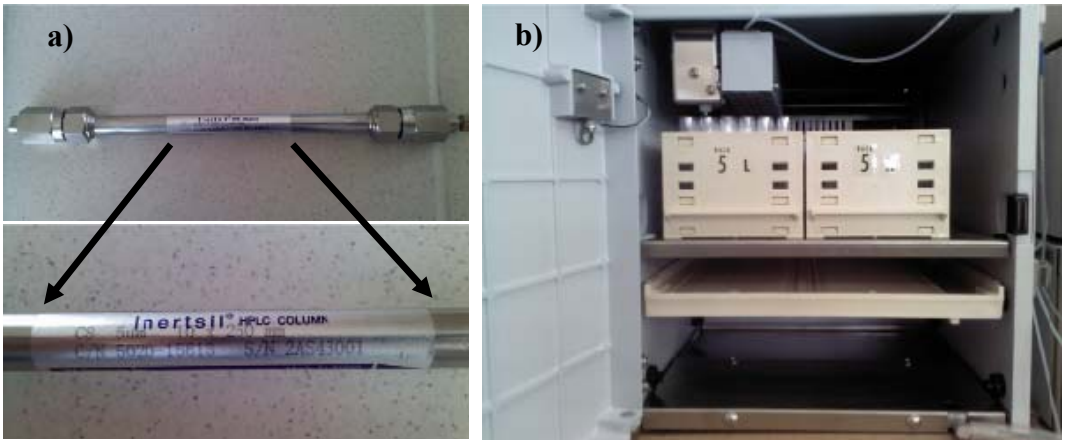


Figure 2.5 Isolation system of HPLC a) semi-preparative column b) fraction collector.

2.8 The Preparation of the Antifouling Paints

The rosin based antifouling paints were prepared with *Z. noltii* powder, *Z. noltii* extract, ZA, diuron, irgarol 1051, mixture of diuron and irgarol and econea. The antifouling effects of ZA were compared with the other biocide. The biocide free paint was prepared as negative control group and commercial antifouling paint was used as positive control. The paints were prepared as follows; 23% (w/w) rosin was dissolved in xylene. Then, sunflower oil, ZnO, Cu_2O, biocide, $CaCO_3$, and Lutanol M40 were incorporated at weight ratios as given in Table 2.1. The steel plates (7x12

cm) were cleaned with sandpaper and the metal plates were coated with primer coating in order to prevent the corrosion. The model paints were applied onto the primer coated plates (Figure 2.6) and allowed to dry over a week under room temperature.

Table 2.1 Antifouling paint compositions prepared for field test.

Paint Component	**Percent by weight (w/w %)**	
Rosin	23	26
Xylene	36	39
Sunflower Oil	8	8
ZnO	12	12
Cu_2O	5	5
Biocide	6	-
$CaCO_3$	2	2
Lutanol M40	8	8

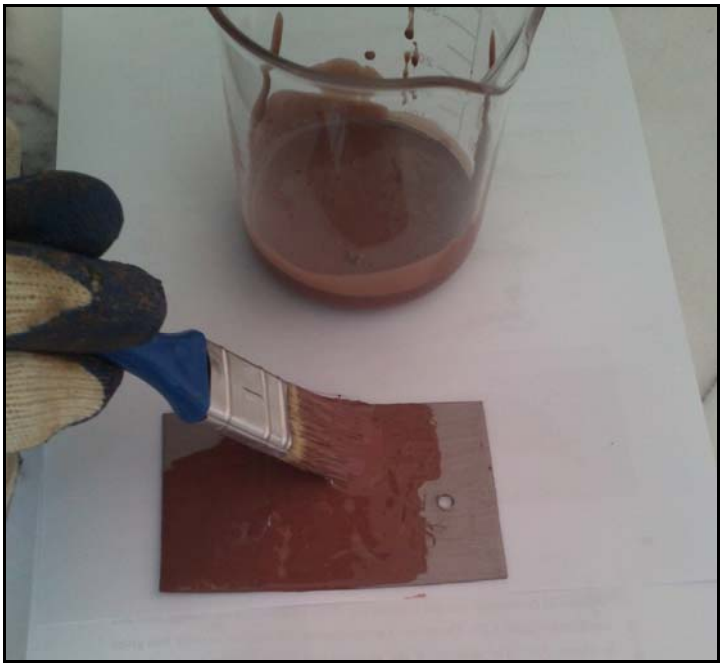


Figure 2.6 Application of prepared antifouling paint.

2.9 The Field Tests

The antifouling performances of the ZA, *Z. noltii* powder, *Z. noltii* extract, commercial biocides (diuron, irgarol and econea), and commercial antifouling paint were evaluated in a seawater immersion test for a period of five months from January

28 to July 3, 2013 at Levent Marina, İzmir, Turkey (Figure 2.7). The paints were tested for a period of 156 days by comparing with paint free and rosin-based biocide free paints as references. The painted steel panels were immersed into seawater at a depth of 50 cm for evaluation of the antifouling performance (Figure 2.8).



Figure 2.7 Levent Marina, İzmir, Turkey, (38° 24' 21.79" N, 27° 04' 08.91" E).



Figure 2.8 Immersion test system with painted plates a) before immersion and b) after 144 days of immersion.

According to the literature, there are several fouling criteria to evaluate the surfaces of antifouling paint test panels according to abundance of settled micro and macro fouling organisms (Arimura, Hiyoshi, Nakamura & Tsuboi, 2004; Karabay, 2011; Alyuruk, 2012). The fouling criteria used in this study constitute five fouling levels and these criteria were given in below,

Level 1. There are no fouling organisms on the surface.

Level 2. Microfilm layer formation is present on the surface.

Level 3. Microfilm layer is present and macrofouling is at the beginning state.

Level 4. Micro- and macrofouling organisms are present on the surface.

Level 5. The surface is heavily fouled (>50%) by micro- and macrofouling organisms.

2.10 The Microscopic Analysis

The fouling organisms attached on paint surface were investigated under optical microscope (Olympus BX51TF, 40x objective lens, zoom 1.00). The samples were taken in methanol at 77^{th} day of immersion.

2.11 The Statistical Tests

For the compound ZA, variability of the amount depends on the site differences was analyzed in Minitab 16. The one-way univariate analysis of variance (ANOVA) following the Tukey's test was applied to the ZA levels obtained from seasonal analysis.

CHAPTER THREE

RESULTS AND DISCUSSION

3.1 The Characterization of the Synthesized Sodium Zosterate

ZA sodium salt was characterized by FT-IR spectroscope and ^{1}H-NMR spectroscope after the synthesis. The results were well in line with the scientific literatures.

There were doublets of doublet peaks in the aromatic region in ^{1}H-NMR spectra of sodium zosterate (Figure 3.1). Since the aromatic hydrogens were symmetric two of the doublet peaks were signs of aromatic hydrogens located at orto and meta positions of aromatic ring. Other doublet peaks were resulted from double bond in the structure of sodium zosterate.

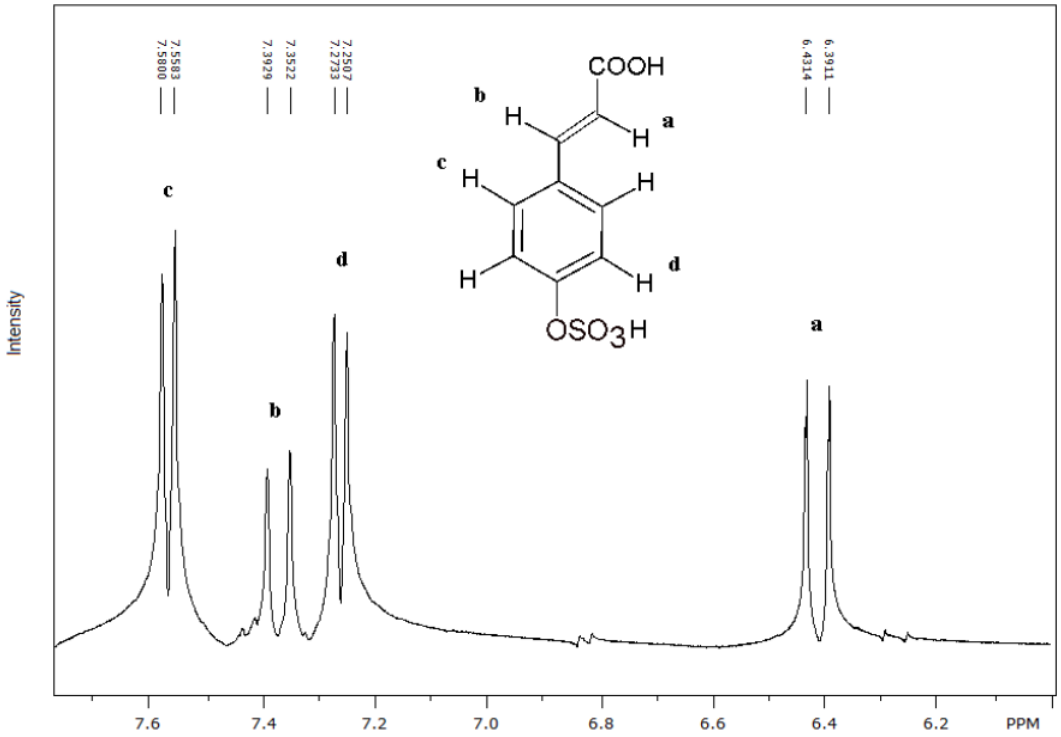


Figure 3.1 ^{1}H-NMR spectra of sodium zosterate.

FT-IR spectra of the sodium zosterate was given in Figure 3.2: O-H stretch of sulphoxy group (3632 cm^{-1}), O-H stretch of carboxyl group (3488 cm^{-1}), aromatic C-H (3036 cm^{-1}), C=O stretch of carboxyl group (1640 cm^{-1}), olefinic C=C (1556 cm^{-1}) and p-substituted aromatic out of plane C-H bending (852 cm^{-1}).

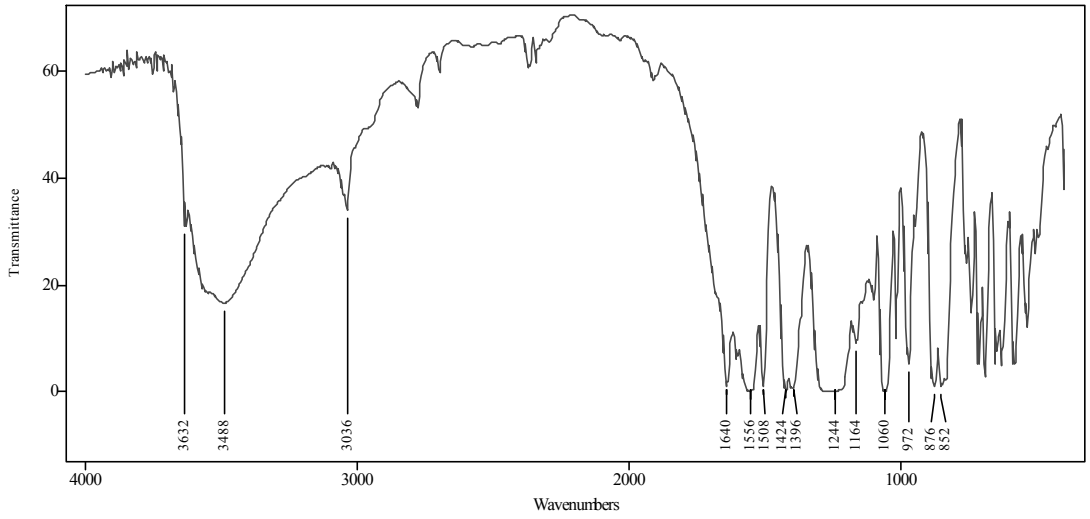


Figure 3.2 FT-IR spectra of sodium zosterate.

3.2 The Characterization of the Synthesized Potassium Zosterate

The synthesized ZA potassium salt was characterized with ^{1}H-, ^{13}C-NMR and elemental analysis at Friedrich-Schiller-University in Jena, Germany. The spectrums were given in Figure 3.3 and Figure 3.4.

The findings were well in line with the published literature (Todd, Zimmerman, Crews & Alberte, 1993; Villa et al., 2010). Found: C: 33.86%, H 1.81%, S 6.35%.

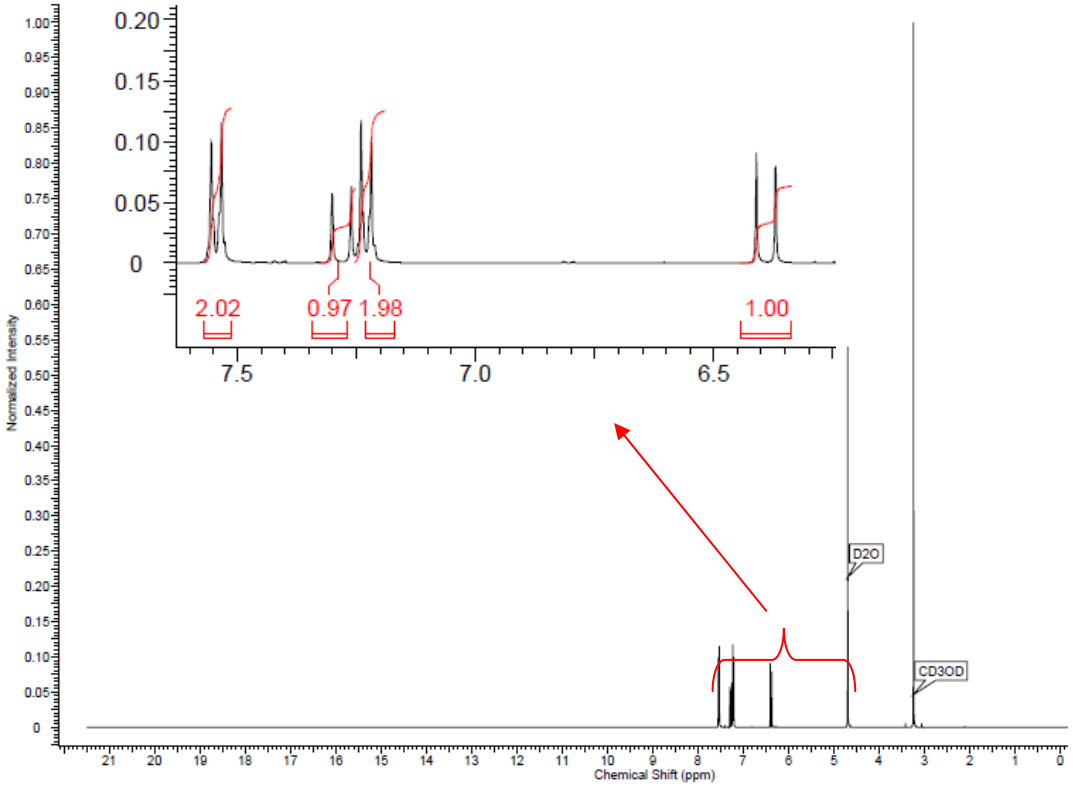


Figure 3.3 [1]H-NMR spectra of potassium zosterate.

[1]H NMR (400MHz, D_2O-CD_3OD (1:1) + 0,6% Formic Acid):

δ 7.54 ppm (2H, *d*, *J* = 8.83 Hz), 7.28 ppm (1H, *d*, *J* = 16.17 Hz), 7.23 ppm (2H, *d*, *J* = 8.54 Hz), 6.39 ppm (1H, *d*, *J* = 16.17 Hz).

[13]C NMR (400MHz, D_2O-CD_3OD (1:1) + 0,6% Formic Acid):

δ 175.56 ppm (1C, C-1), 151.86 ppm (1C, C-7), 139.69 ppm (1C, C-3), 133.17 ppm (1C, C-4), 129.00 ppm (2C, C-5), 124.28 ppm (1C, C-2), 121.74 ppm (2C, C-6).

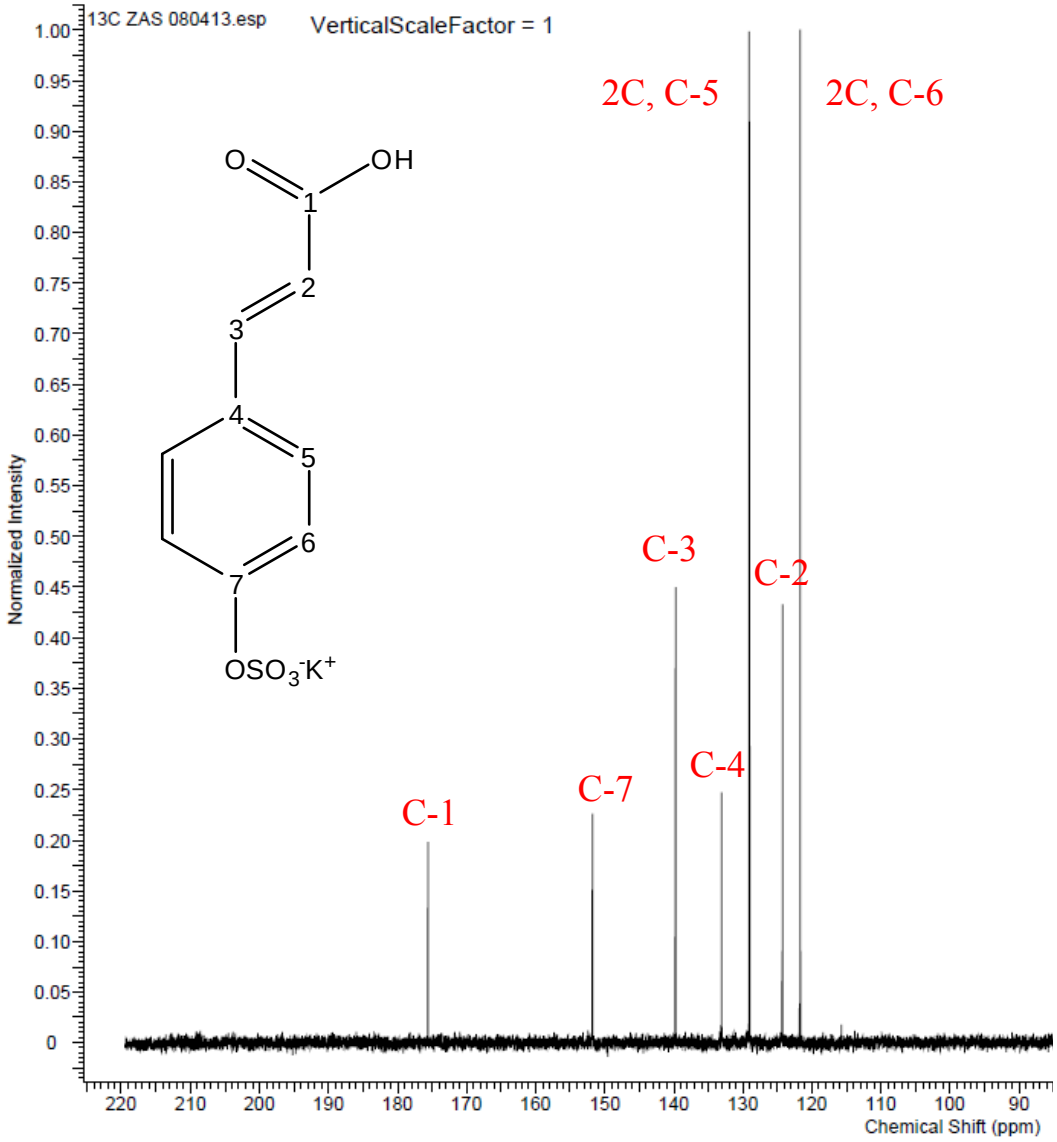


Figure 3.4 ^{13}C-NMR spectra of potassium zosterate.

3.3 The Optimization of the HPLC and Seasonal Zosteric Acid Determination

The HPLC analyses were performed according to the method of Achamlale et al. (2009b) with minor modifications. Two different mobile phases were tried to separate the compounds. At first, ZA sodium salt was separated with the mobile phase of water (A) and methanol (B) (0 min, 1% B; 60 min, 99% B) without TFA, with gradient elution at a flow rate of 1 mL/min. Calibration curve was created for

ZA sodium salt in HPLC grade methanol with six points (5-30 µg/mL). The HPLC chromatogram of 30 µg/mL ZA sodium salt was given in Figure 3.5.

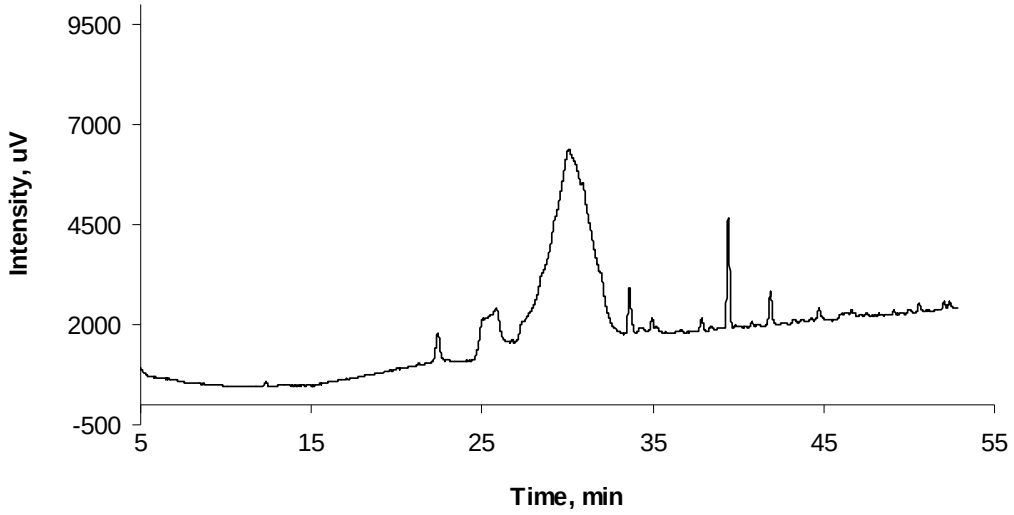


Figure 3.5 The HPLC chromatograms with UV detection (280 nm) of 15 µg/mL ZA sodium salt.

According to the Figure 3.5 the peak shapes obtained with mobile phase without TFA were not gaussian. There are a lot of peaks and it is not clear that which peak belong to ZA. Then, 0.1% (v/v) TFA was added into mobile phase to obtain good separation. The sample was eluted with 0.1% TFA containing mobile phase. The HPLC chromatogram of 15 µg/mL ZA sodium salt was given in Figure 3.6.

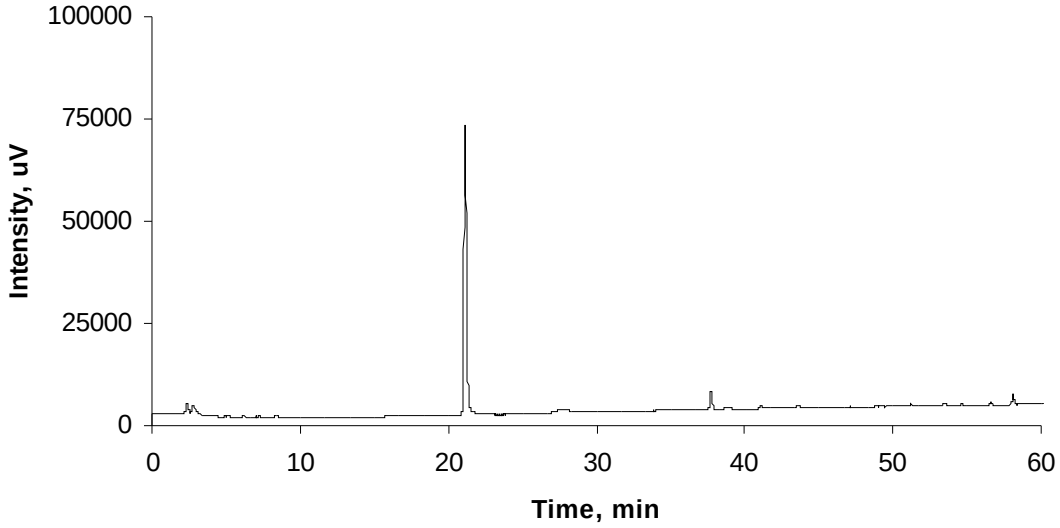


Figure 3.6 The HPLC chromatograms with UV detection (280 nm) of 15 µg/mL ZA sodium salt.

According to the Figure 3.6 mobile phase with TFA had good separation performance compared to the mobile phase without TFA. The peak belong to ZA was clearly obtained. This is also proof that the synthesized ZA is not contain and purities. Since peak was very gaussian, TFA containing methanol and water were used in further analysis. ZA potassium salt was chosen as HPLC standard due to its reliable characterization results.

The analysis time was optimized to avoid loss of time and to reduce the amount of spent solvent. Before optimization, run time was 60 min, stop time 60 min, and post time 65 min. Analysis time was re-set as 20 min for run time, 20 min for stop and 23 min for post time (Figure 3.7). The calibration curve was drawn for ZA potassium salt in this conditions and curve was given in the Figure 3.8. The standard concentration was between 1-30 µg/mL.

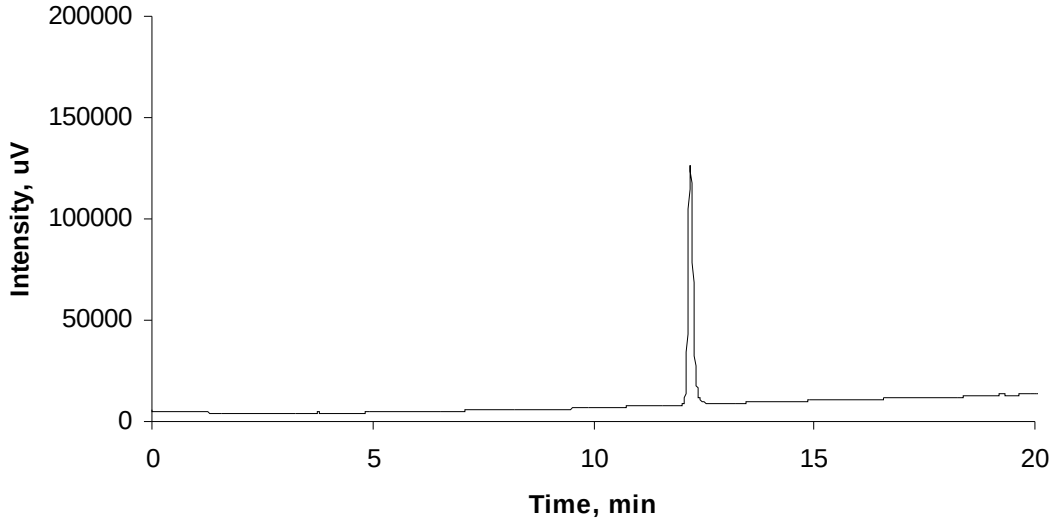


Figure 3.7 The HPLC chromatograms with UV detection (280 nm) of 15 µg/mL ZA potassium salt.

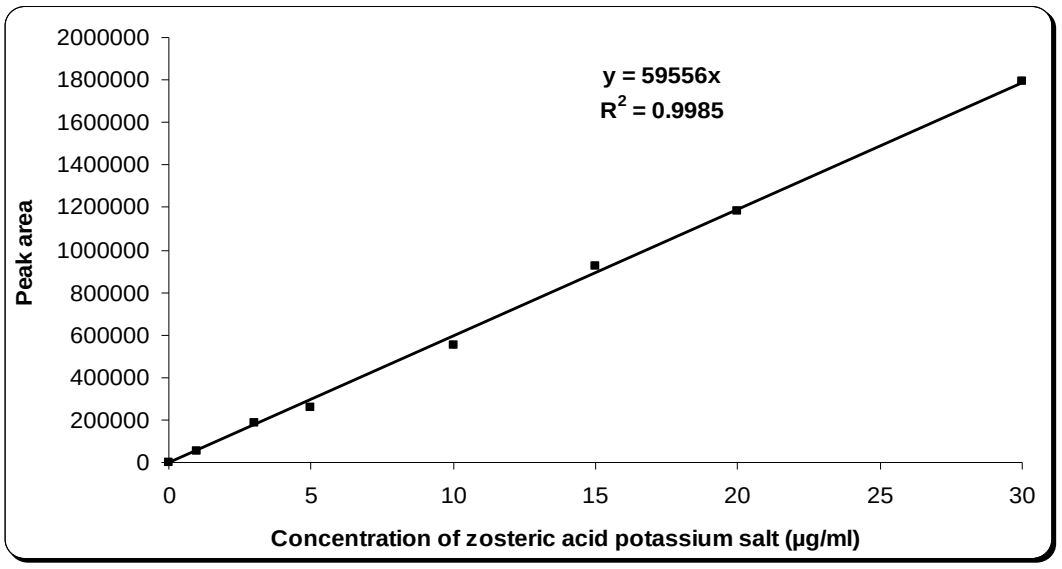


Figure 3.8 Calibration curve for the potassium zosterate.

The regression coefficient and the retention time were found as 0.9985 and 12.0 ± 0.0 for ZA potassium salt, respectively. All peaks belong to ZA salt were symmetrical and gaussian. The peak area of ZA was increased with increasing concentration. The current method was chosen for the determination of ZA level in *Z. noltii* extracts. Before the peak area calculation, the peaks belong to standard ZA and the extracts were superimposed (Figure 3.9).

As shown in the Figure 3.9, the optimized method exhibited a good separation performance. This chromatogram is also proof that the *Z. noltii* sample contains ZA since there is a peak in the chromatogram of *Z. noltii* extract at the same retention time with ZA.

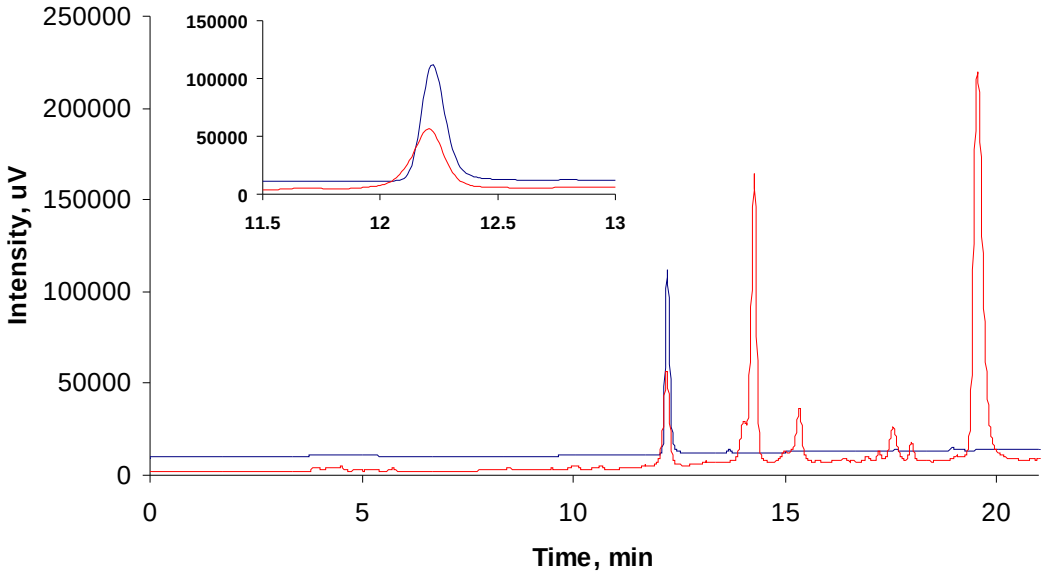


Figure 3.9 The HPLC chromatograms with UV detection (280 nm) of 10 µg/mL ZA potassium salt (blue) and *Z. noltii* extract (red).

HPLC chromatograms of monthly collected samples from Urla, Dikili and Erdek were given between Figure 3.10-Figure 3.37. Although the ZA levels were calculated with the mean peak area of 5 injections, only one chromatogram was given in this thesis. HPLC separation was obtained on a C8 column (5 µm), Inertsil C8 (GL Sciences), (250 x 4.6 mm) and the analytes were eluted using linear gradient with 0.1% TFA (v/v) in water (A) and 0.1% TFA (v/v) in methanol (B) (0 min, 1% B; 20 min 99% B) at a flow rate of 1 mL/min.

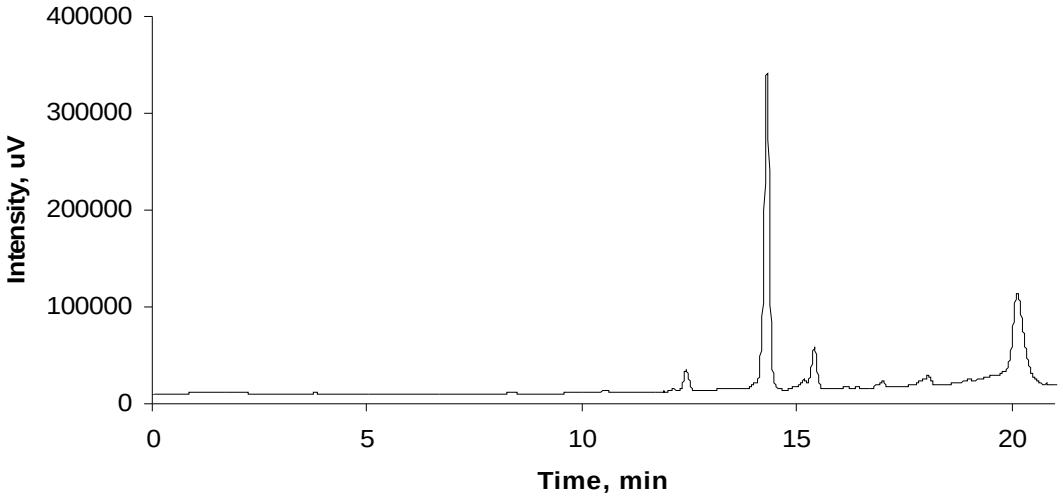


Figure 3.10 The HPLC chromatogram with UV detection (280 nm) of November-2011-Urla sample.

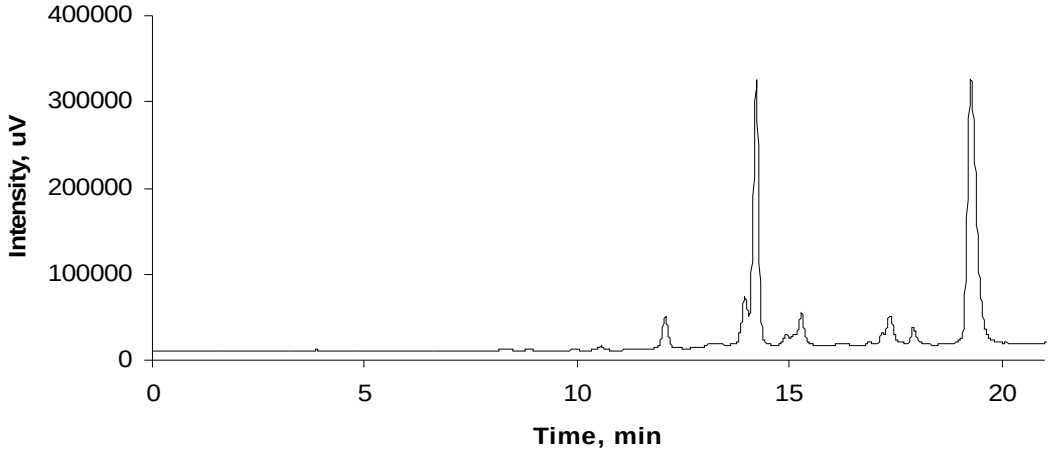


Figure 3.11 The HPLC chromatogram with UV detection (280 nm) of December-2011-Urla sample.

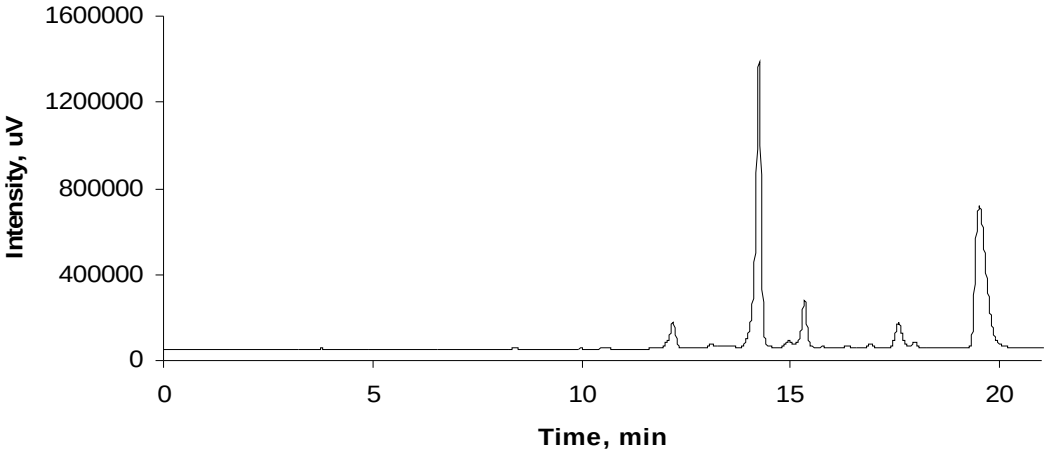


Figure 3.12 The HPLC chromatogram with UV detection (280 nm) of January-2012-Urla sample.

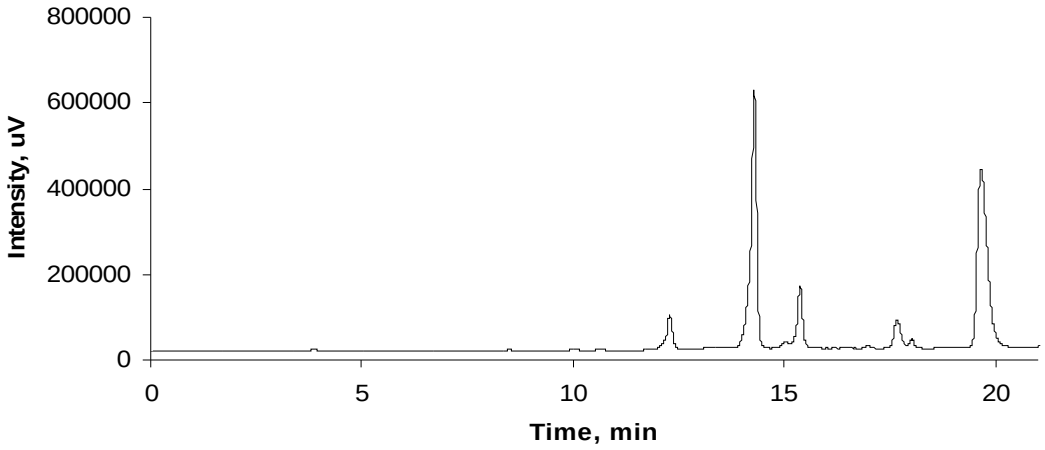


Figure 3.13 The HPLC chromatogram with UV detection (280 nm) of February-2012-Urla sample.

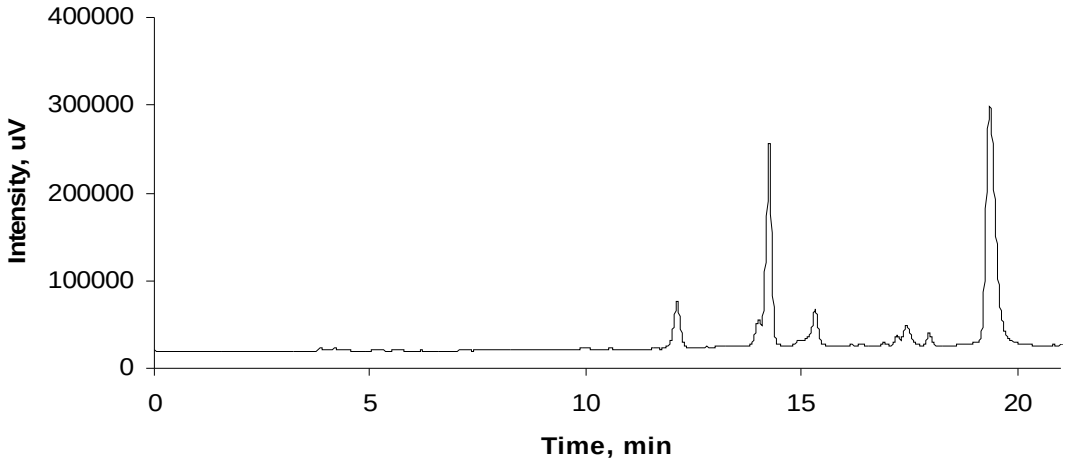


Figure 3.14 The HPLC chromatogram with UV detection (280 nm) of March-2012-Urla sample.

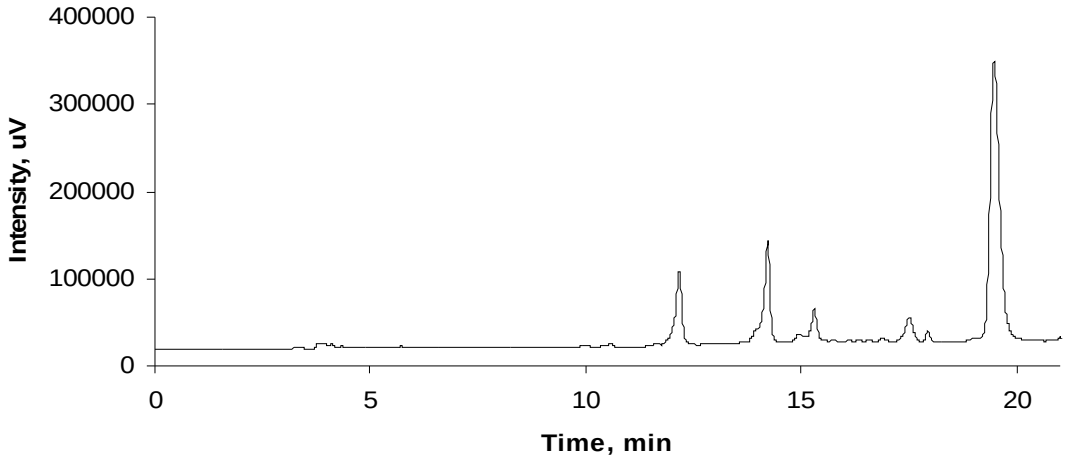


Figure 3.15 The HPLC chromatogram with UV detection (280 nm) of April-2012-Urla sample.

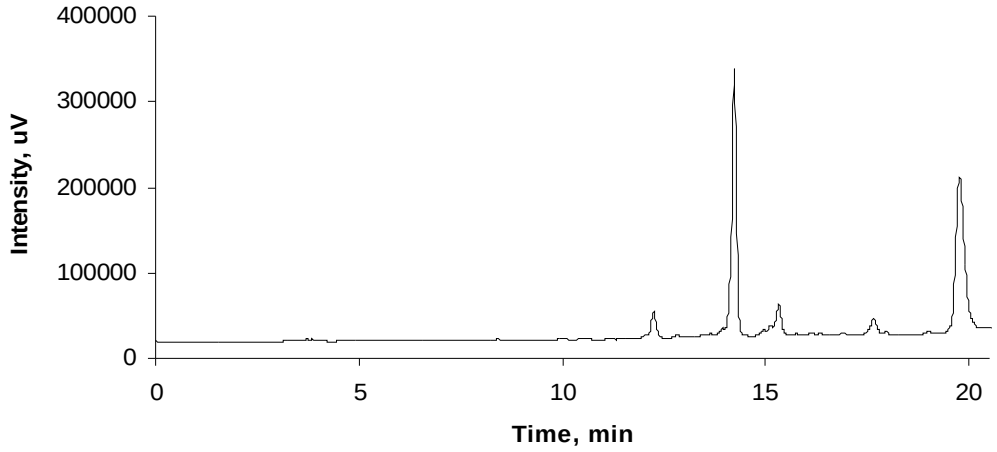


Figure 3.16 The HPLC chromatogram with UV detection (280 nm) of May-2012-Urla sample.

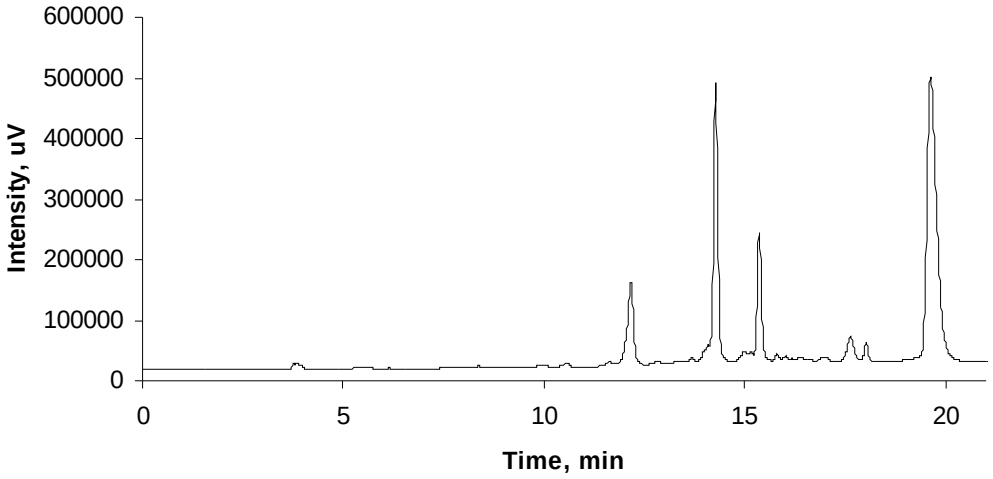


Figure 3.17 The HPLC chromatogram with UV detection (280 nm) of June-2012-Urla sample.

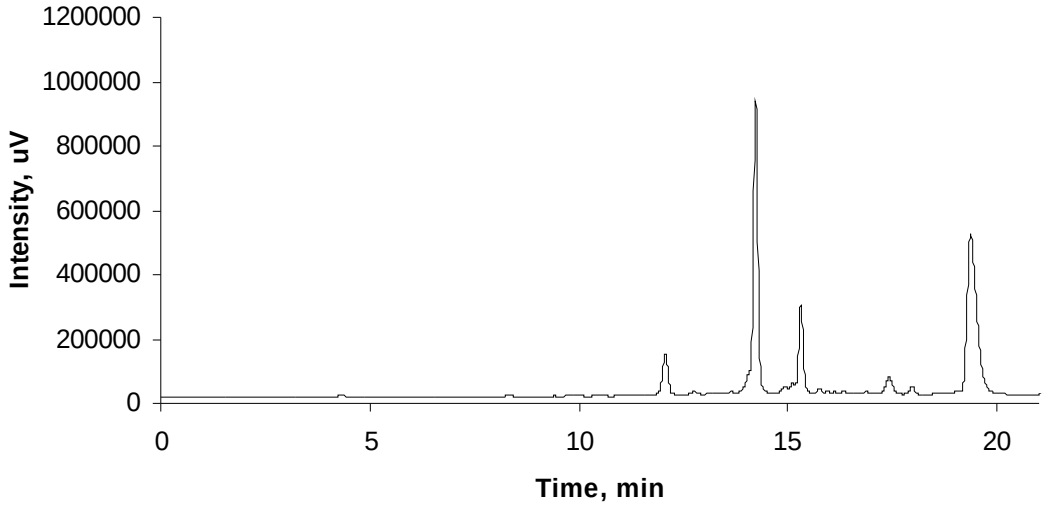


Figure 3.18 The HPLC chromatogram with UV detection (280 nm) of July-2012-Urla sample.

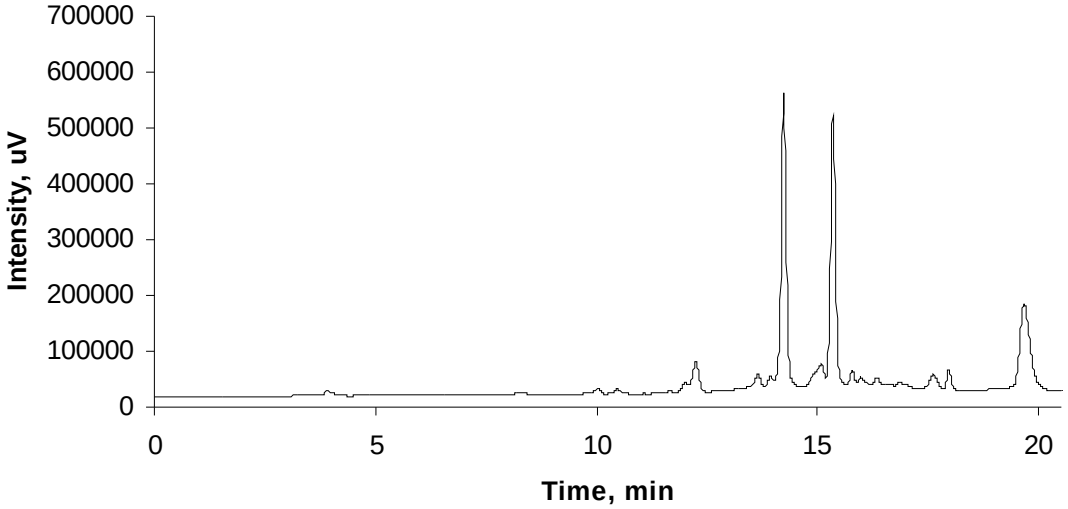


Figure 3.19 The HPLC chromatogram with UV detection (280 nm) of August-2012-Urla sample.

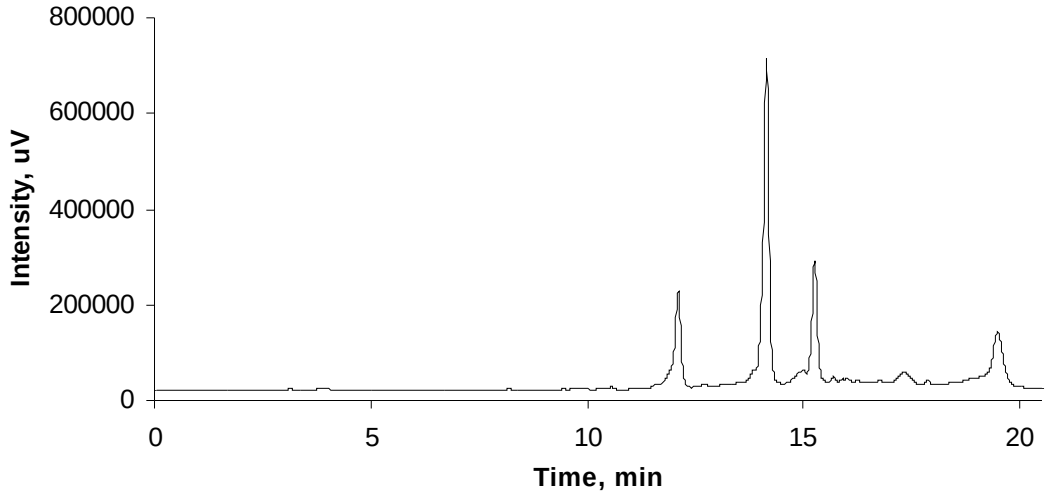


Figure 3.20 The HPLC chromatogram with UV detection (280 nm) of September-2012-Urla sample.

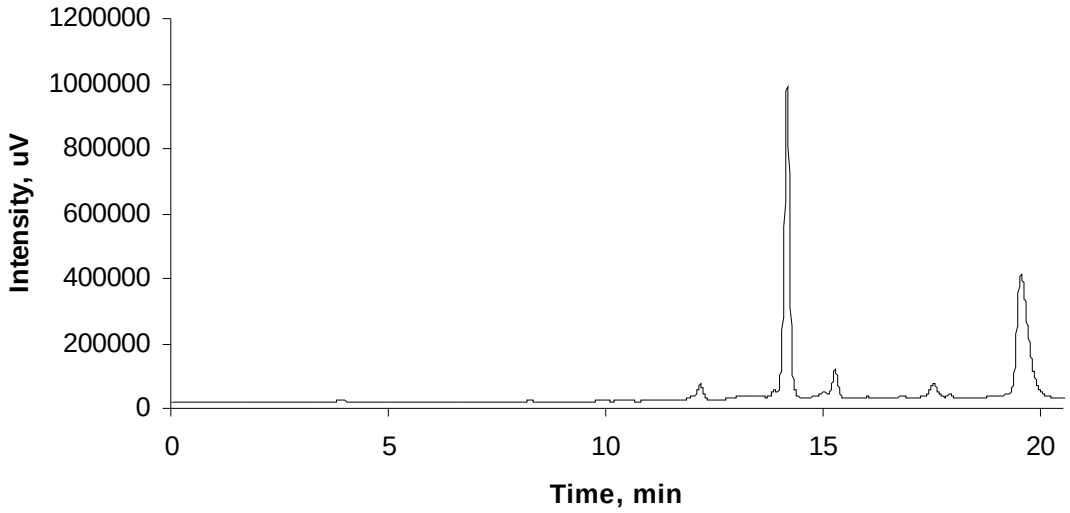


Figure 3.21 The HPLC chromatogram with UV detection (280 nm) of October-2012-Urla sample.

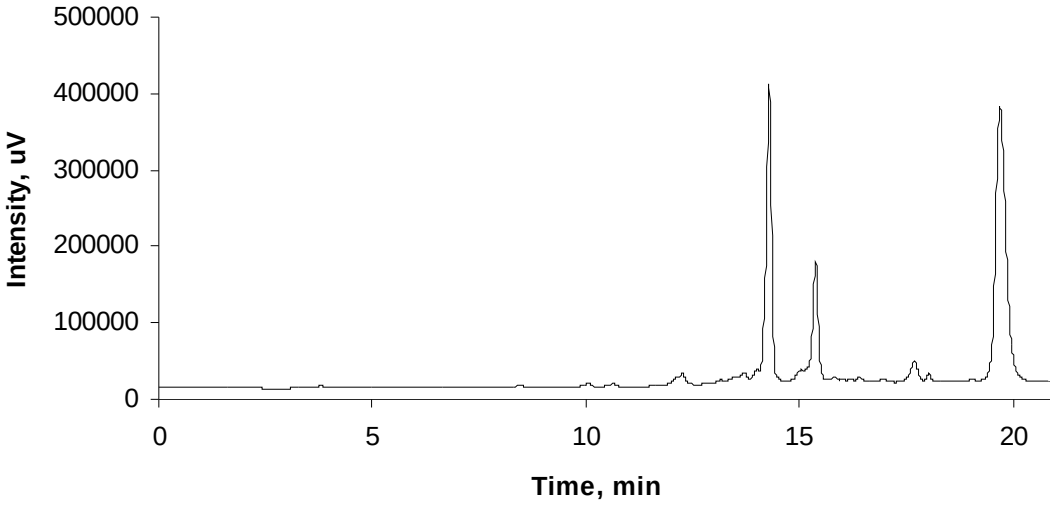


Figure 3.22 The HPLC chromatogram with UV detection (280 nm) of November-2012-Dikili sample.

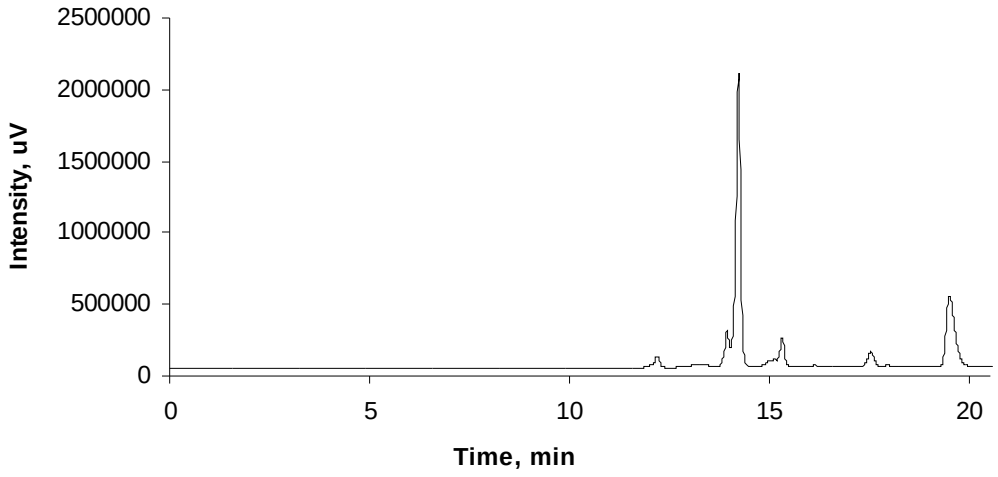


Figure 3.23 The HPLC chromatogram with UV detection (280 nm) of December-2012-Dikili sample.

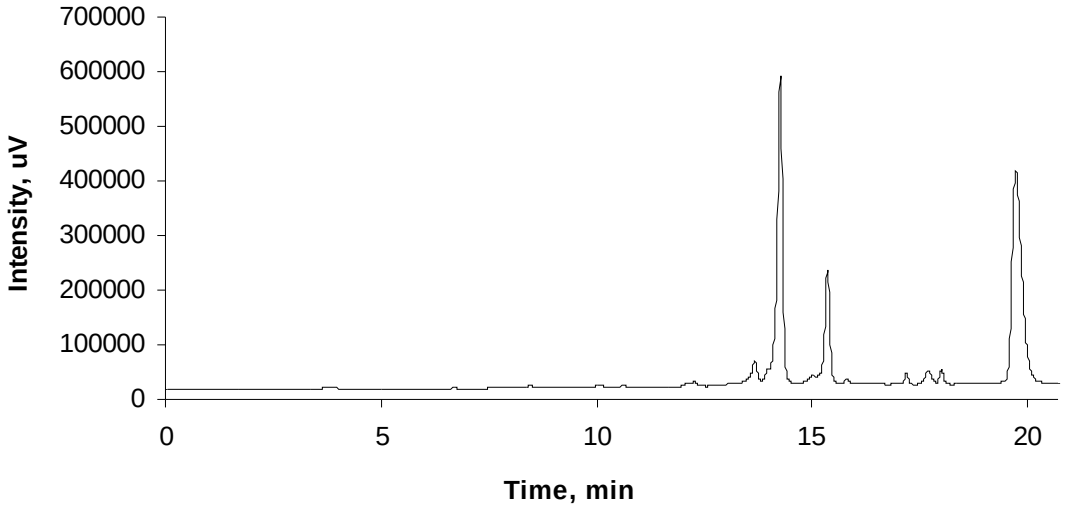


Figure 3.24 The HPLC chromatogram with UV detection (280 nm) of January-2012-Dikili sample.

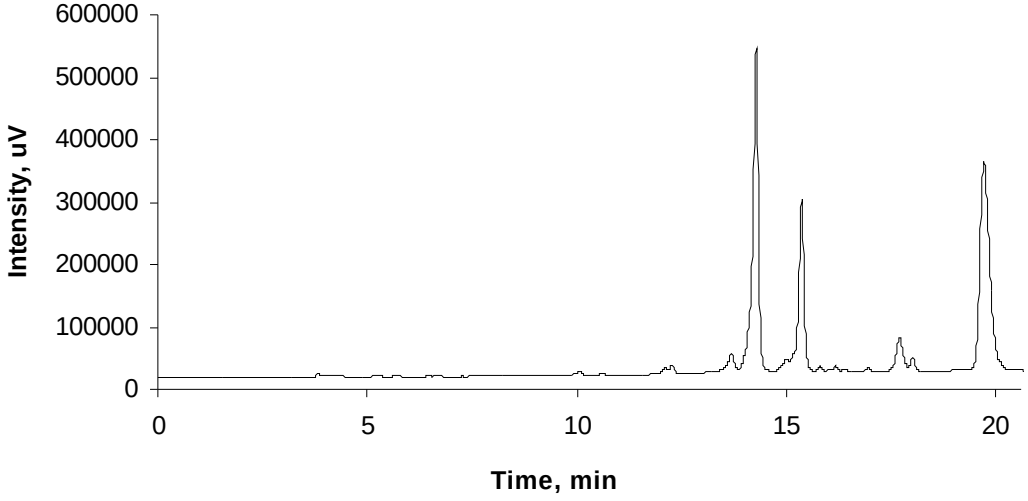


Figure 3.25 The HPLC chromatogram with UV detection (280 nm) of February-2012-Dikili sample.

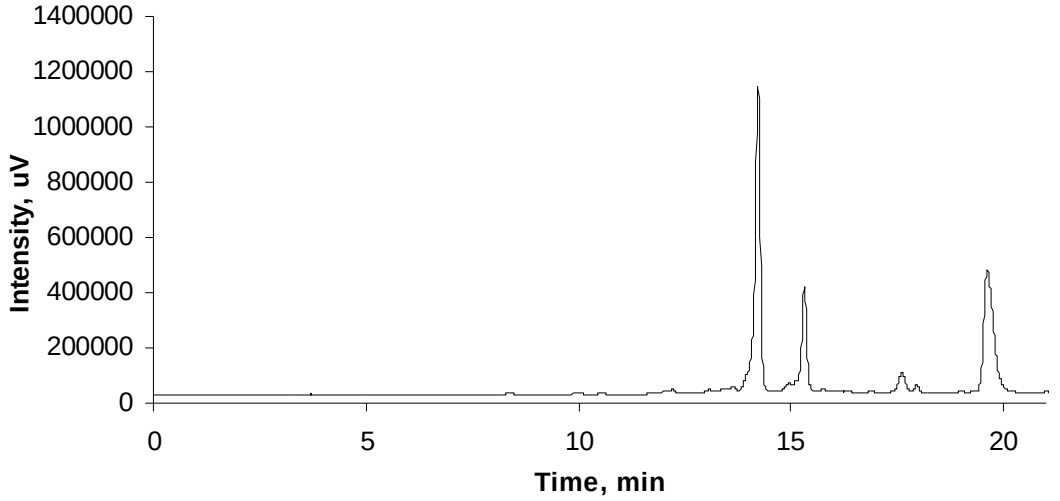


Figure 3.26 The HPLC chromatogram with UV detection (280 nm) of March-2012-Dikili sample.

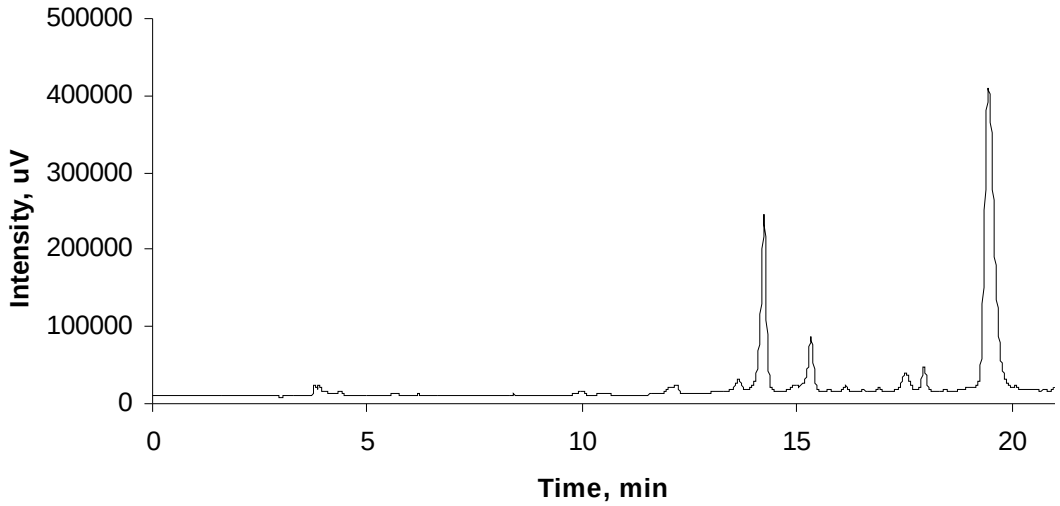


Figure 3.27 The HPLC chromatogram with UV detection (280 nm) of April-2012-Dikili sample.

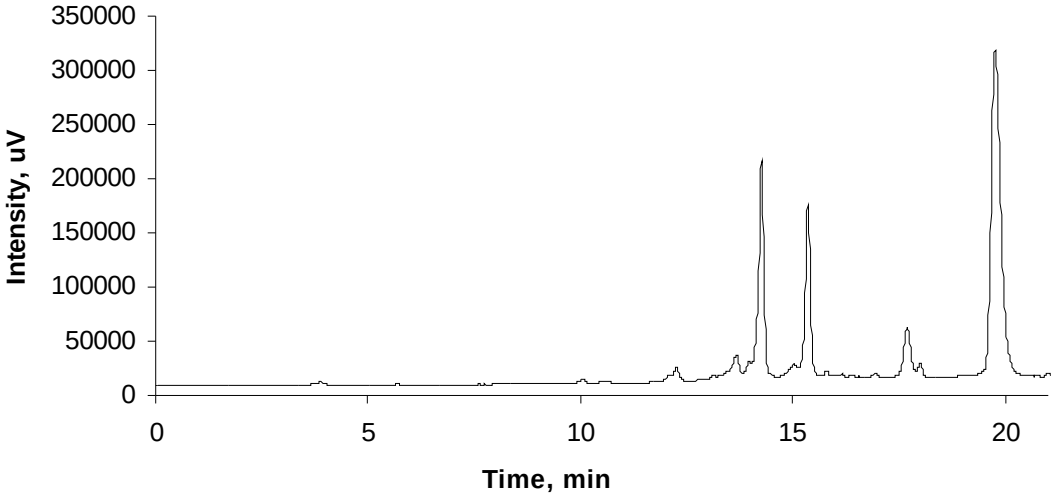


Figure 3.28 The HPLC chromatogram with UV detection (280 nm) of May-2012-Dikili sample.

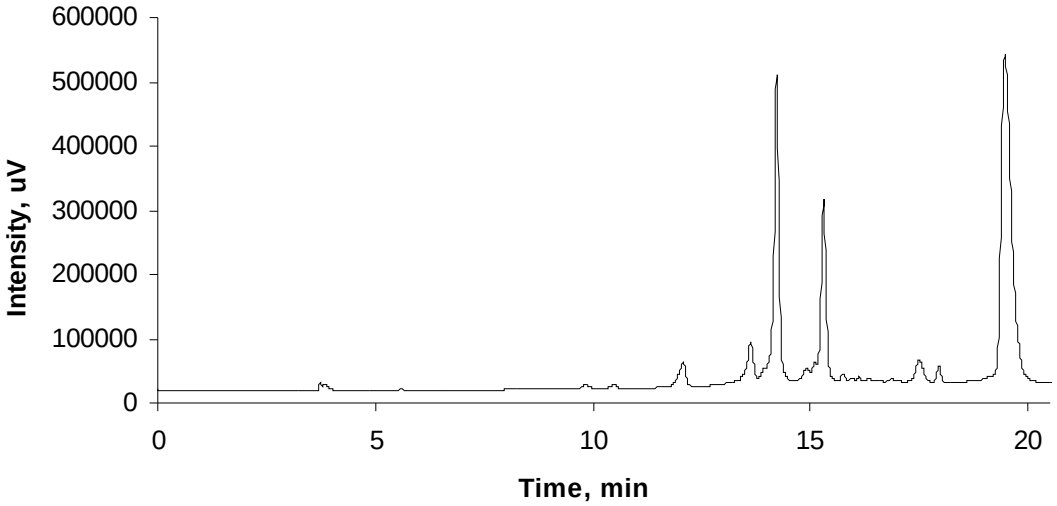


Figure 3.29 The HPLC chromatogram with UV detection (280 nm) of June-2012-Dikili sample.

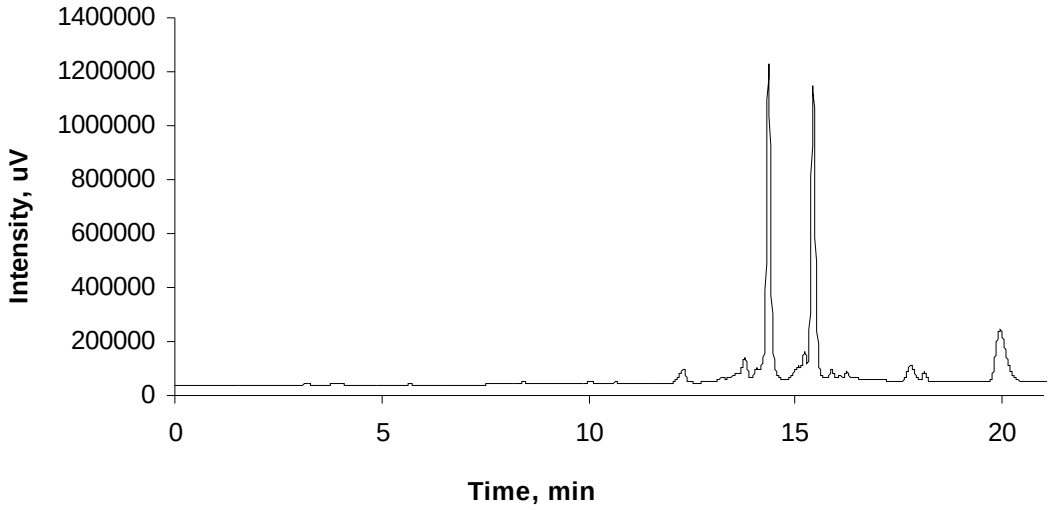


Figure 3.30 The HPLC chromatogram with UV detection (280 nm) of July-2012-Dikili sample.

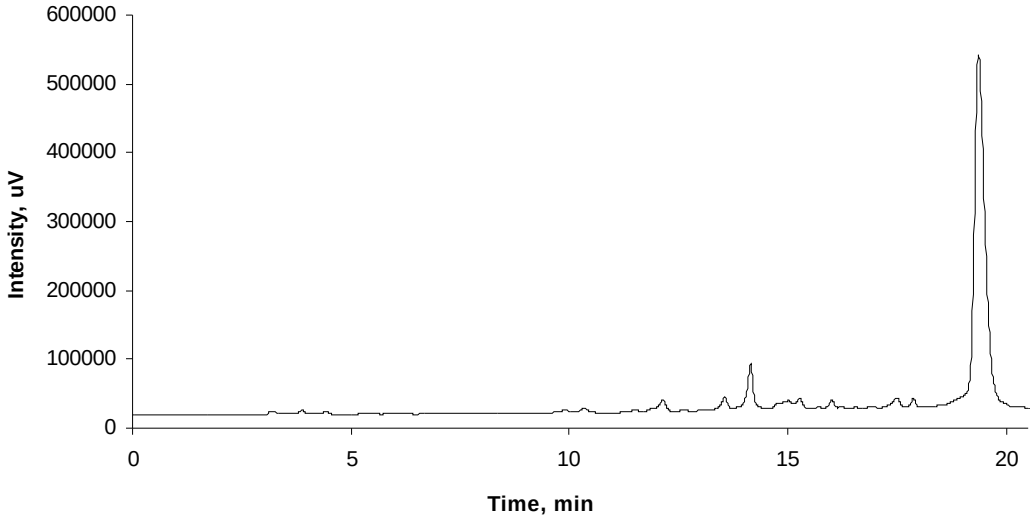


Figure 3.31 The HPLC chromatogram with UV detection (280 nm) of August -2012-Dikili sample.

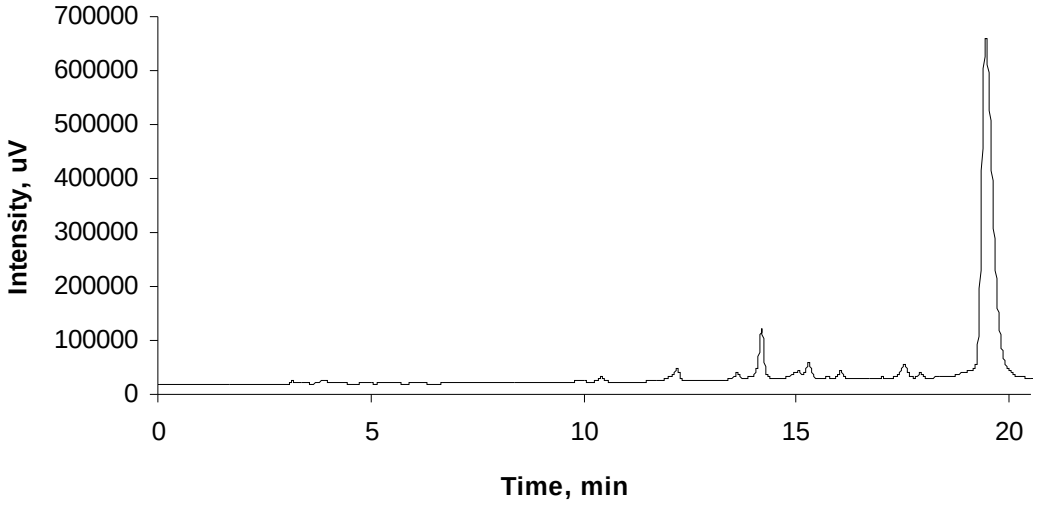


Figure 3.32 The HPLC chromatogram with UV detection (280 nm) of September -2012-Dikili sample.

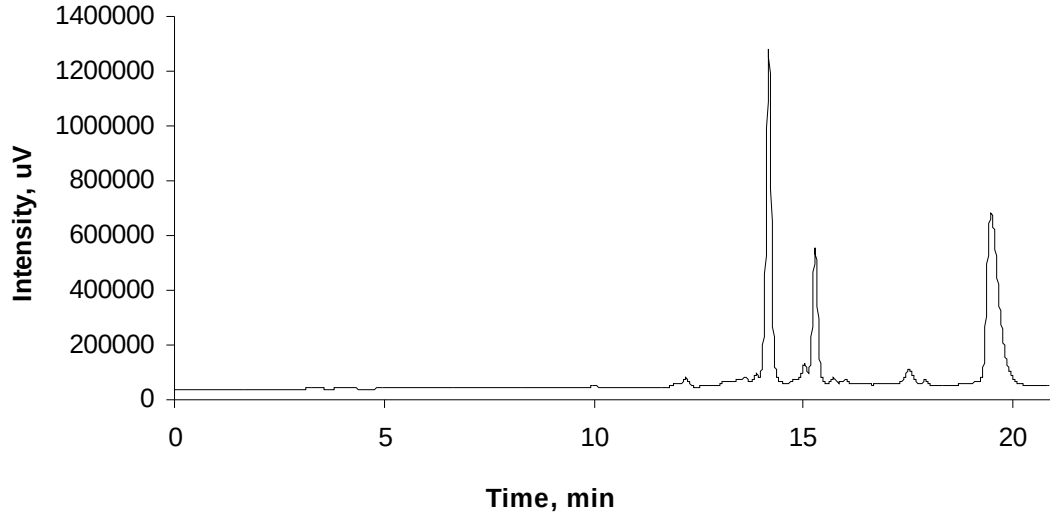


Figure 3.33 The HPLC chromatogram with UV detection (280 nm) of October -2012-Dikili sample.

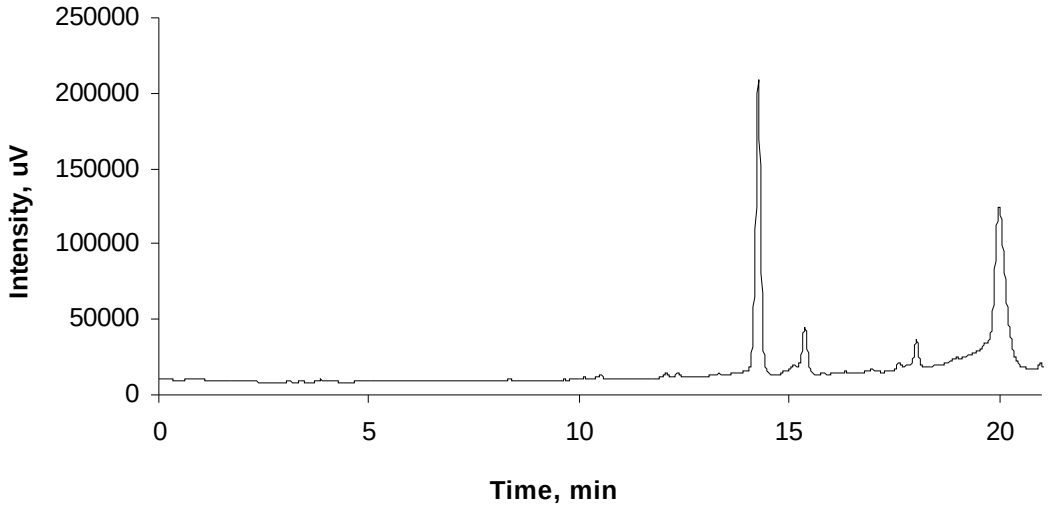


Figure 3.34 The HPLC chromatogram with UV detection (280 nm) of January -2012-Erdek sample.

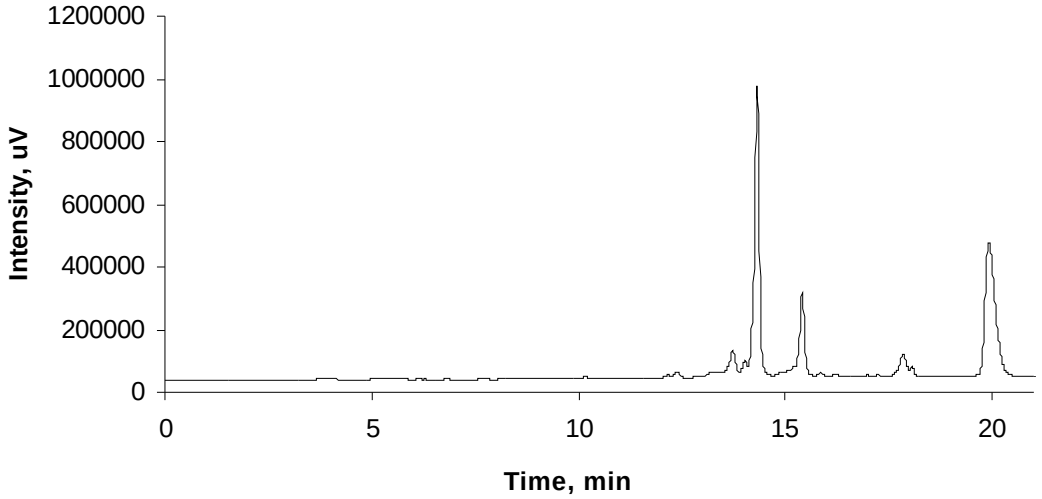


Figure 3.35 The HPLC chromatogram with UV detection (280 nm) of May-2012-Erdek sample.

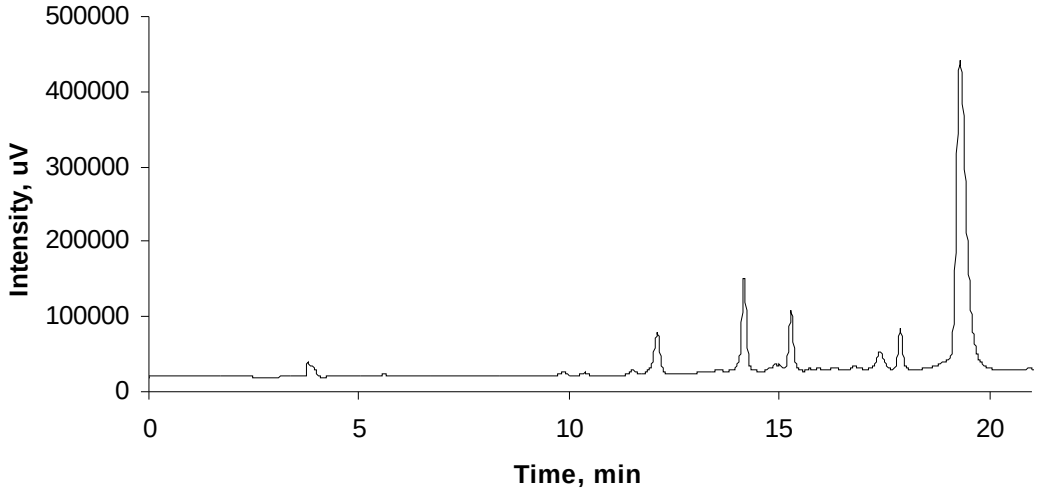


Figure 3.36 The HPLC chromatogram with UV detection (280 nm) of July-2012-Erdek sample.

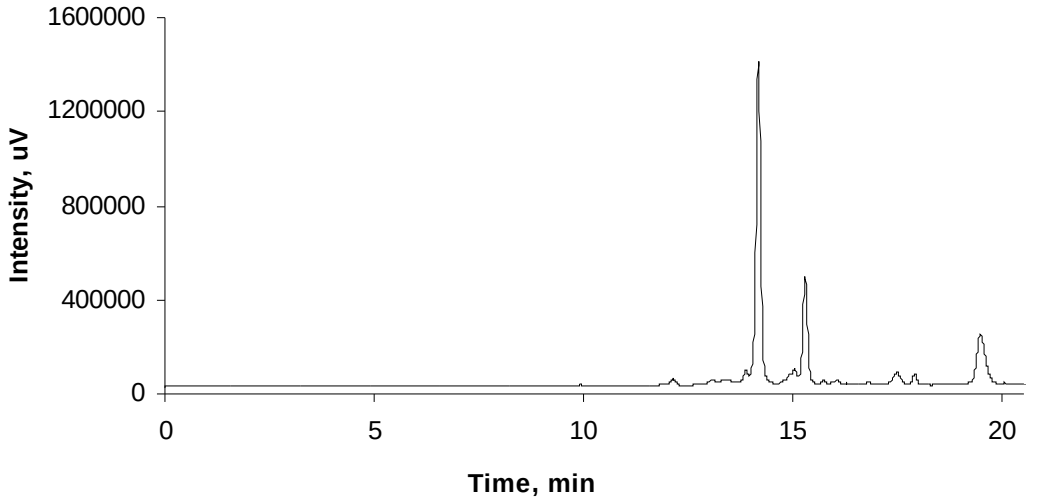


Figure 3.37 The HPLC chromatogram with UV detection (280 nm) of September-2012-Erdek sample.

ZA concentrations in samples were calculated after five individual injections and given as a μg ZA/g DW in the Table 3.1. Seasonal variations were also shown with column chart in the Figure 3.38. The detection limit was found as 0.035 mg ZA/mL.

Table 3.1 Seasonal ZA contents in *Z. noltii* detritus from Turkish coastlines (DW: Dried weight, ±: standard deviation, LOD=0.035 mg ZA/mL).

	ZA content, µg ZA/g DW		
Time	*Dikili*	*Urla*	*Erdek*
November 11	203.2 ± 16.5 (bc)*	104.3 ± 2.7 (h)	-
December 11	241.4 ± 4.8 (b)	246.1 ± 24.6 (fg)	-
January 12	157.2 ± 14.9 (de)	909.1 ± 90.5 (b)	276.7 ± 8.1 (b)
February 12	173.9 ± 17.2 (cd)	743.8 ± 25.8 (cd)	-
March 12	209.2 ± 12.4 (b)	823.1 ± 40.6 (bc)	-
April 12	136.8 ± 7.5 (e)	702.6 ± 114.3 (d)	-
May 12	215.6 ± 15.4 (b)	303.8 ± 24.5 (ef)	251.8 ± 14.2 (b)
June 12	286.1 ± 10.2 (a)	802.0 ± 120.1 (c)	-
July 12	301.4 ± 61.7 (a)	744.5 ± 51.6 (cd)	369.0 ± 26.4 (a)
August 12	29.0 ± 3.1 (f)	368.5 ± 34.1 (e)	-
September 12	27.6 ± 1.5 (f)	1364.8 ± 16.1 (a)	109.7 ± 9.2 (c)
October 12	115.3 ± 9.2 (e)	159.4 ± 4.6 (gh)	-

* Letters in the parenthesis were obtained from One Way ANOVA followed by Tukey's Test, different letters show statistical difference at $p<0.05$.

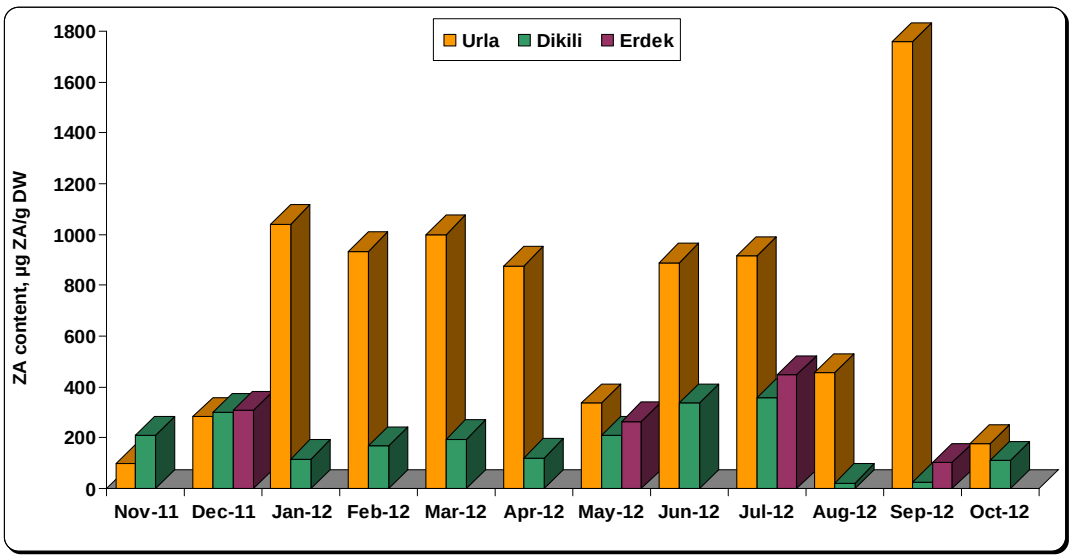


Figure 3.38 Seasonal variation of the ZA content in the *Z. noltii* detritus from three different regions.

The *Z. noltii* detritus were not able to be sampled monthly from Erdek station as these detritus were collected in summer season by the hotels for cleaning of the beaches. The mean ZA contents in samples collected from Urla station were very higher than those of the samples collected from Dikili and Erdek. The highest ZA content was found as 1364.8 ± 16.1 µg ZA/g DW in the samples collected from Urla in September 2012. On the other hand, the lowest ZA content in the samples was

determined in September-2012 from Dikili station (27.6 ± 1.5 µg ZA/g DW). The maximum ZA content of *Z. noltii* detritus from Turkish coastlines were higher compared to published results by Achamlale et al. (2009b) and Grignon-Dubois et al. (2012) as 456 µg ZA/g DW and 727 µg ZA/g DW, respectively. According to the results, ZA levels in samples collected from Urla were higher than those collected from Dikili and Erdek. This could be associated with habitat differences of *Z. noltii* in the sampling regions. *Z. noltii* is dominant species in Urla; however, *Z. noltii* forms mixed vegetation with invasive marine algae *Caulerpa racemosa* var. *cylindracea* and native seagrass *Cymodocea nodosa* in Dikili. The *Z. noltii* samples which have the lowest ZA content in this study could be affected from *Cymodocea nodosa* which is found near to the sampling area. After a tide event in Urla region during autumn and winter seasons, desiccation, increased temperature and light intensity, altered salinity might be some reasons of the variations in ZA concentrations. Moreover, in the Urla region there is a freshwater flow into the coastal water. ZA contents in *Z. noltii* samples collected from Erdek coastline were also lower than those of samples collected from Urla. This could be associated with the habitat and also geographical differences of Erdek, Urla and Dikili coastlines, since Erdek is located in Marmara Sea which is an inland sea that connects the Black Sea to the Aegean Sea. This is the first investigation on the ZA contents of *Z. noltii* from Turkish coastline.

The synthesis of ZA and isolation of ZA were compared in term of cost by calculating the chemical prices that are used. Although the synthesis of 1 mg ZA cost 2.57 TL, the isolation of ZA from *Z. noltii* extract cost 45.10 TL. These synthesis and isolation experiments were achieved in laboratory conditions. But if the attempt is an industrial scale, the coasts may be cheaper. Moreover, the organic synthesis is more hazardous than the isolation because of more chemical usage.

3.4 Isolation of Zosteric Acid from Z. Noltii Extracts

ZA was isolated from *Z. noltii* extracts by using fraction collector and 2 mL loop. Since there are different phenolic acids in *Z. noltii* such as rosmarinic and caffeic

acid, three remarkable peaks observed in HPLC chromatograms of *Z. noltii* extracts were isolated (Figure 3.39).

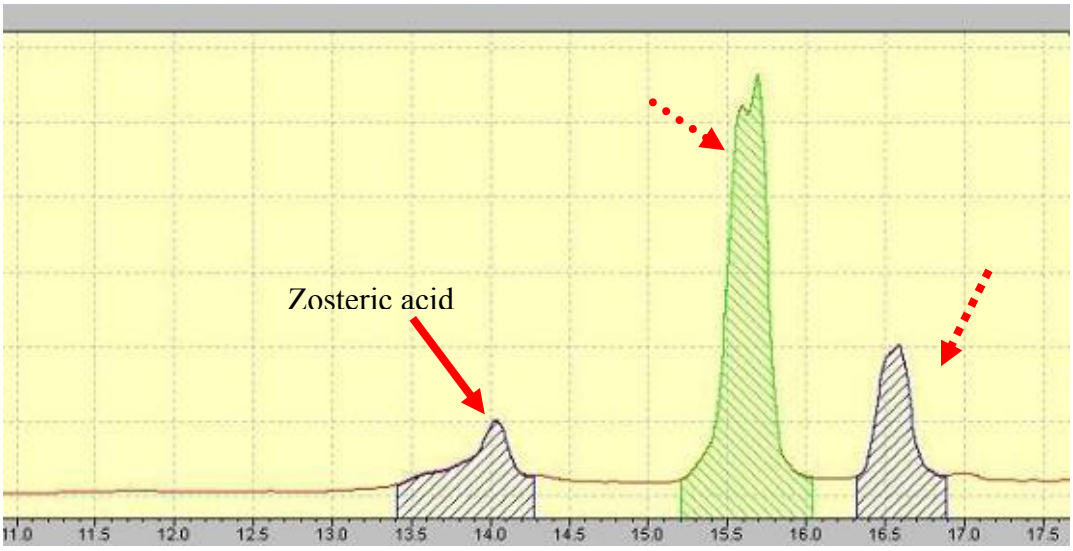


Figure 3.39 HPLC chromatogram with UV detection (280 nm) of January-2012-Urla sample.

The isolated ZA analyzed in analytical HPLC system in order to check the purity and determine the level of the isolated samples. Since the amount of isolated ZA was low, the mobile phase was evaporated by water bath to concentrate the collected ZA. After the evaporation, some impurities were also observed in HPLC chromatogram of ZA (Figure 3.40). Mobile phase was also evaporated under N_2 stream and with rotary evaporator to evaluate the temperature effects on the isolated ZA (Figure 3.41-Figure 3.42).

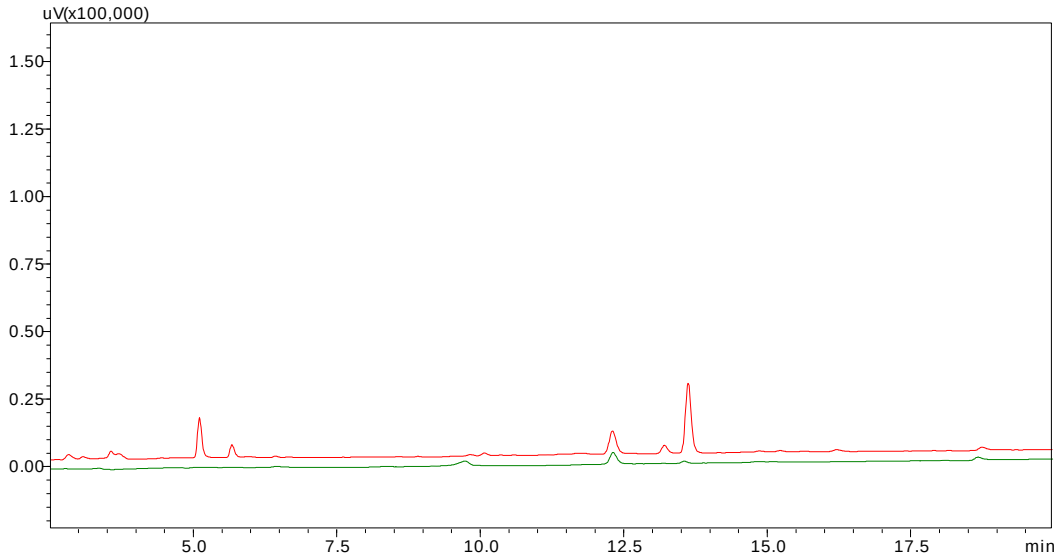


Figure 3.40 HPLC chromatograms of isolated ZA from July-2012-Urla sample, green: before the evaporation of mobile phase, red: after the evaporation of mobile phase by water bath for 4 h at 99°C.

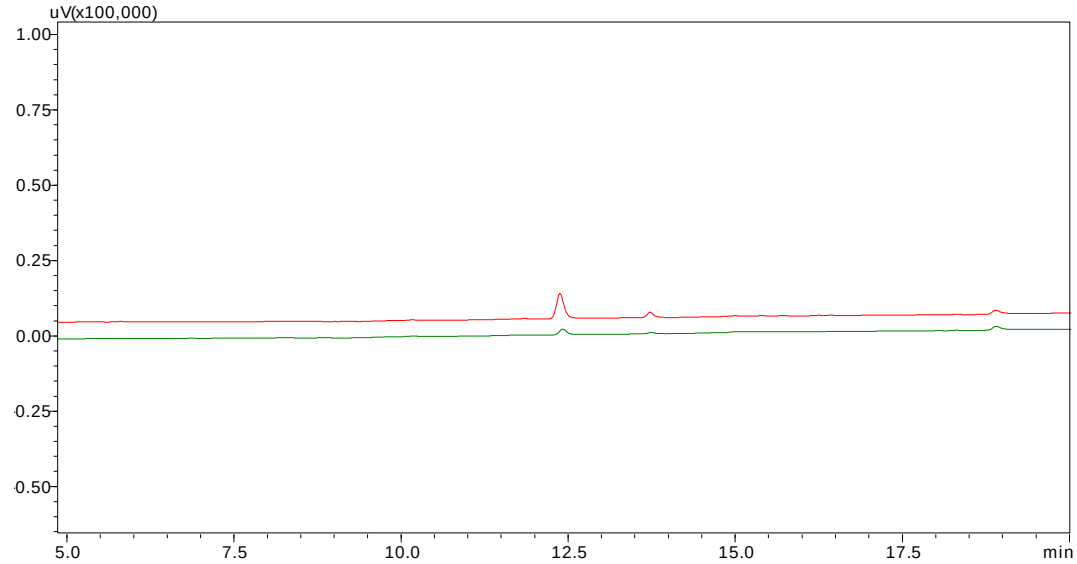


Figure 3.41 HPLC chromatograms of isolated ZA from July-2012-Urla sample, green: before the evaporation of mobile phase, red: after the evaporation of mobile phase under N_2 stream at room temperature.

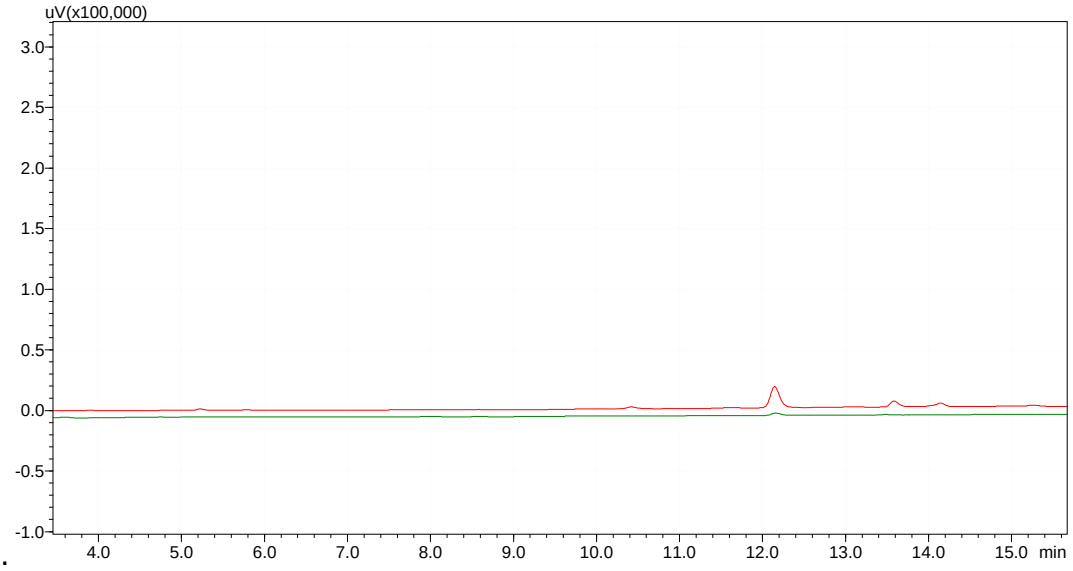


Figure 3.42 HPLC chromatograms of isolated ZA from July-2012-Urla sample, green: before the evaporation of mobile phase, red: after the evaporation of mobile phase with rotary evaporator at 70 °C.

3.5 The Field Test Results

The field tests were carried out for a period of five months from January 28 to July 3, 2013 at Levent Marina, İzmir, Turkey. The all test panels except the painted with commercial antifouling paint, were covered by micro-slime layer non-homogenously in first month. After four months the surfaces of paint free and primer coated panels were started to cover by some macro-fouling organisms. After five months paint free panel was totally covered (Figure 3.44). The best antifouling performance was observed for commercial antifouling paint which contains very high cupper (I) oxide (Figure 3.45). On the other hand, ZA containing paint showed very successful antifouling performance compared to the other prepared paints (Figure 3.47-Figure 3.48). After 156 days only commercial antifouling paint and ZA containing paint prevented the attachment of fouling organisms. The surfaces of diuron and irgarol containing paints were also covered by fouling organism (Figure 3.56-3.58). The all photograph belongs to January 28 to July 3, 2013 seasons were given in between Figures 3.43 and Figure 3.62. Also, the surfaces of test panels were evaluated based on fouling criteria consist of five grades. “I” is attributed that there is

no fouling organism on the painted plates and “V” is attributed for the plate which is totally covered. The results of fouling criteria were given in Table 3.2.

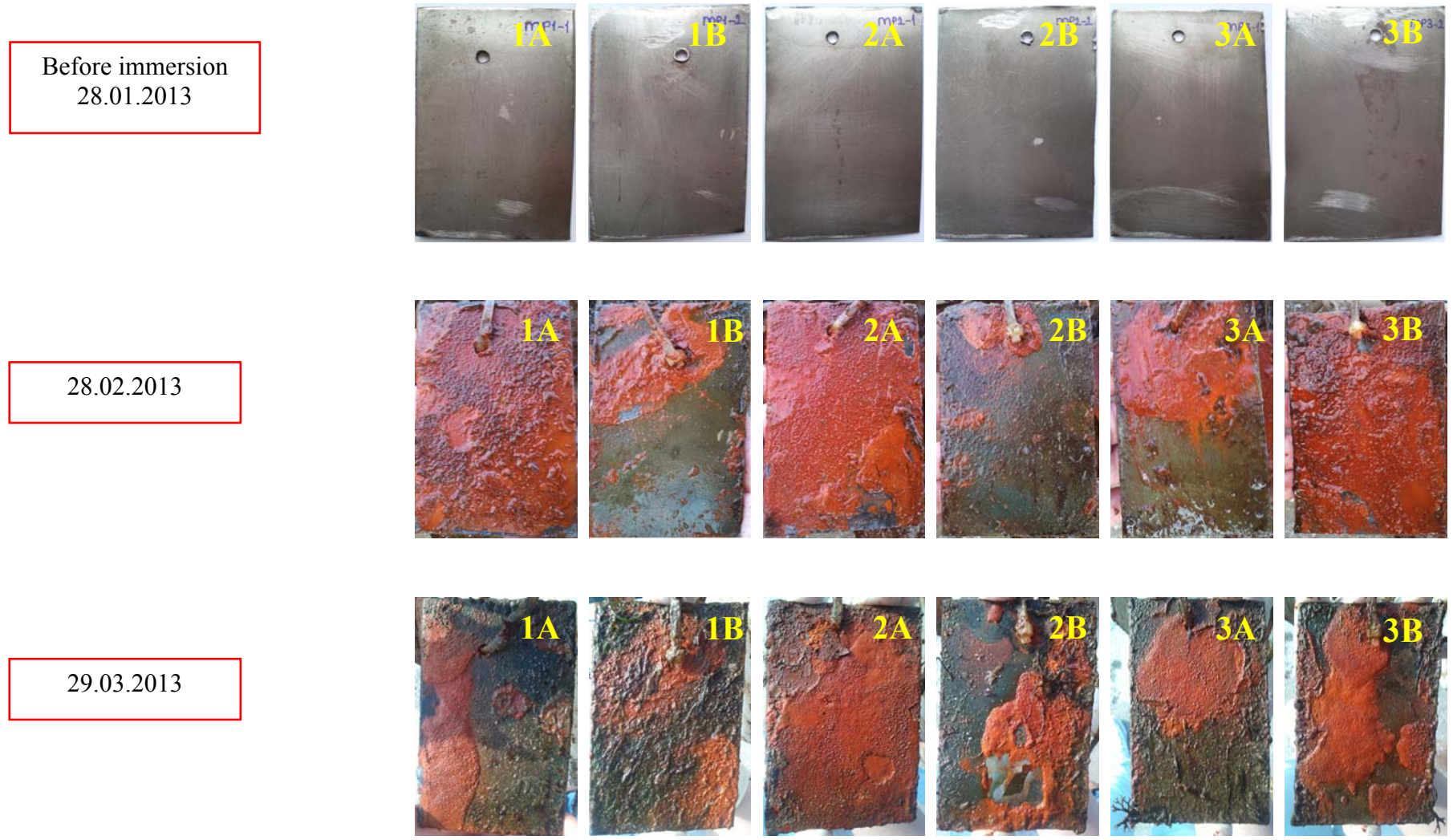


Figure 3.43 The photographs belong to two sides of unpainted test plates (between January and March) (A: front, B: back, 1-3: parallel number).

15.04.2013

22.05.2013

03.07.2013

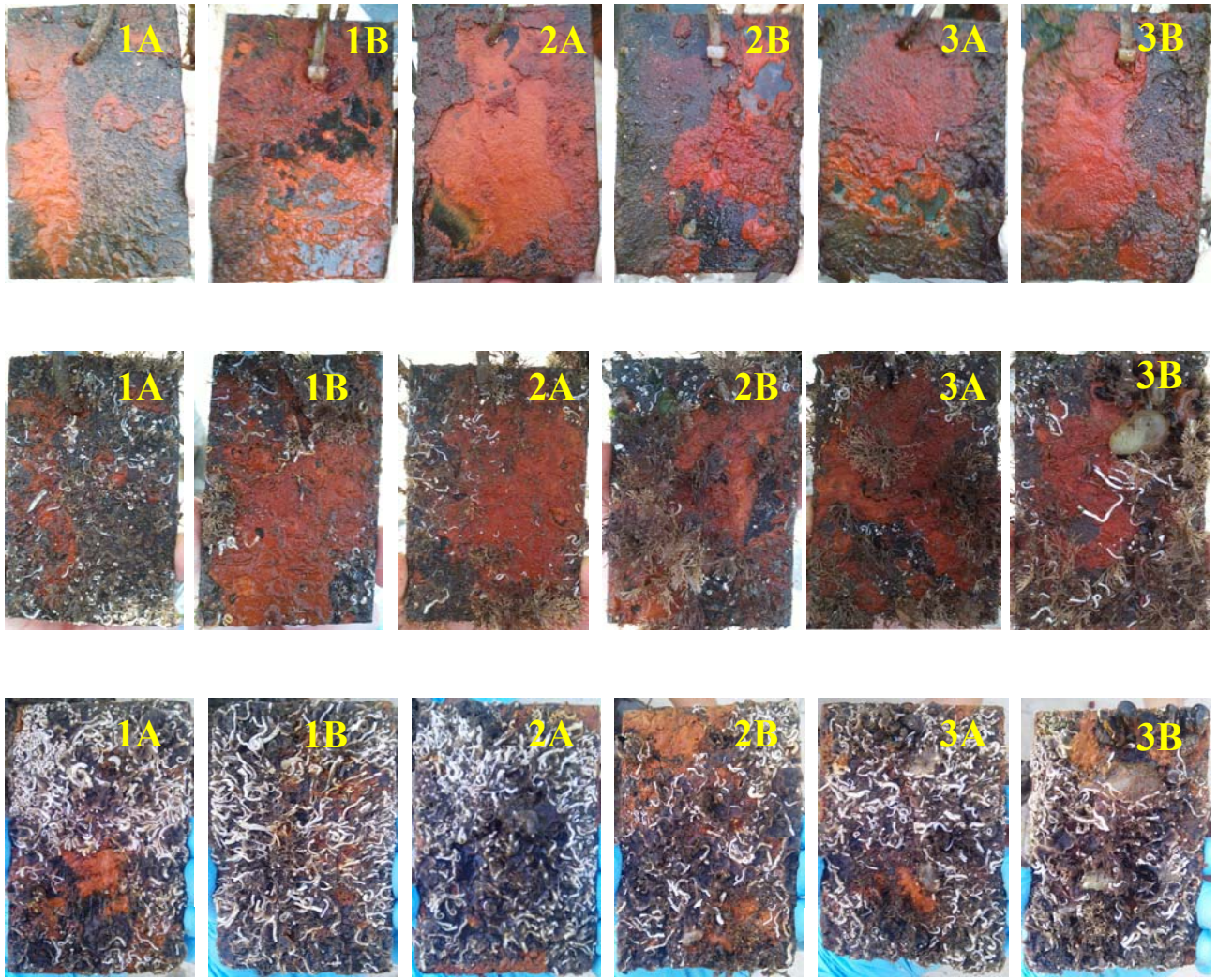


Figure 3.44 The photographs belong to two sides of unpainted test plates (between April and July) (A: front, B: back, 1-3: parallel number).

Before immersion
28.01.2013

28.02.2013

29.03.2013

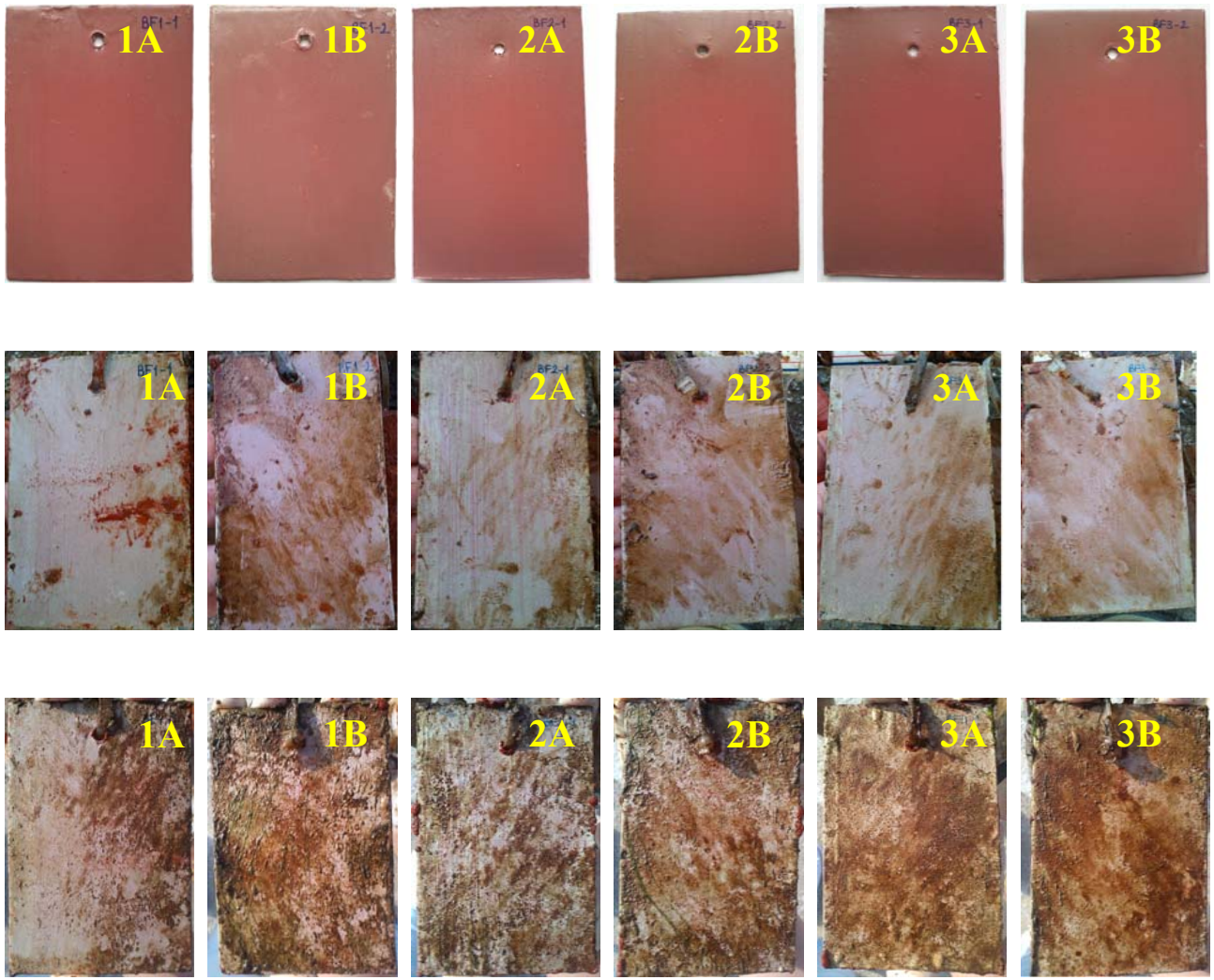


Figure 3.45 The photographs belong to two sides of test plates painted with biocide free paint (between January to March) (A: front, B: back, 1-3: parallel number).

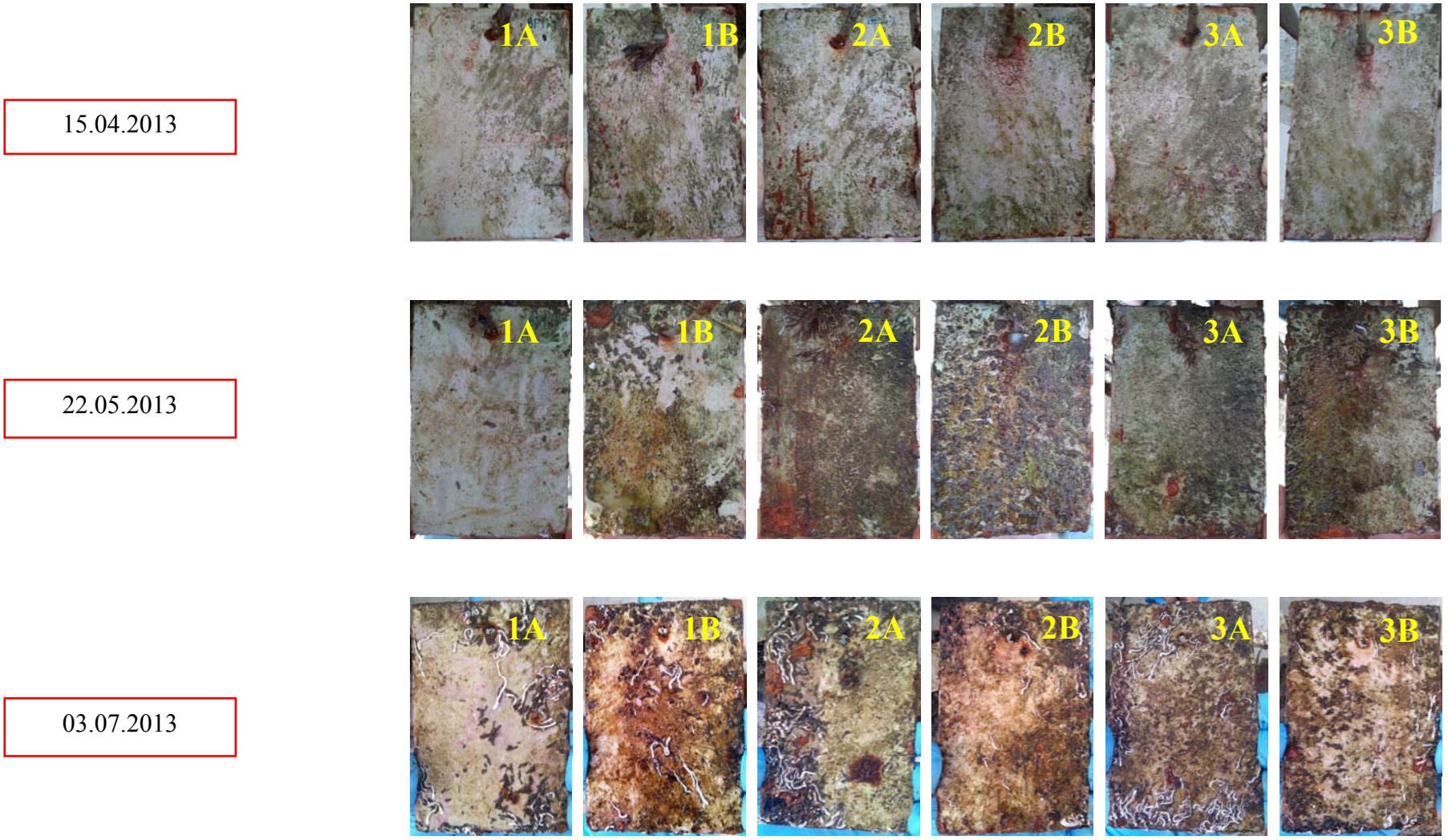


Figure 3.46 The photographs belong to two sides of test plates painted with biocide free paint (between April and July) (A: front, B: back, 1-3: parallel number).

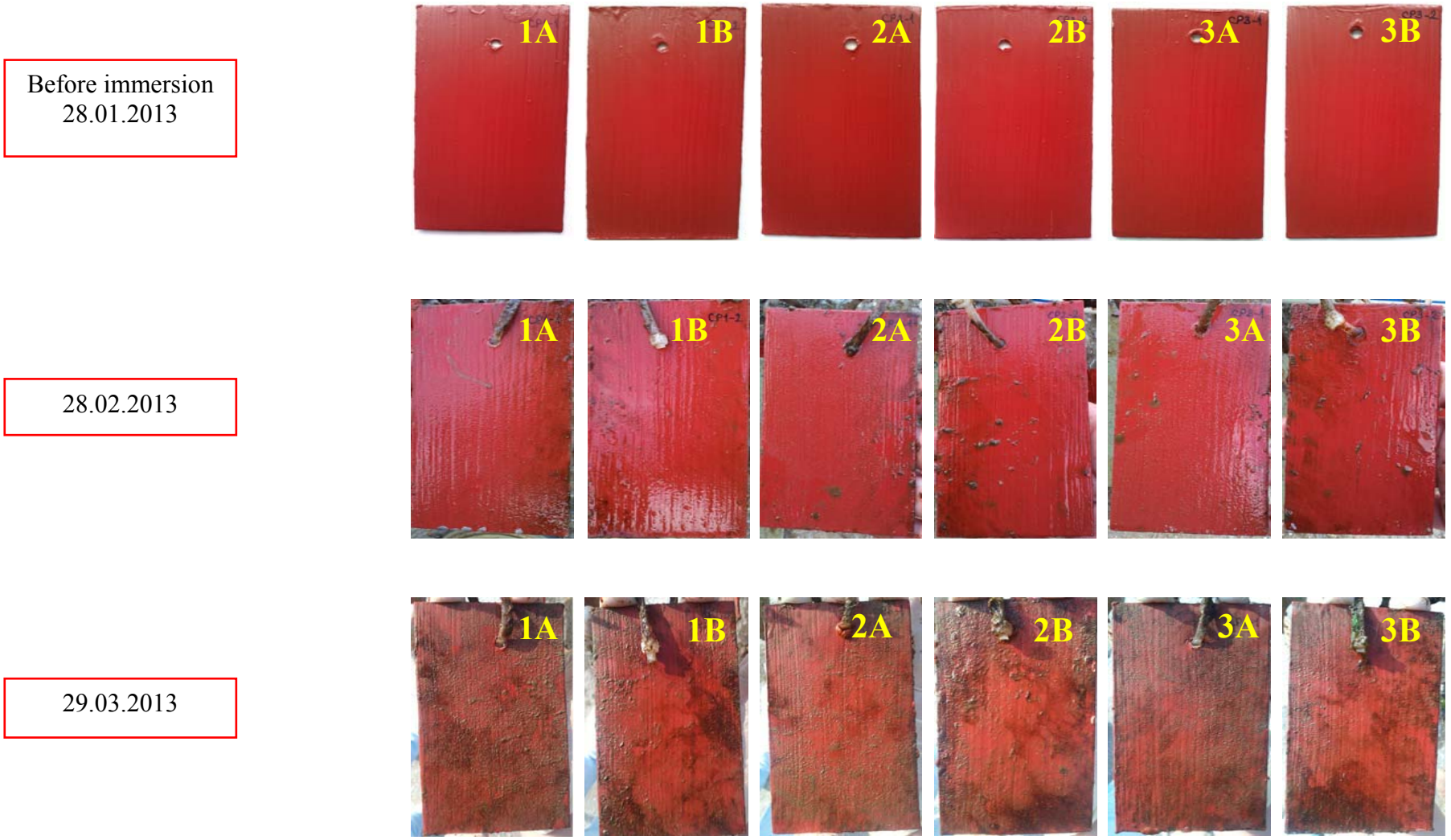


Figure 3.47 The photographs belong to two sides of test plates painted with commercial paint (between January and March) (A: front, B: back, 1-3: parallel number).

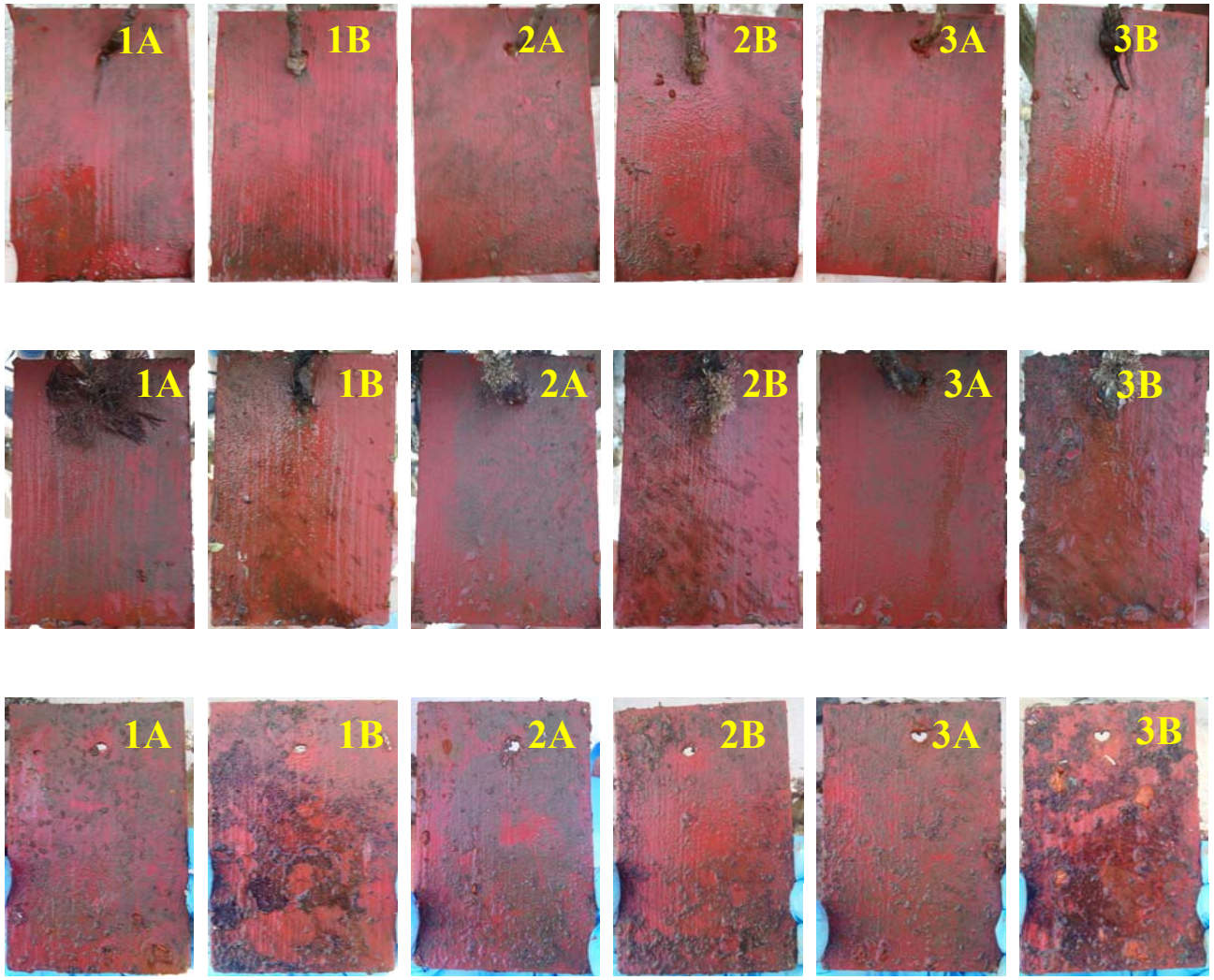


Figure 3.48 The photographs belong to two sides of test plates painted with commercial paint (between April and July) (A: front, B: back, 1-3: parallel number).

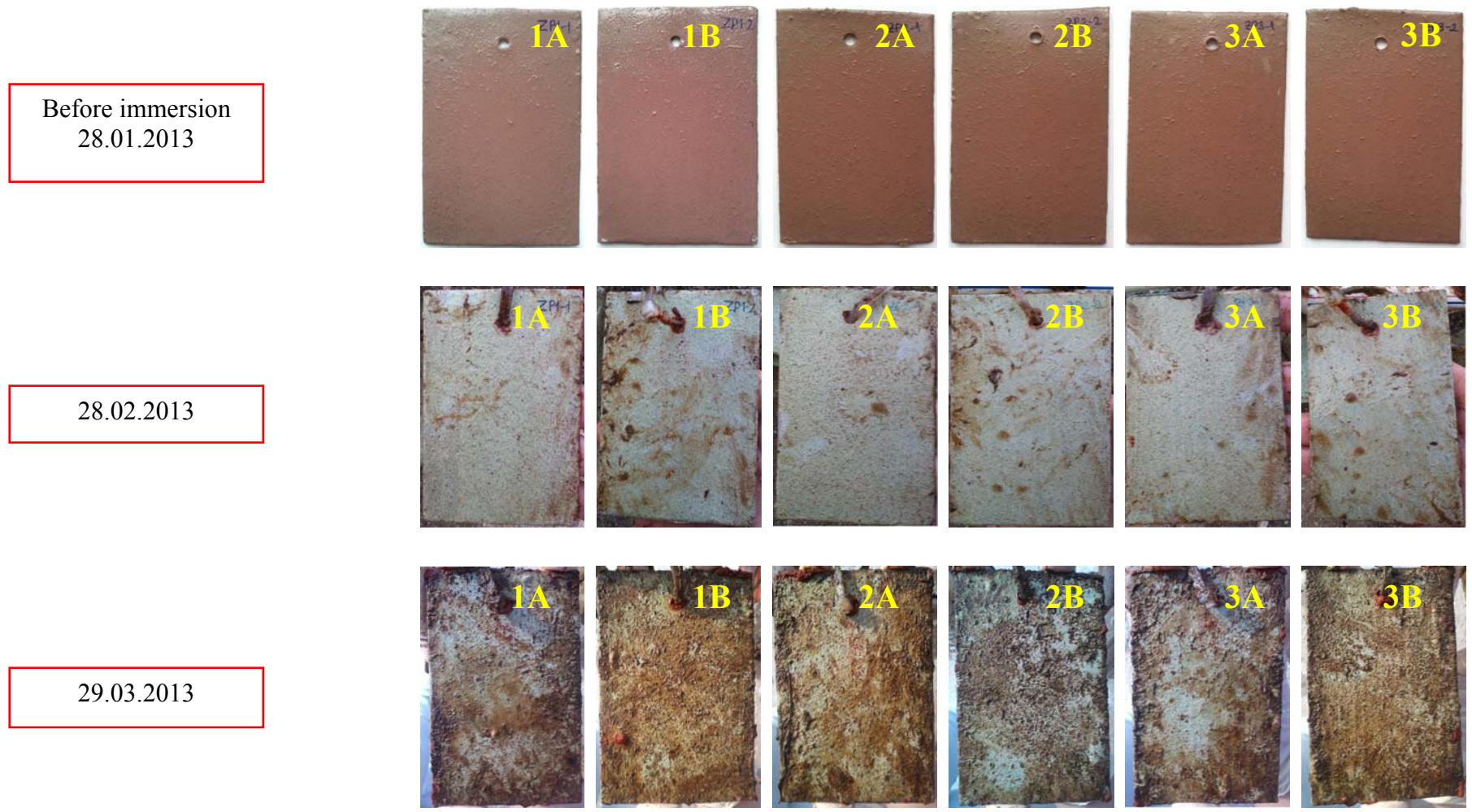


Figure 3.49 The photographs belong to two sides of test plates painted with *Z. noltii* powder containing paint (between January to March) (A: front, B: back, 1-3: parallel number).

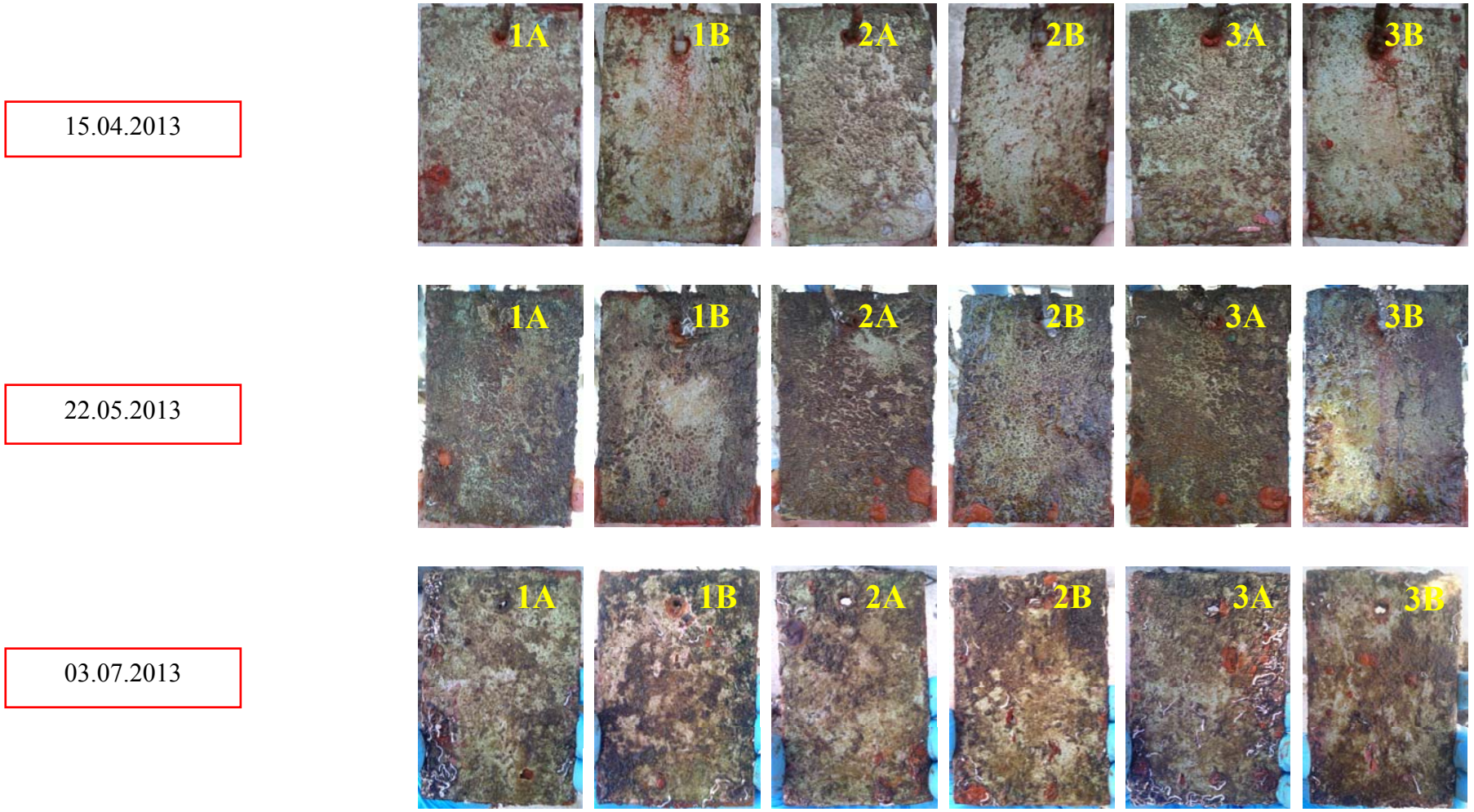


Figure 3.50 The photographs belong to two sides of test plates painted with *Z. noltii* powder containing paint (between April to July) (A: front, B: back, 1-3: parallel number).

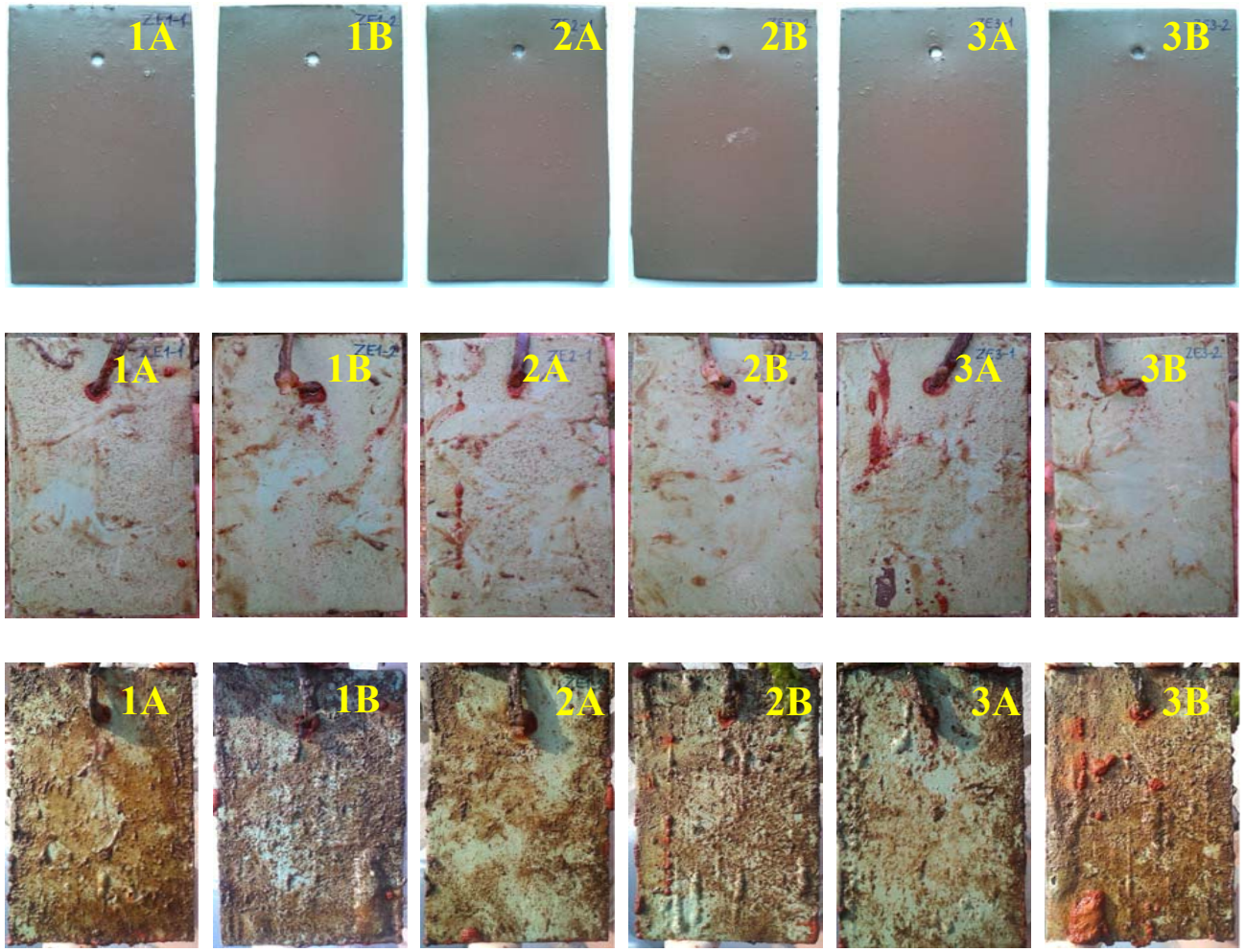


Figure 3.51 The photographs belong to two sides of test plates painted with *Z. noltii* extract containing paint (between January and March) (A: front, B: back, 1-3: parallel number).

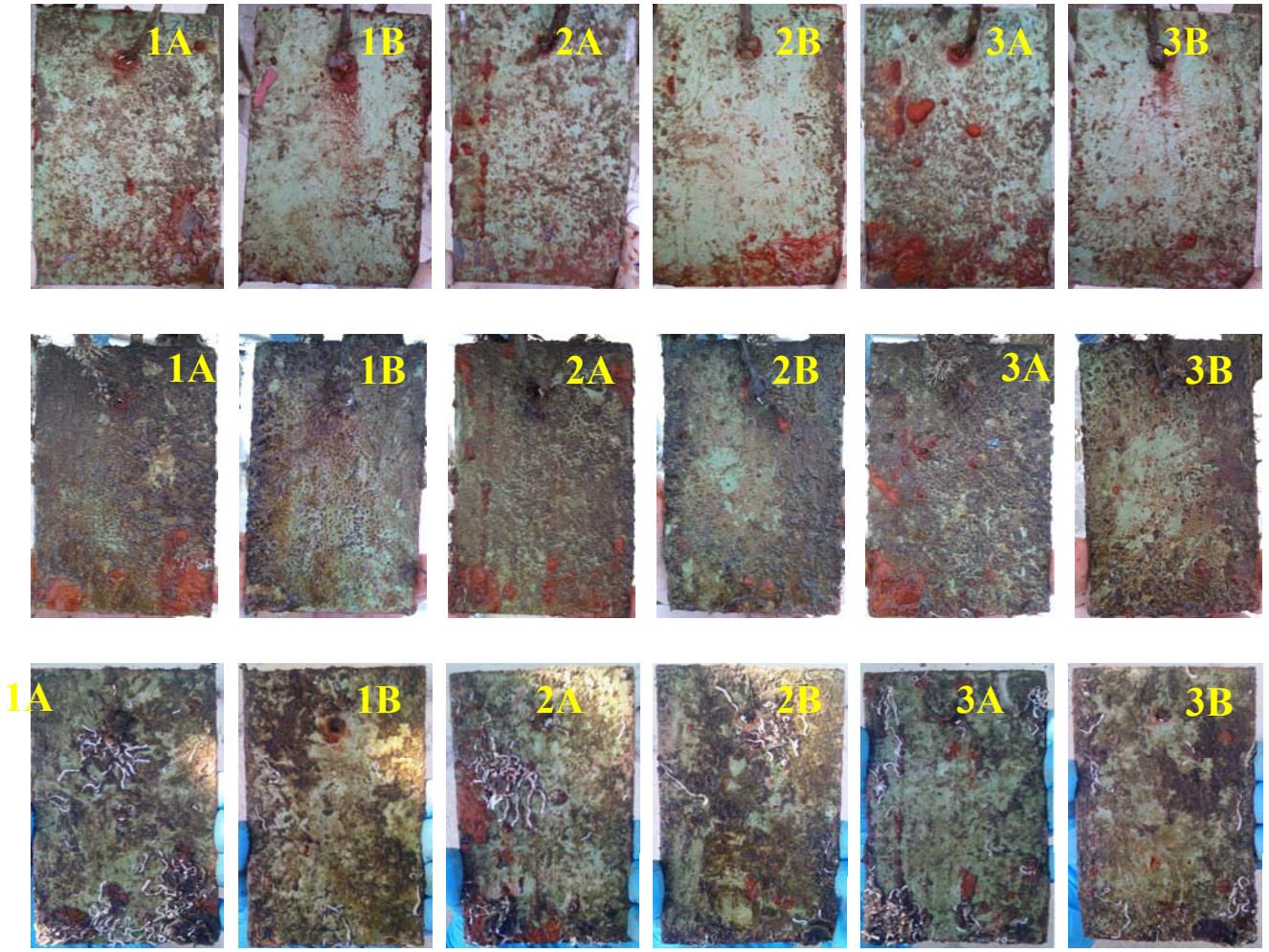


Figure 3.52 The photographs belong to two sides of test plates painted with *Z. noltii* extract containing paint (between April and July) (A: front, B: back, 1-3: parallel number).

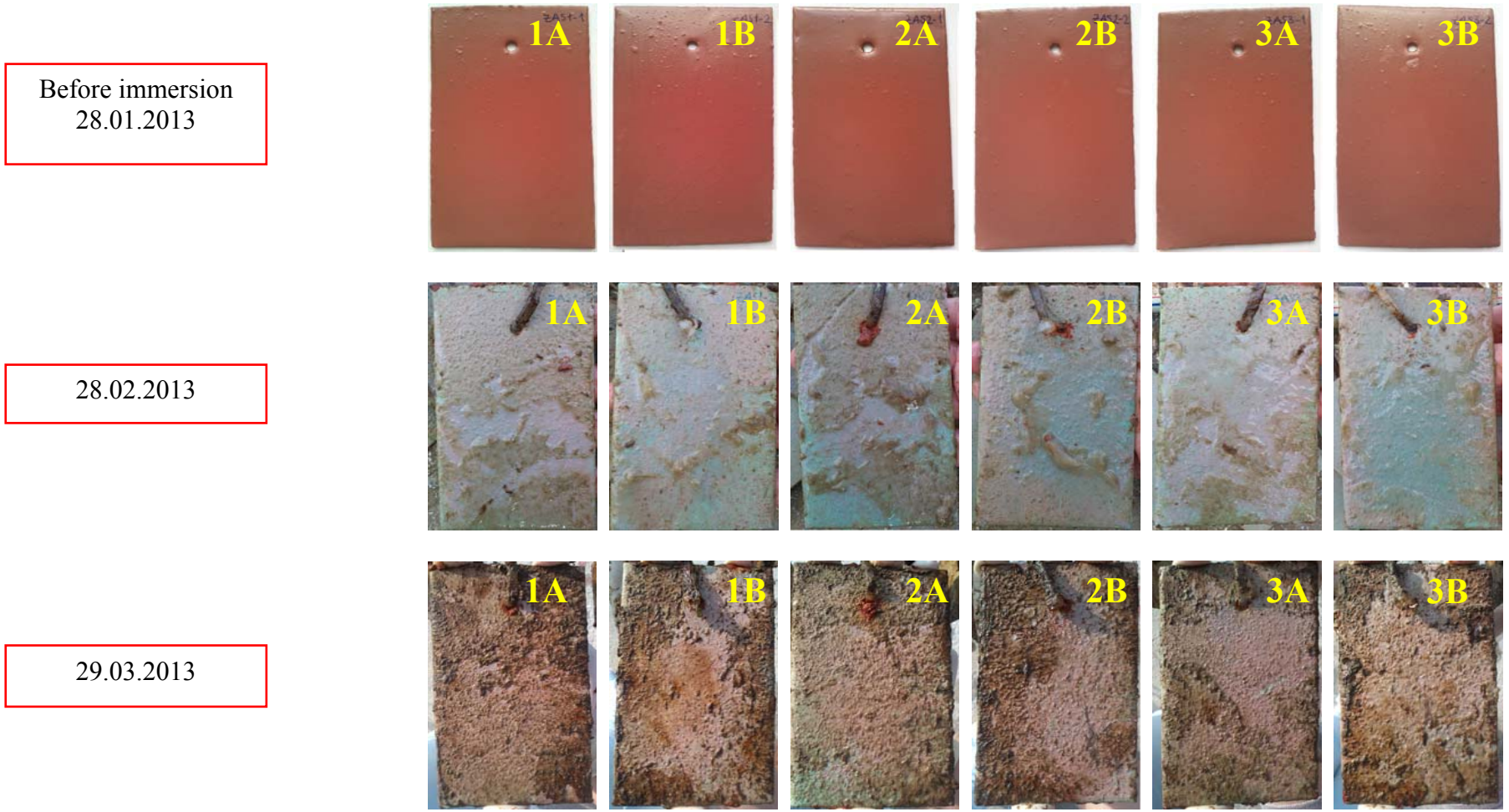


Figure 3.53 The photographs belong to two sides of test plates painted with ZA containing paint (between January and March) (A: front, B: back, 1-3: parallel number).

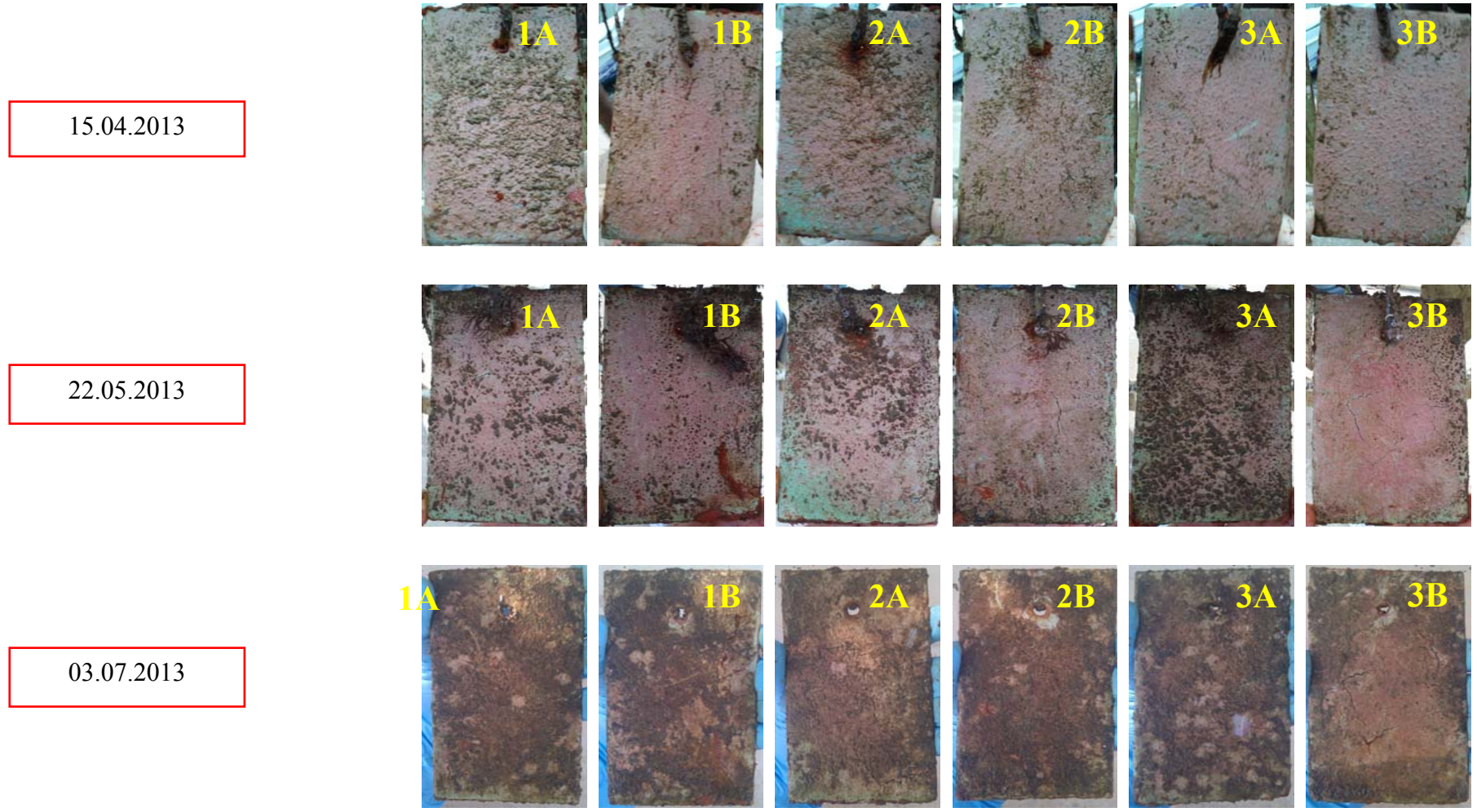


Figure 3.54 The photographs belong to two sides of test plates painted with ZA containing paint (between April and July) (A: front, B: back, 1-3: parallel number).

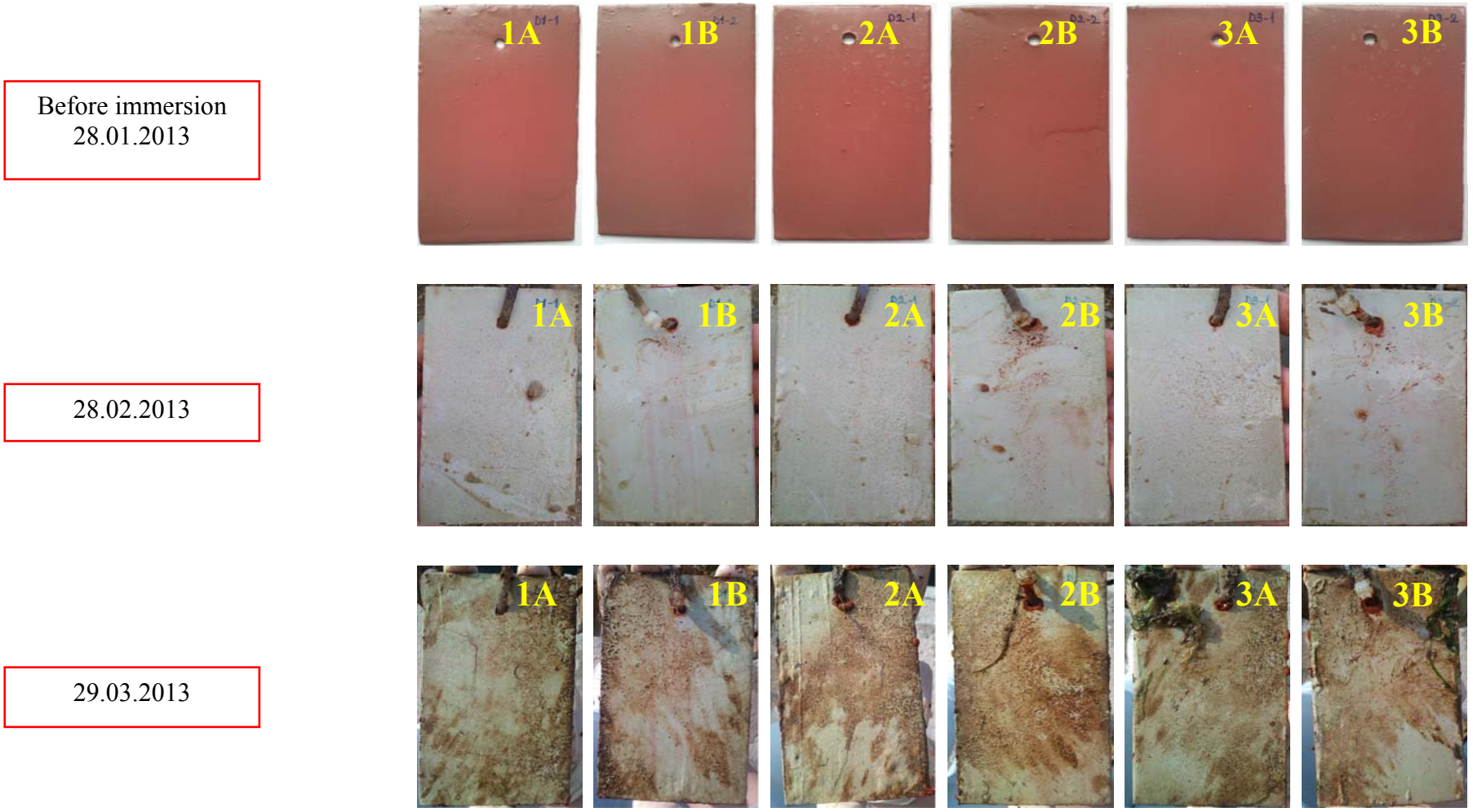


Figure 3.55 The photographs belong to two sides of test plates painted with diuron containing paint (between January and March) (A: front, B: back, 1-3: parallel number).

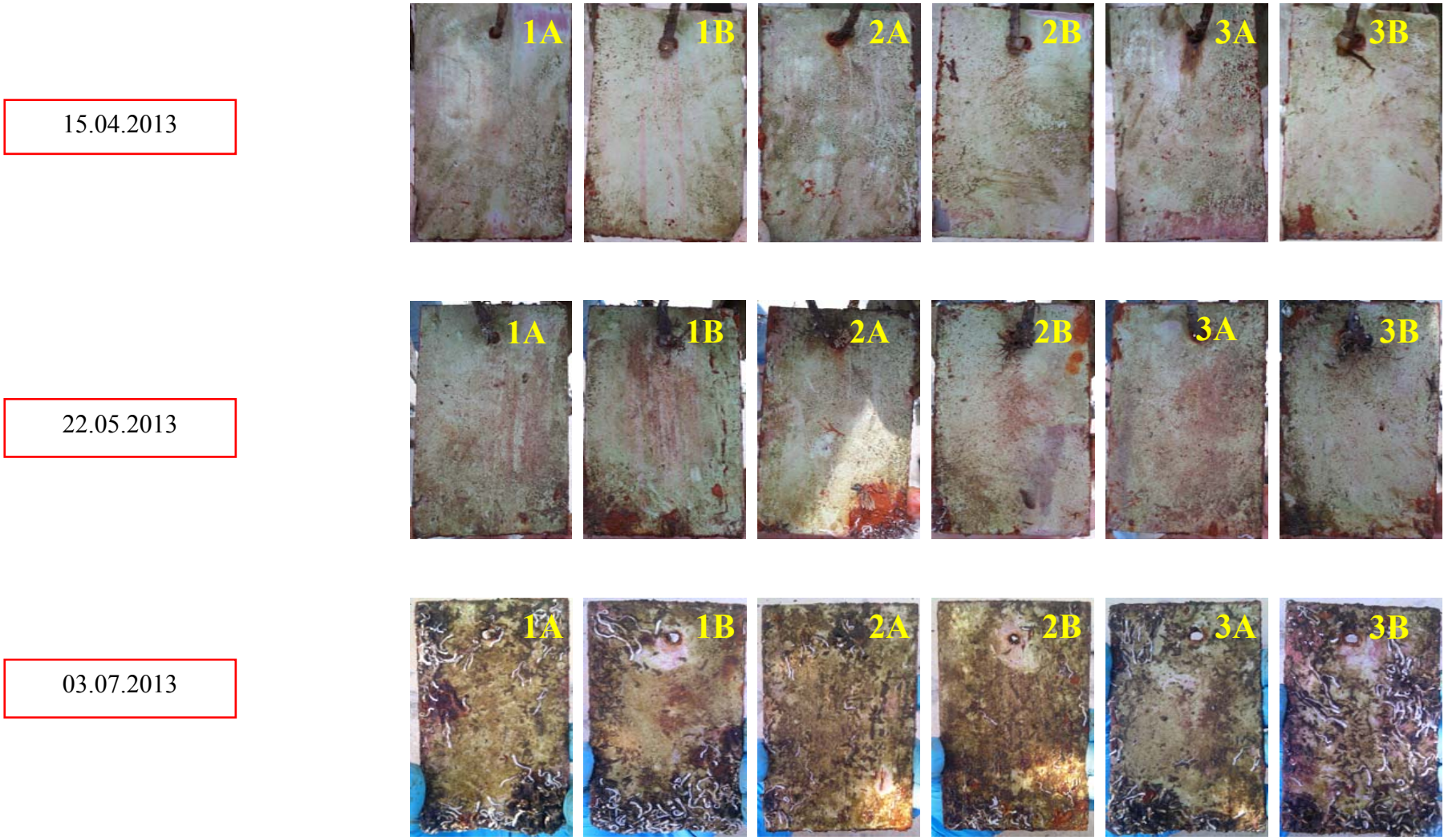


Figure 3.56 The photographs belong to two sides of test plates painted with diuron containing paint (between April and July) (A: front, B: back, 1-3: parallel number).

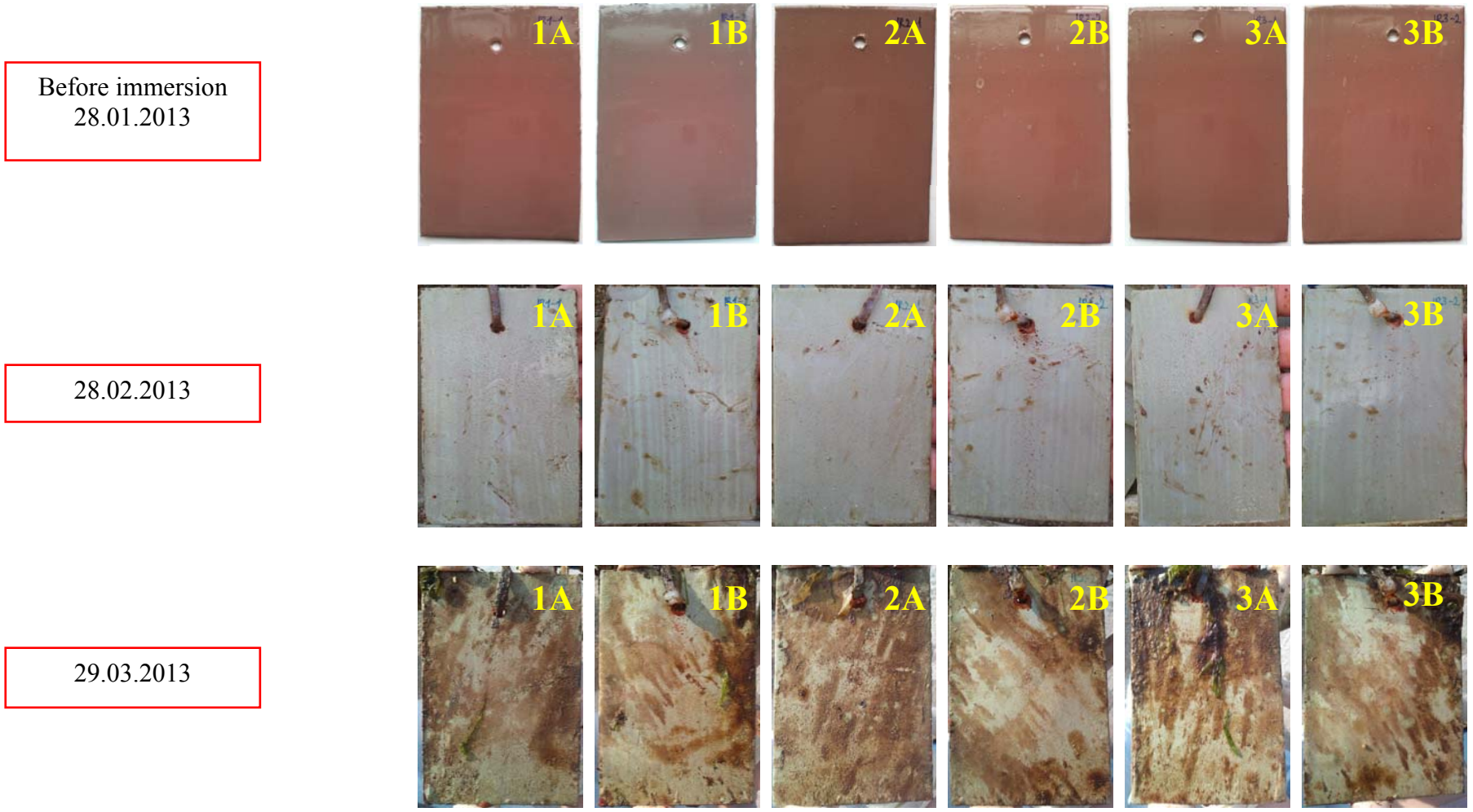


Figure 3.57 The photographs belong to two sides of test plates painted with irgarol 1051 containing paint (between January and March) (A: front, B: back, 1-3: parallel number).

15.04.2013

22.05.2013

03.07.2013

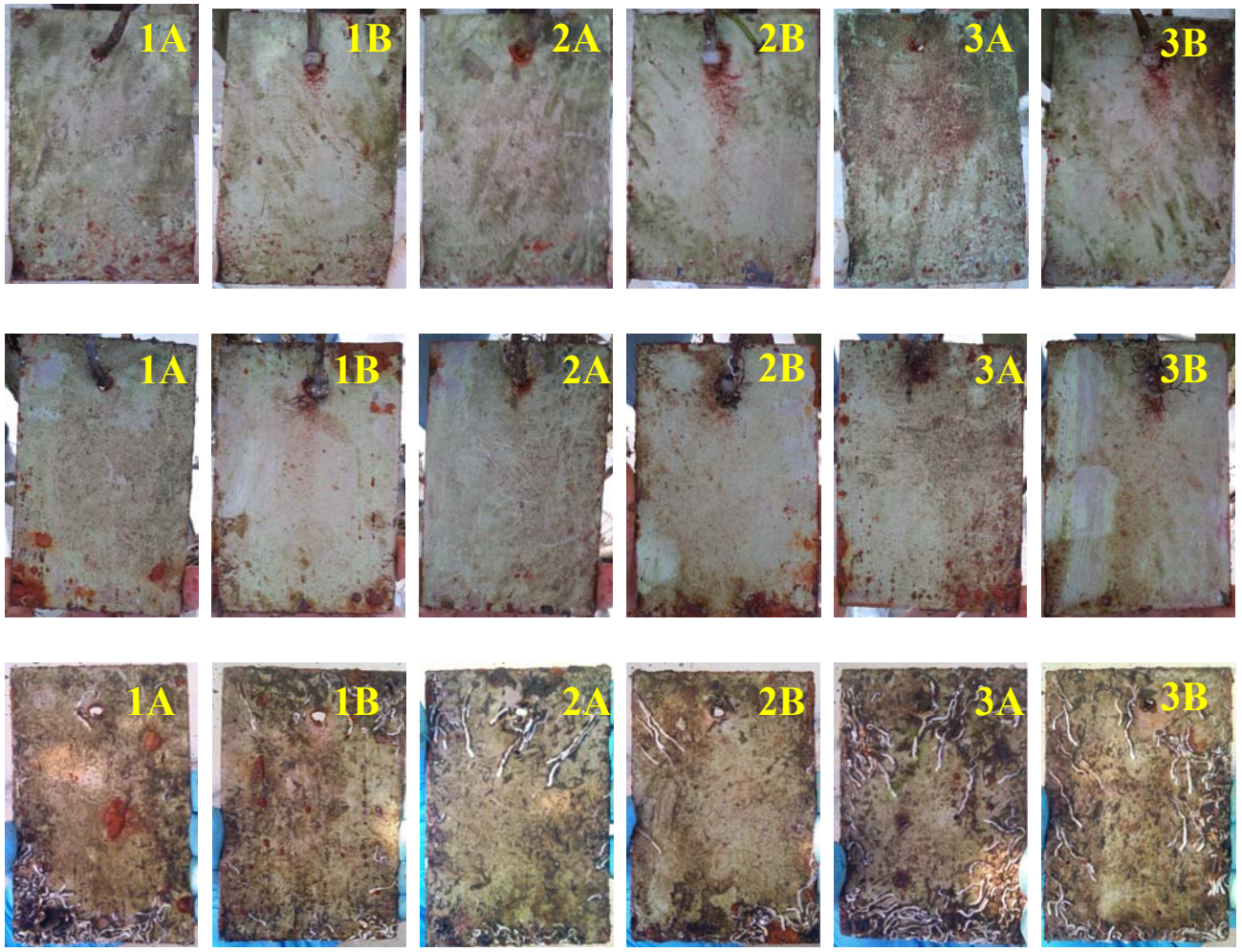


Figure 3.58 The photographs belong to two sides of test plates painted with irgarol 1051 containing paint (between April and July) (A: front, B: back, 1-3: parallel number).

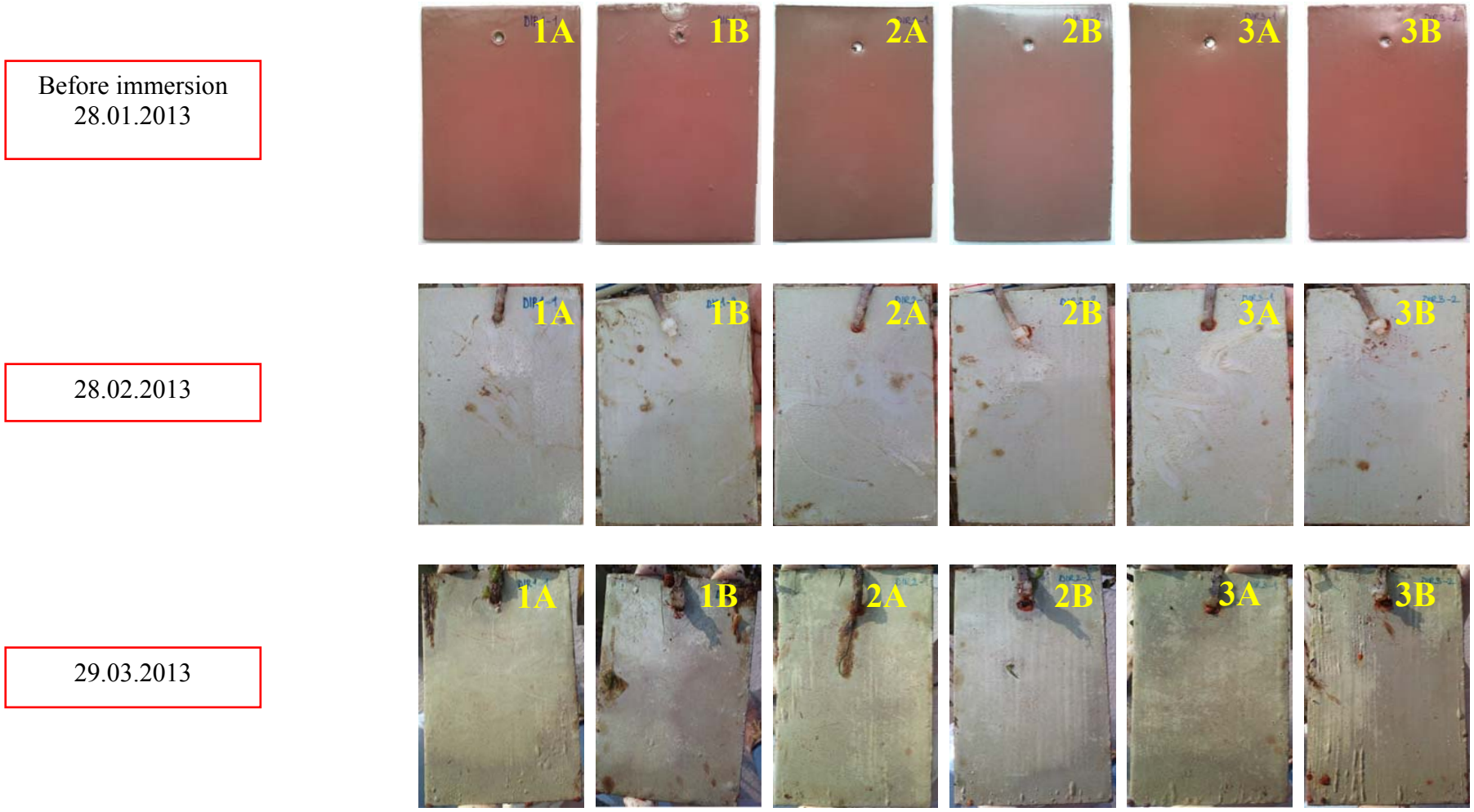


Figure 3.59 The photographs belong to two sides of test plates painted with diuron + irgarol 1051 containing paint (between January and March) (A: front, B: back, 1-3: parallel number).

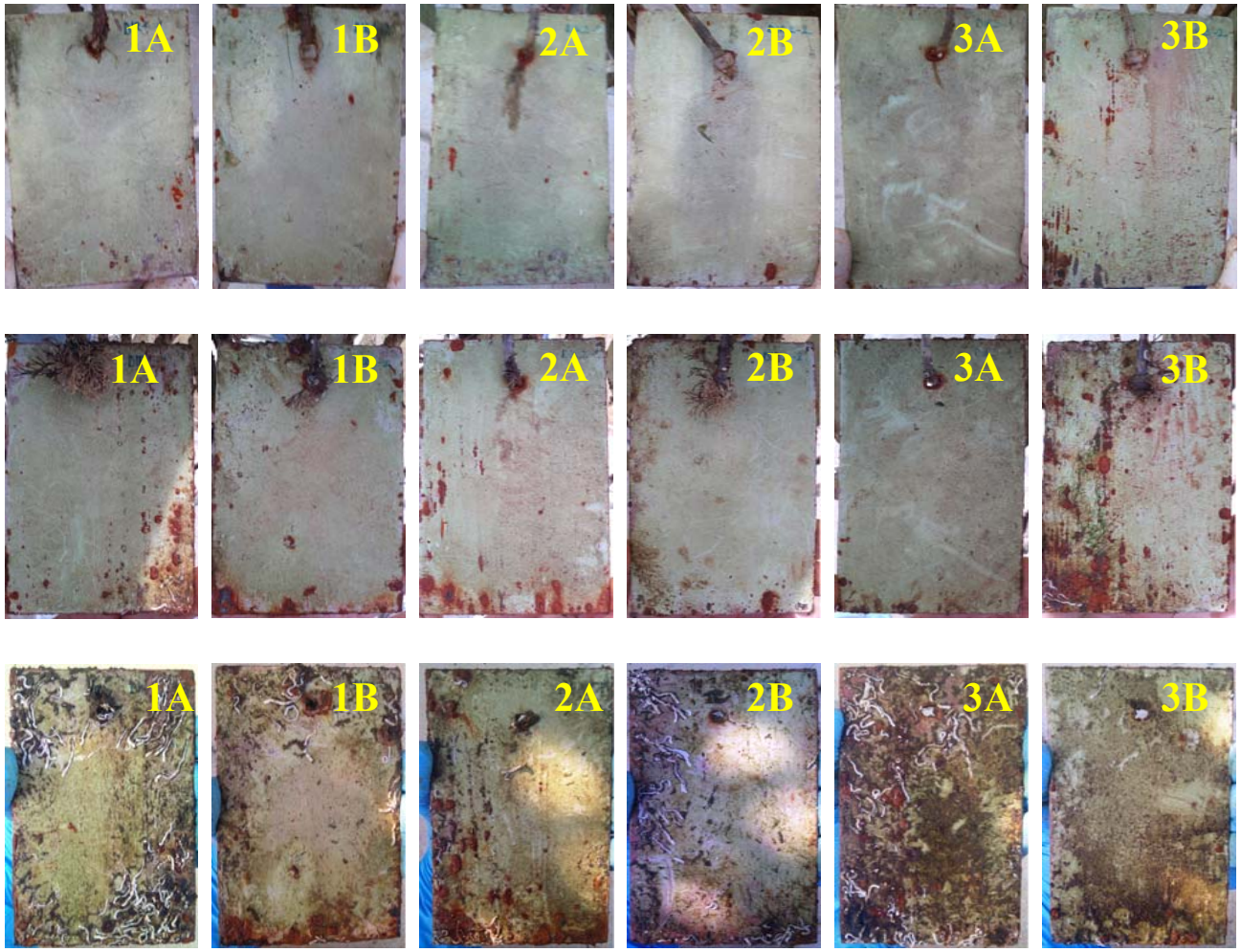


Figure 3.60 The photographs belong to two sides of test plates painted with diuron + irgarol 1051 containing paint (between April to July) (A: front, B: back, 1-3: parallel number).

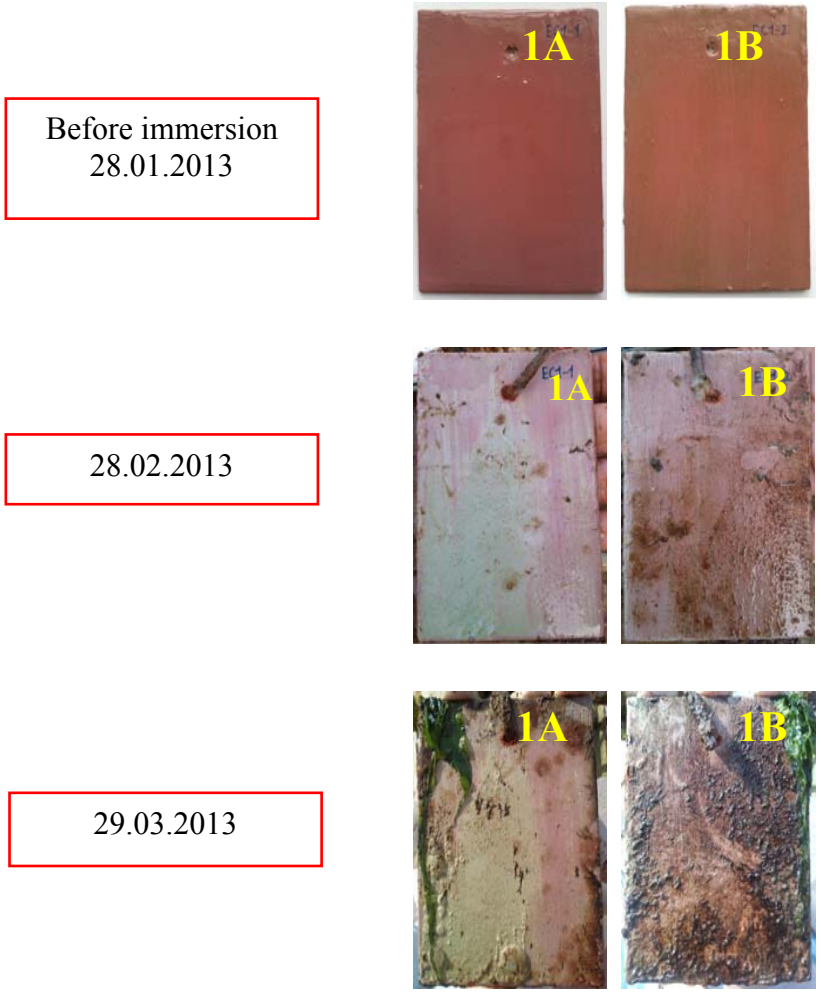


Figure 3.61 The photographs belong to two sides of test plates painted with econea containing paint (between January and March) (A: front, B: back, 1-3: parallel number).



Figure 3.62 The photographs belong to two sides of test plates painted with econea containing paint (between April and July) (A: front, B: back, 1-3: parallel number).

Table 3.2 The assessment of fouling grades on the surface of antifouling paint test panels

Plate Name	**Field Test (156 Days)**	
	Side 1	**Side 2**
Paint Free Panel	V	V
Biocide Free Paint	IV	IV
Commercial antifouling Paint	I	I
Z. noltii powder containing Paint	IV	IV
Z. noltii extract containing Paint	IV	IV
Zosteric acid containing Paint	II	II
Diuron Containing Paint	IV	IV
Irgarol Containing Paint	IV	IV
Diuron + irgarol Containing Paint	IV	IV
Econea containing Paint	III	III

The studies related to the presentation an alternative eco-friendly antifouling agent increased in last decades. For example, Bellotti, Deya´, del Amo, & Romagnoli, (2012) evaluated the antifouling performance of tannin derivative (zinc tannate) from a characteristic argentine tree, Quebracho Colorado, and boosters such as bismuth lactate, a zeolite exchanged with silver cations and the same zeolite modified with silver chloride. They carried out a field test in natural sea water with prepared paints with tannin derivative and these boosters for 9 months. According to the results zinc tannate triple the service life when it used with bismuth lactate in paint formulation as a booster. Bellotti, del Amo, & Romagnoli, (2012) also studied on the antifouling performances of tannin derivatives from a tara tree, *Caesalpinia spinosa*. They evaluated the antifouling performances of two different paint formulations which were prepared with zinc tannat derivatives at 20 °C and 60°C (TZn20 and TZn60, respectively). They immersed the plates in natural water and monitored monthly. The paint prepared with TZn60 showed to have a longer service life than the paint prepared with TZn20. Alyuruk, Doner, Karabay, & Cavas (2010) carried out a study on acute toxicities of potassium sorbate, tannic acid, copper(II)

sulphatepentahydrate, *Caulerpa prolifera* extract were on the model organism *Artemia salina* and LC_{50} values were found as 19.96 g/L, 155.30 g/L, 10.47 g/L and 20.40%, respectively. Antifouling performances of these molecules which were immobilized in phytagel were evaluated with a field test in marine environment. They reported that the molecules in phytagel showed antifouling effect compared with the control group. Silkina, Bazes, Mouget, & Bourgougnon, (2012) carried out a study on the algal growth inhibitory effects of the ethanol and dichloromethane extracts of a brown (*Sargassum muticum*) and a red alga (*Ceramium botryocarpum*) compared with the booster biocides (Diuron, Copper thiocyanate, Tolylfluanid). Three diatom species (*Fragilaria pinnata*, *Cylindrotheca closterium* and *Thalassiosira pseudonana*) were used for 72 hours algal growth inhibition tests. According to the results, methanol extracts of the both algae inhibited the diatom growth (EC_{50} = 4.74 and 5.3 µg/mL for *S. muticum* and *C. botryocarpum* respectively). Although the booster biocides have been found more efficient (EC_{50} = 0.52 µg/mL), Silkina et al., reported that booster biocide are highly toxic unlike marine algae. Armstrong, E., Boyd, K.G., Pisacane, A., Peppiatt, C.J. & Burgess, J.G (2000) isolated active compounds from surface of the seaweed, *Fucus serratus*, and the nudibranch, *Archidoris pseudoargus*. They prepared acrylic base paint resin with the extracts and evaluated antifouling activity of the extracts by measuring their inhibitory ability on bacterial growth. Antifouling ability of these formulations on the marine organisms was presented by Armstrong et al., (2000). Stupak, García, & Pérez, (2003) studied on the antifouling activities of some non-toxic compounds such as sodium benzoate and three different tannins from chestnut, mimosa and guebracho trees. *Balanus amphitrite* nauplii was used for the bioassays conducted in artificial sea water. Stupak et al, (2003) reported that these non-toxic compounds have concentration-dependent narcotic effects and the paints prepared with these compounds prevented the attachment of the barnacle.

3.6 The Results of the Microscopic Analysis

When an artificial surface immersed in seawater, organic compounds such as lipids, proteins and carbohydrates start to adhere to surface quickly with physical

strength. This surface provides a leaving area and nutrients to microorganism and biofouling starts with this adsorption. For this reason, it is important to analyze this microorganism.

Some diatoms were observed on the surface when the plates were examined (Figure 3.63). Most of the paints had these organisms, but the cleanest ones were commercial antifouling paint and diuron containing paint. Since sea water was very dirty in the marina, brown film layer was observed on the most of the paint surface. It was muddy caused by sediment.



Figure 3.63 Some diatoms observed on the test plates.

3.7 The Statistical Analysis Results

According to the One Way ANOVA results, the ZA contents of monthly sampled *Z. noltii* detritus were changed within stations (Table 3.1, $p<0.05$).

CHAPTER FOUR

CONCLUSION

In this thesis, the ZA concentrations in the dead leaves of *Z. noltii* and the antifouling performances of ZA including rosin based antifouling paints were evaluated. *Z. noltii* detritus is accumulated in Turkish coastline seasonally. Seagrasses have important phenolic compounds. Although ZA is one of the bioactive compounds, other phenolic compounds in *Z. noltii* methanol extracts were also observed during this study (Figure 3.39). The characterization of these molecules is of great importance. It could be valuable for Turkish economy to determine the concentrations of these phenolic compounds in widely distributed species along Turkish coastline because of the important biological activities of these phenolic compounds. In the field test regarding synthesized ZA, it was observed that ZA prevented attachment of macro-fouling organisms such as *Balanus* sp and *Hydroides* sp. Although macro-fouling organisms were not observed in the testing plates, micro-slime layer was visible. Since macro-foulers are considered as main problem in antifouling paints, the developed plates could be considered as successful formulations. Since the most important problem is macro-fouling in shipping industry, it can be said that this metabolite could be used in antifouling paint industry.

In this study, *Z. noltii* samples were collected from Dikili and Urla (Aegean Sea) and Erdek (Marmara Sea). The ZA levels just from these regions were determined, however, Turkey has very long coastline, it is approximately 8333 km and ZA levels of *Z. noltii* from the other regions should be studied. ZA potential of *Z. noltii* or *Z.marina* from Black Sea is an original research topic since no published material is existed in the scientific literature yet.

In the literature, there are a lot of study on the determination of the synthetic biocides concentration in sediments and marinas from several countries. Although shipping industry is an important industry for Turkish economy, no detailed study from Turkish coastline on this fact was carried out in the literature. Therefore the

author of the thesis recommends to analytical chemists to determine and evaluate the harmful biocides concentration in Turkish marines and sediments for ecosystem health of the Mediterranean coastline of Turkey.

Currently, the rosin based self-polishing type and the self-polishing copolymer type antifouling paints are the mostly used antifouling paints. Moreover, fouling release type antifouling paints do not contain biocides and they start to become important in the antifouling paint market. However, fouling release type antifouling paints still have some problems with their mechanical strength. Therefore it is very important to develop ecofriendly biocides and ZA could be evaluated as an ecofriendly antifouling agent.

In this study, it is observed that paint containing ZA prevented the attachment of macro-organisms on the test plates. However, the release of ZA from rosin based antifouling paints is very fast. The fast release of ZA from paint formulation could decrease the service time of the paint. Because of this, ZA could be applied to the paint formulation by using different immobilization techniques. In this research, in addition to ZA, the other paint formulations were also compared. It is observed that paint containing *Z. noltii* powder also prevented the attachment of some macro-organisms on the plates. The success of paint containing *Z. noltii* powder can be explained with slow release of ZA and the other phenolic compounds from paint formulation. In summary, release kinetic of ZA from antifouling paints should be studied.

The author of this thesis never recommends the collection of living form of *Z. noltii* under the water because of its importance in the marine ecosystems. However, their detritus from touristic zones could be collected and be evaluated. In a possible industrial collection, local authorities (Ministry of Agriculture, Universities, etc.) must be informed about the scale of the collection.

REFERENCES

Abarzua, S. & Jakubowski, S. (1995). Biotechnological investigation for the prevention of biofouling. I. Biological and biochemical principles for the prevention of biofouling. *Marine Ecology Progress Series 123*, 301-312.

Abbott, A., Abel, P.D., Arnold, D.W. & Milne A. (2000). Cost–benefit analysis of the use of TBT: the case for a treatment approach. *Science of the Total Environment 258*, 5-19.

Abdul Azis, P.K., AI-Tisan, I. & Sasikumar, N. (2001). Biofouling potential and environmental factors of seawater at a desalination plant intake. *Desalination 135*, 69-82.

Achamlale, S., Rezzonico, B. & Grignon-Dubois M. (2009a). Rosmarinic acid from beach waste: Isolation and HPLC quantification in *Zostera* detritus from Arcachon lagoon. *Food Chemistry 113*, 878–883.

Achamlale, S., Rezzonico, B. & Grignon-Dubois M. (2009b). Evaluation of *Zostera* detritus as a potential new source of zosteric acid. *Journal of Applied Phycology 21*, 347–352.

Advisory Committee on Pesticides. (2000). *In: Minutes of the 278th Meeting of the Advisory Committee on Pesticides.*

Alberte, R.S. & Smith, R. (2005). Transgenic plants incorporating traits of *Zostera marina*. *US Patent* (6841718 B2).

Alpar, B., Dogan, E., Yuce, H. & Altıok, H. (2000). Sea level changes along the Turkish coasts of the Black Sea, the Aegean Sea and the Eastern Mediterranean. *Mediterranean Marine Science 1*, 141-156.

Alyuruk, H. & Cavas, L. (2013). Toxicities of diuron and irgarol on the hatchability and early stage development of *Artemia salina*. *Turkish Journal of Biology 37*, 151-157.

Alyuruk, H. (2012). *Antifouling performances of eco-friendly secondary metabolite cocktails from marine plants*, MSc Thesis, Department of Chemistry, The Graduate School of Natural and Applied Sciences, Dokuz Eylül University.

Alyuruk, H., Doner, E., Karabay, Z. & Cavas L. (2010). Antifouling performances and acute toxicities of eco-friendly biocides. *Hacettepe Journal of Biology and Chemistry 38*, 277-286.

Anita, G.J.B., Sascha, B.S., Willem, H. van de Poll, Hans, J.C.K. & Joop, F.B. (2009). Impact of the antifouling agent Irgarol 1051 on marine phytoplankton species. *Journal of Sea Research 61*, 133–139.

Arimura, H., Hiyoshi, S., Nakamura, N., & Tsuboi, M. (2004). (Poly)oxyalkylene block silyl ester copolymer, antifouling coating composition, antifouling coating formed from antifouling coating composition, antifouling method using antifouling coating composition and hull or underwater structure covered with antifouling coating. US Patent (6828030).

Armstrong, E., Boyd, K.G. & Burgess, J.G. (2000). Prevention of marine biofouling using natural compounds from marine organisms. *Biotechnology Annual Review 6*, 221-41.

Armstrong, E., Boyd, K.G., Pisacane, A., Peppiatt, C.J. & Burgess, J.G. (2000). Marine microbial natural products in antifouling coatings. *Biofouling 16,* 215-224.

Auby, I. & Labourg, P.J. (1996). Seasonal dynamics of *Zostera noltii* Hornem in the Bay of Arcachon (France). *Journal of Sea Research 35*, 269-277.

Barrios, C.A., Xu, Q., Cutright, T. & Newby, B.M. (2005). Incorporating zosteric acid into silicone coatings to achieve its slow release while reducing fresh water bacterial attachment. *Colloids and Surfaces B: Biointerfaces 41*, 83-93.

Bellotti, N., del Amo, B. & Romagnoli, R. (2012). *Caesalpinia spinosa* tannin derivatives for antifouling formulations, *Procedia Materials Science 1*, 259-265.

Bellotti, N., Deya´, C., del Amo, B. & Romagnoli, R. (2012). ‘‘Quebracho’’ tannin derivative and boosters biocides for new antifouling formulations, *Journal of Coatings Technology and Research 9*, 551-559.

Boxall, A.B.A., Comber S.D., Conrad A.U., Howcroft J., & Zaman N. (2000). Inputs, monitoring and fate modeling of antifouling biocides in UK estuaries. *Marine Pollution Bulletin 40*, 898-905.

Brady, R.F. (1999). Properties which influence marine fouling resistance in polymers containing silicon and fluorine. *Progress in Organic Coatings 35*, 31–35.

Brancato, M.S. & MacLellan, D. (1999). Impacts of invasive species introduced through the shipping industry. *Marine Technology Society/Institute of Electrical and Electronics Engineers Oceans Conference, Washington, D.C. 2*, 676.

Buskens, P., Wouters, M., Rentrop, C. & Vroon, Z. (2013). A brief review of environmentally benign antifouling and foul-release coatings for marine applications. *Journal of Coatings Technology and Research 10*, 29-36.

Callow, M.E. & Fletcher, R.L. (1994). The influence of low surface energy materials on bioadhesion: a review. *International Biodeterioration & Biodegradation 34*, 333-348.

Chao, P.C., Hsu, C.C. & Yin, M.C. (2009). Anti-inflammatory and anti-coagulatory activities of caffeic acid and ellagic acid in cardiac tissue of diabetic mice. *Nutrition & Metabolism 6*, 33.

Chesworth, J.C, Donkin, M.E. & Brown, M.T. (2004). The interactive effects of the antifouling herbicides Irgarol 1051 and Diuron on the seagrass *Zostera marina* (L.). Aquatic Toxicology *66*, 293-305.

David, R.D. & Haydn, P. (1986). An investigation of the genotoxic effects of an organotin antifouling compound (bis(tributyltin) oxide) on the chromosomes of the edible mussel, *Mytilus edulis. Aquatic Toxicology 8*, 185–195.

Faÿ, F., Linossier, I., Carteau, D., Dheilly, A., Silkina, A. & Vallée-Rééhel K. (2010). Booster biocides and microfouling. *Biofouling* 26, 787-798.

Gibbs, P.E., Pascoe, P.L. & Bryan G.W. (1991). Tributyltin-induced imposex in stenoglossan gastropods: pathological effects on the female reproductive system. *Comparative Biochemistry and Physiology 1*, 231–235.

Green, E.P. & Short, F.T. (2003). *World Atlas of Seagrasses* (Cloth edition ISBN 0-520-24047-2). USA: University of California Press.

Grignon-Dubois, M., Rezzonico, B. & Alcoverro, T. (2012). Regional scale patterns in seagrass defences: Phenolic acid content in *Zostera noltii*. *Estuarine, Coastal and Shelf Science 114*, 18–22.

Gulcin, I. (2006). Antioxidant activity of caffeic acid (3,4-dihydroxycinnamic acid). *Toxicology 217*, 213-220.

Hagger, J.A., Fisher, A.S., Hill, S.J., Depledge, M.H., Jha, A.N. (2002). Genotoxic, cytotoxic and ontogenetic effects of tri-n-butyltin on the marine worm, *Platynereis dumerilii* (Polychaeta: Nereidae). *Aquatic Toxicology 57*, 243–255.

Hall, L.W., Giddings, J.M., Soloman, K.R. & Balcomb, R. (1999). An ecological risk assessment for the use of Irgarol 1051 as an algaecide for antifoulant paints. *Critical Reviews in Toxicology 29*, 367-437.

Haynes, D., Muller, J. & Carter, J. (2000). Pesticide and herbicide residues in sediments and seagrasses from the Great Barrier Reef World Heritage Area and Queensland coast. *Marine Pollution Bulletin 41*, 279–287.

Hellio, C., De La Broise, D., Dufossé, L., Le Gal, Y. & Bourgougnon, N. (2001). Inhibition of marine bacteria by extracts of macroalgae: potential use for environmentally friendly antifouling paints. *Marine Environmental Research 52*, 231-247.

Hwang, H.J., Park, H.J., Chung, H.J., Min, H.Y., Park, E.J., Hong, J.Y. & Lee, S.K. (2006). Inhibitory effects of caffeic acid phenethyl ester on cancer cell metastasis mediated by the down-regulation of matrix metalloproteinase expression in human HT1080 fibrosarcoma cells. *The Journal of Nutritional Biochemistry 17*, 356-362.

Kang, N.J., Lee, K.W., Shin, B.J., Jung, S.K., Hwang, M.K., Bode, A.M., Heo, Y.S., Lee, H.J. & Dong, Z. (2009). Caffeic acid, a phenolic phytochemical in coffee, directly inhibits Fyn kinase activity and UVB-induced COX-2 expression. *Carcinogenesis 30*, 321-330.

Karabay, Z. (2011). *Antifouling performances of some eco-friendly biocides*, MSc Thesis, Department of Chemistry, The Graduate School of Natural and Applied Sciences, Dokuz Eylül University.

Keough, M.J. & Raimondi, R.T. (1995). Responses of settling invertebrate larvae to bioorganic films: effects of different types of films. *Journal of Experimental Marine Biology and Ecology 185*, 235-253.

Kirschner, C.M. & Brennan, A.B. (2012). Bio-inspired antifouling strategies. *Annual Review of Materials Research 42*, 211-229.

Konstantinou, I.K, & Albanis, T.A. (2004). Worldwide occurrence and effects of antifouling paint booster biocides in the aquatic environment: a review. *Environment International 30*, 235-248.

Liu, C.X., Zhang, D.R., He Yi, Zhao, X.S. & Bai, R. (2010). Modification of membrane surface for anti-biofouling performance: Effect of anti-adhesion and anti-bacteria approaches. *Journal of Membrane Science 346*, 121–130.

Marbà, N., Cebrian, J., Enriquez, S. & Duarte C.M. (1996). Growth patterns of Western Mediterranean seagrasses: species-specific responses to seasonal forcing. *Marine Ecology Progress Series 133*, 203–215.

Mehrotra, A., Shanbhag, R., Chamallamudi, M.R., Singh, V.P. & Mudgal, J. (2011). Ameliorative effect of caffeic acid against inflammatory pain in rodents. *European Journal of Pharmacology 666*, 80-86.

Milchakova, N.A. (1999). On the status of seagrass communities in the Black Sea. *Aquatic Botany 65*, 21-32.

Murthy, P.S. & Venkatesan, R. (2008). Chapter: Industrial biofilms and their control. *Marine and Industrial Biofouling* (65-101), New York: Springer-Verlag Berlin Heidelberg.

Negri, A., Vollhardt, C., Humphrey, C., Heyward, A., Jones, R., Eaglesham, G. & Fabricius, K. (2005). Effects of the herbicide diuron on the early life history stages of coral. *Marine Pollution Bulletin 51*, 370-383.

Omae, I. (2003). Organotin antifouling paints and their alternatives. *Application of Organometallic Chemistry 17*, 81–105.

Papenbrock, J. (2012). Highlights in Seagrasses' Phylogeny, Physiology, and Metabolism: What Makes Them Special? *International Scholarly Research Network Journals (ISRN Botany)*.

Peña, S.T. (2010). Biofilms and their impact on food industry. *Veterinary Health Surveillance Center (VISAVET) Outreach Journal* http://www.*vigilanciasanitaria*.es/en/articles/biofilms-impact-food-industry.php.

Philippart, C.J.M. (1995). Seasonal variation in growth and biomass of an intertidal *Zostera noltii* stand in the Dutch Wadden Sea. *Netherlands Journal of Sea Research 33*, 205-218.

Phillips, R.C. & Menez, E.G. (1988). *Seagrasses*. Washington: Smithsonian Institution Press.

Readman, J.W, Kwong, L.L.W., Grondin, D., Bartocci, J., Villeneurve, J.P. & Mee L.D. (1993b.) Coastal water contamination from a triazine herbicide used in antifouling paints. *Environmental Science & Technology 27*, 1940–1942.

Readman, J.W., Albanis, T.A., Barcelo, D., Galassi, S., Tronczynski, J. & Gabrielides, G.P. (1993a). Herbicide contamination of Mediterranean estuarine waters: results from a MED POL pilot survey. *Marine Pollution Bulletin 26*, 613–619.

Rees, C.R., Costin, J.M., Fink, R.C., McMichael, M., Fontaine, K.A., Isern, S. & Michael, S.F. (2008). In vitro inhibition of dengue virus entry by p-sulfoxy-cinnamic acid and structurally related combinatorial chemistries. *Antiviral Research 80*, 135-142.

Ribera, M.A. (1995). Introduced marine plants, with special reference to macroalgea: mechanism and impact. *Progress in Phycological Research 11*, 187-268.

Silkina, A., Bazes, A., Mouget, J.L. & Bourgougnon, N. (2012). Comparative efficiency of macroalgal extracts and booster biocides as antifouling agents to control growth of three diatom species. *Marine Pollution Bulletin 64*, 2039–2046.

Stupak, M.E., García, M.T., & Pérez, M.C. (2003). Non-toxic alternative compounds for marine antifouling paints. *International Biodeterioration & Biodegradation 52*, 49-52.

Sundberg, D.C., Vasishtha, N., Zimmerman, R.C. & Smith, C.M. (1997). *Chapter 5: Selection, Design and Delivery of Environmentally Benign Antifouling Agents.* Virginia: Office of Naval Research.

Taxonomy Browser: Algeabase. (14.10.2013). http://www.algaebase.org/browse/taxonomy/?id=7301.

Thomas, K.V., Fileman, T.W., Readman, J.W. & Waldock, M.J. (2001). Antifouling paint booster biocides in the U.K. coastal environment and potential risks of biological effects. *Marine Pollution Bulletin 42*, 677–688.

Tian, L., Chen, X.D., Yang, Q.P., Chen, J.C., Shi, L. & Li, Q. (2012). Effect of calcium ions on the evolution of biofouling by *Bacillus subtilis* in plate heat exchangers simulating the heat pump system used with treated sewage in the 2008 Olympic Village. *Colloids Surf B Biointerfaces 94*, 309-316.

Todd, J.T., Zimmerman, R.C., Crews, P. & Alberte, R.S. (1993). Isolation of p-sulfoxy cinnamic acid from *Zostera marina* L. (eelgrass) and the antifouling activity of phenolic acid sulfate esters. *Phytochemistry 34*, 401-404.

Valle, M., Borja, Á., Chust, G., Galparsoro, I. & Garmendia, J.M.. (2011). Modelling suitable estuarine habitats for *Zostera noltii*, using Ecological Niche Factor Analysis and Bathymetric LiDAR. *Estuarine, Coastal and Shelf Science 94*, 144–154.

Vermaat, J.E., Beijer, J.A.J., Gijlstra, R., Hootsmans, M.J.M., Philippart, C.J.M., van den Brink, N.W. et al. (1993). Leaf dynamics and standing stocks of intertidal *Zostera noltii* Hornem. and *Cymodocea nodosa* (Ucria) Ascherson on the Banc d'Arguin (Mauritania). *Hydrobiologia 258*, 59-72.

Villa, F., Albanese, D., Giussani, B., Stewart, P.S., Daffonchio, D. & Cappitelli, F. (2010). Hindering biofilm formation with zosteric acid. *Biofouling 26*, 739-752.

Voulvoulis, N., Scrimshaw, M.D. & Lester J.N. (1999). Alternative antifouling biocides. *Applied Organometallic Chemistry 13*, 135–143.

Voulvoulis, N., Scrimshaw, M.D. & Lester J.N. (2000). Occurrence of four biocides used in antifouling paints, as alternatives to organotin compounds, in waters and sediments of a commercial estuary in the U.K. *Marine Pollution Bulletin 40*, 938–946.

Wahl M. (1989). Marine epibiosis. I. Fouling and antifouling: some basic aspects. *Marine Ecology Progress Series 58*, 175-189.

Wang, G.F., Shi, L.P., Ren, Y.D., Liu, Q.F., Liu, H.F., Zhang, R.J. et al. (2009). Anti-hepatitis B virus activity of chlorogenic acid, quinic acid and caffeic acid in vivo and in vitro. *Antiviral Research 83*, 186-190.

Woods Hole Oceanographic Institution (WHOI). 1952. US Naval Institute, Annapolis, Iselin, COD.

Woods Hole Oceanographic Institution: Barnacles and Biofilms, http://www.whoi.edu/page.do?pid=7342&tid=3622&cid=155889.

Yan, T., Yan, W.X., Dong, Y., Wang, H.J., Yan, Y. & Liang, G.H. (2009). Marine fouling on floating installations west of Dongsha Islands, the northern South China Sea. *International Biodeterioration & Biodegradation 63*, 1079–1087.

Yang, S.Y., Hong, C.O., Lee, G.P., Kim, C.T. & Lee, K.W. (2013). The hepatoprotection of caffeic acid and rosmarinic acid, major compounds of *Perilla frutescens*, against t-BHP-induced oxidative liver damage. *Food and Chemical Toxicology 55*, 92-99.

Yebra, D.M., Kiil, S. & Dam-Johansen, K. (2004). Antifouling technology-past, present and future steps towards efficient and environmentally friendly antifouling coatings. *Progress in Organic Coatings 50*, 75–104.